Habilitační práce

Petr Adámek

Václav Janovec

SYMMETRY PROPERTIES OF DOMAIN STRUCTURES

Thesis for habilitation

Prague, June 1994

This thesis for habilitation consists of 11 papers collected in the Part 2 and of Introductional commentary (Part 1). The papers have been published within the period 1972 - 1994 and have been worked out mainly in the Institute of Physics, Academy of Sciences of the Czech Republic in Prague. They are all devoted to the symmetry properties of domain structures.

Contents

1. Introductory commentary

1.1. Basic domain formations

At phase transitions accompanied by a lowering of symmetry the homogeneous high symmetry *parent phase* changes almost always into a heterogeneous domain structure which consists of homogeneous regions (domains) of the low symmetry *distorted phase*. In real conditions the domain structure usually appears as a complicated geometrical pattern the form of which depends on the kinetics of the transitions, on external forces, defects, etc. In any case, the concrete form of the domain structure determines to a large extent the physical properties of the crystalline material.

Theoretical explanation of real domain structures represents a complex problem which involves highly non-linear objects (domain walls), long-range elastic and electric interactions, metastable states, surface effects, etc. Any reasonable model of a domain structure tractable by recently available mathematical tools and computer facilities necessarily involves severe simplifications and approximations.

The symmetry analysis of domain structures is in this respect exceptional since it needs no approximations and its conclusions, based on the group theory, are exact. Though the predictions deduced from symmetry have serious limitations (e.g., in most cases do not yield numerical results) they provide a unique reliable guide in the deciphering of domain structures. This exceptional position and predictive power of the symmetry analysis follows from the fact that the very basic reason for domain formation is the symmetry lowering at the phase transition.

Domain structures are traditionally described in terms of domains and domain walls. Such a picture usually exhibits no obvious symmetry. To

disclose the profound symmetry properties of domain structures we have introduced other objects the symmetry of which can be expressed in exact terms of the group theory. We call these objects *basic domain formations.* Papers /P1/-/P11/ deal with following basic domain formations: domain states, domain pairs, domain twins and walls, and perfect domain textures.

Basic domain formations have the following common features:

- Their definitions apply both for a miscroscopic or a continuum approach and can be used for magnetic crystals as well.
- Their symmetry can be expressed by crystallographic groups (space or point groups, ordinary or magnetic groups, dichromatic groups, layer groups, etc.).
- They can be partitioned into classes of crystallographically equivalent formations that can be symmetrically classified.

The concepts of basic domain formations have developed in the course of our study in an effort to reach more exactness and to cover more general situations. This explains certain shifts in their definitions, changes in the terminology and in designation used in different papers in the Part 2.

1.2. Domain states and their degeneracy

We consider a structural phase transition from a homogeneous parent phase with the symmetry G to a distorted phase with the symmetry F which is a subgroup of G, $F < G$. We denote this phase transition by $F \downarrow G$ and the corresponding *order parameter* of the transition by **P.**

As a rule, the distorted phase does not appear as a homogeneous single domain (as all theories of phase transitions tacidly assume) but as a non-homogeneous formation called *domain structure* which consists of many domains. A *domain* is a region with homogeneous distorted structure. The boundary of a domain is formed either by the surface of the crystal or by the transient regions between neighbouring domains called *domain walls*.

Very often (also in our older papers /P1-P3/) the term "domain" is used not only in the sense decriberd above but also for the bulk structure of the domain. To make this distinction clear we define a *domain state* $\mathbf{S_i}$ as the bulk structure (extended into the entire space) of a possible domain in a

domain structure. A *domain* $\mathbf{D_i}$ is then defined by the domain state $\mathbf{S_i}$ and by the connected region Ω_i to which the structure of $\mathbf{S_i}$ is confined in a real domain structure.

In the simplest case the crystal in the distorted phase consists of one domain only (the region Ω_i covers the whole crystal). Then we call the corresponding domain state $\mathbf{S_i}$ the *single domain state*.

As it is explained in /P1/ (where the term "domain" is used instead of "single domain state") possible single domain states $\mathbf{S_1},\mathbf{S_2},...,\mathbf{S_n}$ are *crystallographically equivalent (c.e.) with respect to the group G*, i.e. any single domain state, say $\mathbf{S_i}$, can be brougth into coincidence with another single domain state, say $\mathbf{S_j}$, by an operation g_{ij} of the group $\boldsymbol{G}$ (all single domain states form an *orbit in G*). The *symmetry groups* $\boldsymbol{F_i}$ and $\boldsymbol{Fj}$ of single domain states $\mathbf{S_i}$ and $\mathbf{S_j}$, resp, are conjugate subgroups of $\boldsymbol{G}$.

The single domain states $\mathbf{S_1},\mathbf{S_2},...,\mathbf{S_n}$ are specified by corresponding values of the order parameter $\mathbf{P_1},\mathbf{P_2},...,\mathbf{P_n}$, resp. The order parameter $\mathbf{P}$ is the proper (primary) order parameter of the transition $\boldsymbol{F\downarrow G}$, consequently, $\mathbf{S_1},\mathbf{S_2},...,\mathbf{S_n}$ can be denoted as the *proper single domain states.*

Further it can be shown (see /P1/) that the single domain states $\mathbf{S_1},\mathbf{S_2},...,\mathbf{S_n}$ are in one-to-one correspondence to the left cosets of the decomposition of $\boldsymbol{G}$ into left cosets of $\boldsymbol{F_i}$ and that number n of all proper single domain states equals the index of $\boldsymbol{F_i}$ in $\boldsymbol{G}$ (see Theorem I, where q is used instead of n).

This last result illustrates well the power and elegance of symmetry predictions: The number n of all possible single domain states can be determined from very simple formulae (see,e.g. Eqs (3.9), (310) in /P1/ and Eqs (6), (7) in /P2/) without any knowledge of the strucure or of the order parameter; the only input information needed is the group $\boldsymbol{G}$ and $\boldsymbol{F_i}$

If there exists an intermediate group $\boldsymbol{K}$ such that $\boldsymbol{F<K<G}$ then the notion of the improper (secondary) domain states can be introduced /P1/ (This concept is a generalization of the concept of partial ferroelectric or ferroelastic domain states introduced by Aizu). Let $\mathbf{I}$ be the order parameter of the virtual phase transition $\boldsymbol{K\downarrow G}$ from the parent phase with symmetry $\boldsymbol{G}$ to a phase with symmetry $\boldsymbol{K}$ (the parameter $\mathbf{I}$ is the improper (secondary) order parameter of the transition $\boldsymbol{F\downarrow G}$). Then an *improper single domain*

state $\mathbf{Q^{(i)}}$ is such a distorted structure in which the improper order parameter **I** has constant value $\mathbf{I^{(i)}}$. The essential point here is that there exist $d.>1$ different proper domain states $\mathbf{S_1,S_2,...,S_d}$ with the same value of the improper order parameter $\mathbf{I^{(1)}}$, d another different proper domain states with the same improper order parameter $\mathbf{I^{(2)}}$, etc. The number d, which we call the *degeneracy of improper single domain states* $\mathbf{Q^{(i)}}$, equals the index of F in K (see Eq. (4.11) in /P1/) and the number m of improper domain states equals the index of K in G. The degeneracy and the numbers of improper and proper single domain states fulfil simple relation $n = md$ (see Eqs. (3.12), (4.11) and (4.12) in /P1/).

The fact that both proper and improper single domain states form c.e. sets (orbits) allows one to classify them according to the transformation properties of the corresponding order parameters. Thus one speaks about *ferroelectric, ferroelastic, piezoelectric,... single domain states* if the corresponding order parameter transforms as a vector V, symmetrized square $[V^2]$ or the product $V[V^2]$, resp.

The concept of improper domain states allows partitionig of domain states into sets with the same property, e.g. domain states with the same symmetry group (see Theorem III in /P1/), with the same macroscopic (ferroic) properties (see Eq. (6) in /P2/), etc. This concept is useful in experimental studies since it determines the "resolution" of certain experimental techniques (e.g. an observation in polarized light enables one to discriminate only domain states that differ in spontaneous deformation which may be an improper order parameter. Then one ferroelastic domain can consist of several smaller domains which differ in the primary order parameter, e.g., polarization). Concrete examples of single domain states can be found in /P1/,/P2/,/P3/,/P6/,/P8/,/P11/.

In non-ferroelastic phases the single domain states are identical with domain states in any polydomain structure (see /P10/). In ferroelastic phases the distinction between single domain states and domain states in a polydomain structure is essential (see /P11/, esp. Fig.1 and 2). Due to mechanical compatibility, the single domain states split into so called *disoriented domain states*. Symmetry groups of these domain states are so called *isotropy groups (stabilizers)* of disoriented domain states which can be subgroups of the symmetry groups of single domain states. Then the number

of c.e. disoriented domain states is greater than the number of the single domain states. Another difference is that the disoriented domain states cannot be associated with the order parameter. In any case, however, domain states in ferroelastic domain structures can be related in a unique way to the single domain states.

In what follows we shall use for brevity the term domain state for single domain state and in all situatuations where the difference is not essential or when the distinction should be clear from the context.

Original contribution: Basic symmetry properties of domain states formulated in a consistent group-theoretical language /P1,P2,P12/.

1.3. Domain pairs and distinction of domains

Domain pair is the simplest domain formation which allows one to study relations between two domain states. It was introduced in /P1/ as a purely theoretical concept but later on it has proved to be indispensable for examining distinction of domains and has provided the starting point for the symmetry analysis of domain twins and walls.

A *domain pair* is a set of two domain states $\mathbf{S_i}$ and $\mathbf{S_j}$ that are treated irrespectively of their coexistence. From the mathematical point of view we have to discriminate two types of domain pairs (see /P1/ and /P6/): In an *ordered domain pair* $(\mathbf{S_i},\mathbf{S_j})$ the *transposed domain pair* $(\mathbf{S_j},\mathbf{Si})$ is not identical with the original domain pair $(\mathbf{S_i},\mathbf{S_j})$ unless $i=j$ (trivial domain pair). In an *unordered domain pair* $\{\mathbf{S_i},\mathbf{S_j}\}$ the identity $(\mathbf{S_i},\mathbf{S_j}) = (\mathbf{S_j},\mathbf{Si})$ holds for all i and j. Further, the term "domain pair" will be used for both ordered and unordered domain pairs when the distinction is not significant or when it is clear from the context.

Domain pairs can be visualized as a superposition of the structures $\mathbf{S_i}$ and $\mathbf{S_j}$ which are "coloured" (e.g. $\mathbf{S_i}$ black and $\mathbf{S_j}$ red). In an ordered domain pair one discriminates the colours whereas in an unordered domain pair not, i.e. the unordered pair is a "colour-blind" (black only) picture of the corresponding ordered domain pair. Examples of such geometrical representations of unordered domain pairs can be found in /P6/, Fig. 4, /P9/ Fig. 1 and /P11/ Fig. 1.

Symmetrical equivalence between two domain pairs is defined in /P1/ Eq. (5.4) and in /P6/ Eq. (4.2). It enables one to divide ordered domain pairs into two main classes: *ambivalent domain pairs* (for which the ordered domain pair is c.e. with the transposed domain pair) and *polar domain pairs* (the ordered domain pair is not c.e. with the transposed domain pair) - see /P1/ Eq. (5.9) and Theorem IV.

From n domain states one can form $n(n-1)$ non-trivial ordered pairs. The crystallographical equivalence of domain pairs divides these domain pairs into c.e. classes (orbits). It has been shown in /P1/ that there exists one-to-one correspondence between these classes and double cosets of $\boldsymbol{F_i}$ in $\boldsymbol{G}$. This correspondence also allows one to find representative domain pair of each class and to determine whether the class consists of ambivalent or polar domain pairs (see Theorem V in /P1/).

Thus unlike for single domain states (which are all c.e.) domain pairs can form several c.e. classes (orbits). Domain pairs from different orbits differ in some inherent properties, whereas domain pairs from the same orbit have essentially equal properties since after performing some operation from $\boldsymbol{G}$ they can be brought into coincidence. The double coset decomposition thus reduces the task of examining $n(n-1)$ ordered domain pairs to a considerable lower (especially for large n) number of representative domain pairs corresponding to double cosets.

The importance of left and double coset resolutions in domain analysis has led to tabulation of coset decompositions for all crystallographical point groups and it subgroups /1/ and has encouraged the development of computer programs for IBM compatible personal computers both for point group decompositions /P5/ and space group decompositions /P8/.

The *symmetry group* $\boldsymbol{F_{ij}}$ *of an ordered domain pair* $(\mathbf{S_i},\mathbf{S_j})$ consists of operations common to symmetry groups $\boldsymbol{F_i}$ and $\boldsymbol{Fj}$ of domain states $\mathbf{S_i}$ and $\mathbf{S_j}$, resp. (see /P1/, Eq. (5.3)). The *symmetry group* $\boldsymbol{J_{ij}}$ *of an unordered domain pair* $\{\mathbf{S_i},\mathbf{S_j}\}$ is

$$\boldsymbol{J_{ij} = F_{ij} + j_{ij}F_{ij}}, \qquad (1)$$

where $\boldsymbol{j_{ij}}$ is an operation from $\boldsymbol{G}$ that transposes (exchanges) domain states $\mathbf{S_i}$ and $\mathbf{S_j}$ and is, therefore, an allowable operation of the unordered domain pair (see /P3/,/P6/,/P10/ and /P11/). An operation $\boldsymbol{j_{ij}}$ exists for any

ambivalent ordered domain pair but does not exist for polar domain pairs for which $J_{ij} = F_{ij}$. The group J_{ij} can be treated as a dichromatic (black & white) group in which the operations of the left coset $j_{ij}F_{ij}$ comprise all "colour-changing" operations that transpose domain states $\mathbf{S_i}$ and $\mathbf{S_j}$

Symmetry group J_{ij} allows one to classify domain pairs. Thus, e.g., a domain pair $\{\mathbf{S_i},\mathbf{S_j}\}$ for which

$$\mathrm{Fam}(J_{ij}) = \mathrm{Fam}(F_{ij}) , \qquad (2)$$

where Fam means crystal family of the group given in the parenthesis, is non-ferroelastic, i.e. the domain states $\mathbf{S_i}$ and $\mathbf{S_j}$ have the same spontaneous deformation (for other examples of the classication see /P3/).

If, especially, the symmetry groups F_i and F_j of both domain states are equal, $F_i = F_j = F_{ij}$, (we call in /P11/ such a domain pair *totally transposable domain pair*) the group J_{ij} expresses in a convenient way the relation between two domain states (*'twin law"* of the pair) which determines the distinction of two domain states $\mathbf{S_i}$ and $\mathbf{S_j}$.

In /P10/ we have shown that within continuum description *all* non-ferroelastic domain pairs fulfilling the condition (2) are in a non-ferroelastic phase totally transposable and their symmetry has the simple form

$$J_{ij} = F + j_{ij}F_{ij} , \qquad (3)$$

where F is the symmetry of the distorted non-ferroelastic phase. .From the condition (2) we have found all non-ferroelastic twin laws (3). For each twin law we have determined the irreducible representation according to which transform the tensor components that are different in two domain states of the pair. From them it is easy to find, for particular material tensors, number of components that are distinct (have opposite signs in a properly chosen coordinate system) in two domain states under consideration. Table II in /P10/ displays these results for all non-ferroelastic twin laws and for important material tensors. These results are useful,e.g. for determining which material property can be used for visualization of non-ferroelastic domains which are not directly visible in a polarized light.

Similar procedure has been applied in /P11/ to totally transposable ferroelastic domain pairs which form only part of possible ferroelastic

domain pairs. Here, moreover, the effect of disorientations of ferroelastic domain states has been discussed.

Original contribution: The concept of domain pairs and their classification /P1,P2,P3/. Description of their symmetry by dichromatic groups (/P3,P10,P11/). Enumeration of all symmetries (twin laws) of non-ferroelastic domain pairs, determination of tensor distinction of domains in non-ferroelastic phases /P10/ and in totally transposable ferroelastic domain pairs /P11/.

1.4. Domain twins and domain walls

Each domain structure can be resolved into simple twins consisting of two domains that meet along a domain wall. We consider an infinite *domain twin* consisting of two domains that are joined along a planar coherent *domain wall*. Such a domain twin (and the wall as well) is defined by the orientation and position of the central plane of the domain wall and by the domain states $\mathbf{S_i}$ and $\mathbf{S_j}$ on the negative and positive side of the normal to the domain wall (for details see /P6/ part V). The symmetry of this twin (and also of the wall) is described by a layer group $\boldsymbol{T_{ij}}$ (this is a subperiodic subgroup of a space group which specifies symmetries of 3-dimensional objects with 2-dimensional periodicity). The layer group T_{ij} can be derived from the symmetry $\boldsymbol{J_{ij}}$ of the corresponding domain pair $\{\mathbf{S_i},\mathbf{S_j}\}$ (see Eq (2) and (3) in /P3/ and (5.4) and (5.5) in /P6/). According to the form of the group $\boldsymbol{T_{ij}}$ the twin and the wall can be classified and partitioned into c.e. classes.

The displacements of atoms (or ordering of molecules) within the wall are controlled by site symmetries at corresponding Wyckoff positions. These site symmetries can be deduced from the layer group $\boldsymbol{T_{ij}}$ that describes the symmetry of the wall. The symmetry of the wall restricts in this way possible structural changes within the wall. In crystals with higher symmetry this constrains determine the topology of the local displacements or ordering, i.e. those characteristics of the structural changes that are independent on numerical values, like the thickness of the wall, magnitudes of displacements,etc.

This approach has been successfully tested on two concrete examples: on the order-disorder domain walls of zero thickness in KSCN /P6/ and on displacive walls of finite thickness in Hg_2Cl_2 /P9/. The results illustrate the dependences of the wall structure on the orientation and position of the wall.

From the layer symmetry of the wall one can also deduce tensorial properties of the wall. Due to the structural gradients within walls the wall symmetry is in most cases lower than that of the domain bulk. As a result the wall exhibits new tensorial properties which are not present in the domain bulk. Thus, e.g., spontaneous polarization appears in domain walls in non-polar phases of quartz /P7/ and of calomel /P9/.

Original contribution: Symmetry description of domain twins and domain walls by layer groups. An algorithm for finding these symmetries from the symmetries of domain pairs /P2,P3/. Conclusions that can be deduced from these symmetries concerning the structure and physical properties of domain walls. Illustration on concrete examples /P6,P7,P9/.

1.5. Perfect domain textures

In /P4/ we have put forward an alternative continuum description of incommensurate phases close to the phase transition to commensurate phase. It consists in replacing the discommensurations by a mesoscopic regular pattern formed by c.e. domain walls with negative energy. This description, which we call a *domain texture approximation of the incommensurate phase,* allows one to visualize and treat complicated situations (which have been observed by electron microscopy) like non-homogeneous modulated structures with several q-vectors of modulation consisting of "incommensurate domains" (textural blocks) (see /P7/), planar and linear defects of the modulation /2/, transitions between incommensurate phases, etc.

This approach also enables one to determine the macroscopic symmetry of incommensurate phases which cannot be found in an usual way via the factor group since the translation group of the incommensurate phase is not defined. A particular prediction obtained from domain texture approximation, namely that the triangular texture in quartz has polar

macroscopic symmetry 6 and that the textural blocks behave like ferroelectric domains (see p. 125 in /P7/), has been recently confirmed experimentally /3/.

Original contribution: The concept of a perfect domain texture. Application of perfect domain textures for approximate description of incommensurate phases. Determination of the macroscopic (averaged) symmetry of the incommensurate phases from the mesoscopic symmetry of the domain texture. The concepts of textural blocks and their basic symmetry properities. Application of the results on concrete incommensurate structures, especially those observed in quartz (see /P4/ and P7/).

1.6. Concluding remarks.

1. All conclusions that follow from the symmetry analysis of domain structures are exact but some of its predictions are only qualitative in nature (e.g. in the tensor distinction of domains the analysis determines which components of a material tensor are the same and which have opposite sign in two non-ferroelastic domains but cannot offer any information about their numerical values).

2. The only input information are the symmetry groups of the parent and distorted phases. In some microscopic considerations (e.g. microscopic structure of domain walls) they are to be supplemented with the Wyckoff positions of atoms in the parent structure. Symmetry analysis always represents an efficient and useful first step in deciphering any real domain structure.

3. The results of the papers /P1/ - /P11/ have been utilized by other researches (e.g., the Science Citation Index gives several tens of quotations in the last 3 years of these publications, in the book /4/ a considerable part of the chapter about domains is taken from /P1/ and /P2/), book /5/ talks in connection with symmetry analysis about "Prague school", etc.).

1.7. References to Part 1

/1/ V. Janovec, E. Dvořáková, Subgroups of crystallographic point groups: Conjugation, normalizers, left and double coset decompositions, Report V-FzU 75/1, Institute of Physics, Prague (1974).

/2/ P. Saint-Grégoire, V. Janovec, Analysis of linear defects in triply incommensurate phase of quart-type, Ferroelectrics 97, 299 (1989).

/3/ E. Snoeck, P. Saint-Grégoire, V. Janovec, C. Roucau, TEM study of the 3-q modulated phase of quartz-type under electric field, Ferroelectrics (1994), to appear.

/4/ Yu. A. Izyumov, V. N. Syromyatnikov, Phase transitions and crystal symmetry, Kluwer Academic Publishers, Dordrecht (1990).

/5/ E.K.H. Salje, Phase transitions in ferroelastic and co-elastic crystals, Cambridge University Press, Cambridge (1990).

2.1. List of selected publications

GROUP ANALYSIS OF DOMAINS AND DOMAIN PAIRS

V. JANOVEC

*Institute of Physics, Czechosl. Acad. Sci., Prague**)

Basic symmetry properties of transformation twins and of ferroelectric or ferromagnetic domains are examined in terms of the abstract group theory. It is shown that the crystallographical relations between domains (twin components) and between domain pairs can be deduced from the decomposition of the symmetry group of the high symmetry phase into the left and double cosets of the group of the low symmetry phase. Expressions are derived for the numbers of proper and improper domains, for the number of crystallographically equivalent low symmetry phases, and for the number of crystallographically non-equivalent domain pairs. A classification of domain pairs according to their symmetry is proposed. The domain structure of the monoclinic phase in WO_3 and the Dauphiné twinning in quartz are analysed as illustrative examples.

1. INTRODUCTION

Phase transitions accompanied by a symmetry reduction exhibit, besides other similarities, the following common feature: The homogeneous high symmetry phase splits at a phase transition into a heterogeneous aggregate consisting of homogeneous regions of lower symmetry which are in well-defined spatial relations. These regions are called *domains* (especially in ferroelectric and ferromagnetic materials) or *twin components* (e.g., in martensitic transformations or in quartz) and the entire phenomenon may be called the *domain structure formation* or *transformation twinning*. A symmetry operation which brings a domain (twin component) into coincidence with another domain (twin component) is called the *twinning operation* and the plane along which domains or twin components meet a *domain wall* or a *composition plane.*[1])

Ferroelectric crystals provide a suitable material for the domain structure investigation since ferroelectric domains can be represented by a polar vector of spontaneous polarization and can be visualized optically or by etching. The fundamental principles of the crystallographical approach to ferroelectric domain structures were formulated by Zheludev and Shuvalov [1, 2, 3]. Important contributions were also given by Aizu [4, 5] and by Ascher [6, 7]. The basic symmetry relations of twinning are clearly summarized by Indenbom [8]. Many ideas of these works can be generalized and provide starting points of our consideration.

In this paper we are aiming at a general approach to main crystallographical features of transformation twinning. Instead of investigating domains themselves we examine their transformation laws which are concealed in the algebraic structure of

---

*) *Na Slovance 2, Praha 8, Czechoslovakia.*

[1]) We shall use both kinds of terms interchangeably, i.e. expressions like domain, domain structure will not be restricted to ferroelectric or ferromagnetic materials.

the symmetry groups of high and low symmetry phases. Such formulation does not rely on geometric imagination and can be applied to any phase transition connected with a symmetry reduction.

In Section 2 the relation between the symmetry change at the transition and possible characterization of domains is discussed. The notion of crystallographical equivalence of objects is introduced in Section 3 where, further, the connection between the symmetry reduction and the number of domains is elucidated. In Section 4 we demonstrate that, generally, several crystallographically equivalent low symmetry phases can appear at the transition and we find domains compatible with one low symmetry phase. In next two Sections the symmetry relations between domains and domain pairs[2]) are analysed. In section 5 we examine twinning operations which transform the first domain into the second domain of an ordered pair and we put forward a classification of ordered domain pairs. In Section 6 we divide all pairs into classes of crystallographically equivalent pairs and find representatives of all these classes. In this way a complete set of non-equivalent pairs can be constructed which enables an efficient analysis of the twinning structure of the low symmetry phase. For convenience, the main results of Sections 3 through 5 are summarized in Theorems. Section 7 illustrates possible use of general results. First, the domain structure of the monoclinic phase of tungsten trioxide is analysed. Further, it is shown that some conclusions take a simpler form if the group of the low symmetry phase is an invariant subgroup of the group of the high symmetry phase. As an example, the Dauphiné twinning in quartz is discussed. For simplicity, examples are treated within non-magnetic point groups though the exposition and Theorems are formulated in a general way and can be used also for space groups and magnetic groups.

No attention is paid to the conditions of real coexistence of domains. A continuum theory of coherent stress-free domain walls is discussed elsewhere [9].

2. SYMMETRY CHANGES AT PARAMETRIC PHASE TRANSITIONS

At a structural phase transition one phase changes into another phase and the former differs from the latter in symmetry. In many cases one phase has specific properties which do not exist in the other phase. Thus we speak about a ferroelectric (ferromagnetic, ferroelastic) transition if an electric polarization (magnetization, mechanical strain) forms in one phase but does not exist in the other phase. Generally, we shall call *parametric* such a *phase transition* the symmetry change of which can be described as a consequence of specific geometrical or physical properties which appear in one phase only. Any property (set of properties) the appearance of which accounts fully for the symmetry change at the transition will be referred to as a *transition*

[2]) We reserve the term "twin" for an edifice in which two domains coexist along a domain wall of given orientation. The expression "domain pair" should imply that no attention is paid to the question of a real coexistence of domains.

parameter. Those properties which manifest themselves at the transition but cannot explain the symmetry change will be called *partial* or *improper*[3]) *parameters*.

Transition parameters and improper parameters, or appropriate quantities which describe them, will be denoted by $\boldsymbol{P}$ and $\boldsymbol{I}$, respectively. Superscripts (i), (j) etc. will specify the spatial relations of the parameters to the phase with $\boldsymbol{P} = 0$. Thus $\boldsymbol{P}^{(i)}$ denotes a transition parameter of a given spatial orientation with respect to the phase in which $\boldsymbol{P} = 0$ (e.g., for proper ferroelectrics $\boldsymbol{P}^{(i)}$ signifies the vector of spontaneous polarization of a fixed orientation relative to the paraelectric phase).

Let us denote by G and $F^{(i)}$ the symmetry group with $\boldsymbol{P} = 0$ and $\boldsymbol{P}^{(i)}$, respectively. From the definition of the transition parameter it follows that[4])

(2.1) $$F^{(i)} = \text{maximal subgroup of } G \text{ which leaves } \boldsymbol{P}^{(i)} \text{ invariant} .$$

Obviously, $F^{(i)}$ is a proper subgroup of G,

(2.2) $$F^{(i)} \subset G .$$

Thus, *at a parametric phase transition symmetry always lowers*. The phase with zero transition parameter can be called a *high symmetry phase* whereas the phase with non-zero transition parameter a *low symmetry phase*.[5])

The relation between G, $F^{(i)}$ and $\boldsymbol{P}^{(i)}$ can be, formally, expressed in a more compact way. By applying a symmetry operation g from G on the parameter $\boldsymbol{P}^{(i)}$ we get, generally, a parameter $\boldsymbol{P}^{(j)}$ with different spatial orientation (j),[6])

(2.3) $$g\boldsymbol{P}^{(i)} = \boldsymbol{P}^{(j)}, \quad g \in G .$$

Some operations $f \in G$ may, however, leave $\boldsymbol{P}^{(i)}$ unchanged,

(2.4) $$f\boldsymbol{P}^{(i)} = \boldsymbol{P}^{(i)}, \quad f \in G .$$

From (2.1) it follows that (2.4) holds for all elements of $F^{(i)}$, and only for elements of G belonging to $F^{(i)}$. In algebra, the set of all elements obeying (2.4) is called the

---

[3]) The former term has been introduced by Aizu [4, 5], the latter one is coined recently by Dvořák [10]. For transitions of the second order the transition parameter is equivalent to Landau order parameter [11].

[4]) Similar formulation was put forward by Ascher [12].

[5]) Alternative expressions like prototype [4, 5], initial phase [2], high form [13] and ferroic phase [4, 5], low form [13] are also used for high symmetry and low symmetry phases, respectively. A critical review of the nomenclature is given in [14].

[6]) In algebra, the operation of a group G on a set $\mathcal{P}$ is a mapping $G \times \mathcal{P} \to \mathcal{P}$ such that

$$(g_1 g_2)\,\boldsymbol{P}^{(i)} = g_1(g_2 \boldsymbol{P}^{(i)}), \quad \text{and} \quad e\boldsymbol{P}^{(i)} = \boldsymbol{P}^{(i)},$$

for all elements $g_1, g_2 \in G$ and $\boldsymbol{P}^{(i)} \in \mathcal{P}$ (e is the identity element of G) [15]. These requirements are met in our case so that *the relation* (2.3) *can be treated as an operation of the group G on the set* $\mathcal{P}$ *of all conceivable parameters*. The concrete form of the "mapping" (2.3) is given by the transformation laws of the parameter (e.g., for tensorial parameters by the transformation laws for tensors). Fortunately, the explicit form of (2.3) is not needed in our consideration.

isotropy group of $\mathbf{P}^{(i)}$ *in* G (or the *stabilizer of* $\mathbf{P}^{(i)}$ *in* G) and is denoted by $G_{\mathbf{P}^{(i)}}$ [15]. Thus

$$F^{(i)} = G_{\mathbf{P}^{(i)}}\,; \tag{2.5}$$

the group $F^{(i)}$ *of the low symmetry phase equals the isotropy group* $G_{\mathbf{P}^{(i)}}$ *of the transition parameter* $\mathbf{P}^{(i)}$ *in the group* G *of the high symmetry phase.*[7])

Finally, we mention a useful extension of the notion of parametric transitions. Let a phase α (symmetry group ${}^{(\alpha)}F$) change in a phase β (symmetry ${}^{(\beta)}F$), where neither ${}^{(\alpha)}F \subset {}^{(\beta)}F$ nor ${}^{(\beta)}F \subset F^{(\alpha)}$. Obviously, no transition parameter can be found in this case. If, nevertheless, a symmetry group G exists (at least theoretically) such that

$${}^{(\alpha)}F \subset G \quad \text{and} \quad {}^{(\beta)}F \subset G \tag{2.6}$$

then the phases α and α can be treated as two different modifications of a common "mother phase" of symmetry G, and the transition $\alpha \to \beta$ as the change from the state with α more stable than β to the state with β more stable than α.[8]) (Clearly, such transition must be of the first order.) All our further considerations apply also for such *extended parametric transitions*; we just have to treat separately each of the phases α and β as being formed from a common high symmetry mother phase in ordinary parametric transitions $G \to {}^{(\alpha)}F$ and $G \to {}^{(\beta)}F$, respectively.

3. CRYSTALLOGRAPHICALLY EQUIVALENT PARAMETERS: PROPER AND IMPROPER DOMAINS

In this Section we show that a symmetry reduction at a parametric transition provides conditions for domain structure formation. Let us start with the following definition:

Parameters $\mathbf{P}^{(i)}$, $\mathbf{P}^{(j)}$ are said to be *crystallographically equivalent with respect to the group* G if an element $g \in G$ exists such that

$$\mathbf{P}^{(j)} = g\mathbf{P}^{(i)}\,, \quad g \in G\,. \tag{3.1}$$

Symbolically we write $\mathbf{P}^{(j)} \overset{G}{\sim} \mathbf{P}^{(i)}$.

Utilizing the group properties of G one can easily demonstrate that the relation $\overset{G}{\sim}$ satisfies three requirements of the equivalence relation [19],

$$\mathbf{P}^{(i)} \overset{G}{\sim} \mathbf{P}^{(i)} \quad \text{(reflexivity)}\,, \tag{3.2}$$

$$\text{if } \mathbf{P}^{(j)} \overset{G}{\sim} \mathbf{P}^{(i)} \text{ then } \mathbf{P}^{(i)} \overset{G}{\sim} \mathbf{P}^{(j)} \quad \text{(symmetry)}\,, \tag{3.3}$$

$$\text{if } \mathbf{P}^{(i)} \overset{G}{\sim} \mathbf{P}^{(j)} \text{ and } \mathbf{P}^{(j)} \overset{G}{\sim} \mathbf{P}^{(k)} \text{ then } \mathbf{P}^{(i)} \overset{G}{\sim} \mathbf{P}^{(k)} \quad \text{(transitivity)}\,. \tag{3.4}$$

---

[7]) Relations between G, $F^{(i)}$ and $\mathbf{P}^{(i)}$ can also be given in terms of the representation theory [11, 16]. These formulations provide useful tools for finding the transformation properties of the transition parameter $\mathbf{P}^{(i)}$ for a given symmetry change $G \to F^{(i)}$.

[8]) Similar approach has been applied in the thermodynamical treatment of the polymorphism of $BaTiO_3$ [17], and, recently, of the Rochelle salt [18].

The relation can, therefore, be used to divide the set $\mathscr{P}$ of all conceivable parameters into disjoint *classes of parameters crystallographically equivalent with respect to G*. Symbol $G\mathbf{P}^{(i)}$ will denote such a class where $\mathbf{P}^{(i)}$ is the representative of this class. Obviously, the representative $\mathbf{P}^{(i)}$ can generate the entire class if it is exposed to all transformations $g \in G$. From group properties of G it follows that any element of the class $G\mathbf{P}^{(i)}$ may be taken as the representative. In algebra, the set $G\mathbf{P}^{(i)}$ is called the *orbit of* $\mathbf{P}^{(i)}$ *under* G [15].

The physical significance of the crystallographical equivalence with respect to a group G is evident: If a parameter $\mathbf{P}^{(i)}$ forms at a transition from G to $F^{(i)}$ then any other parameter $\mathbf{P}^{(j)}$ crystallographically equivalent[9]) to $\mathbf{P}^{(i)}$ may appear with the same probability. Thus the parameters of the class $G\mathbf{P}^{(i)}$ represent all possible *proper domains* of the low symmetry phase. For brevity, we shall call parameters of the class $G\mathbf{P}^{(i)}$ *domains (twin components)*[10]).

We decompose now the group G into subsets so that each element of a subset transforms the domain $\mathbf{P}^{(i)}$ into one domain from $G\mathbf{P}^{(i)}$. The number of subsets will give us the number of domains in $G\mathbf{P}^{(i)}$. Moreover, if we choose one element of each subset as its representative, the entire class $G\mathbf{P}^{(i)}$ can be effectively formed by applying representatives of all subsets to $\mathbf{P}^{(i)}$.[11])

First, let us notice that each element of a left coset[12]) $t_{ij}F^{(i)}$ transforms the domain $\mathbf{P}^{(i)}$ into the domain $\mathbf{P}^{(j)} = t_{ij}\mathbf{P}^{(i)}$:

$$t_{ij}F^{(i)}\mathbf{P}^{(i)} = t_{ij}\mathbf{P}^{(i)} = \mathbf{P}^{(j)} . \tag{3.5}$$

Conversely, if an element $g \in G$ transforms $\mathbf{P}^{(i)}$ into $\mathbf{P}^{(j)}$ then g belongs to the left coset $t_{ij}F^{(i)}$: $g\mathbf{P}^{(i)} = \mathbf{P}^{(j)} = t_{ij}\mathbf{P}^{(i)}$, therefore $t_{ij}^{-1}g\mathbf{P}^{(i)} = \mathbf{P}^{(i)}$, hence $t_{ij}^{-1}g \in F^{(i)}$, i.e. $g \in t_{ij}F^{(i)}$. Thus, all elements transforming $\mathbf{P}^{(i)}$ into $\mathbf{P}^{(j)}$ are contained in the left coset $t_{ij}F^{(i)}$, and two different cosets of $F^{(i)}$ generate from $\mathbf{P}^{(i)}$ two different domains. Further, in algebra it is proved that a group G can be expressed as a set-theoretic sum of disjoint left cosets of the subgroup $F^{(i)}$,

$$G = eF^{(i)} + t_{i2}F^{(i)} + \ldots + t_{iq}F^{(i)} \tag{3.6}$$

where e is the identity element. The (cardinal) number q of distinct left cosets in the resolution (3.6) is called the *index of* $F^{(i)}$ *in* G and denoted by $[G : F^{(i)}]$. For finite

---

[9]) Unless stated otherwise, the expression "crystallographically equivalent" will indicate the equivalence with respect to the group G of the high symmetry phase.

[10]) Other expressions have also been proposed, e.g., orientation states [4, 5] or modification multiplets [13].

[11]) The expression for the number of domains was given by Zheludev and Shuvalov [1] for ferroelectric transitions, and recently derived by Aizu [5]. We, nevertheless, sketch the proof here since we shall use a similar reasoning in the next Section.

[12]) The *left coset* $t_{ij}F^{(i)}$ consists of products $t_{ij}f$ where t_{ij} is a fixed element of G and f runs over all elements of $F^{(i)}$. The element t_{ij} is called the *representative of the coset*. It can be proved that any element of a coset may be taken as the representative, $tF^{(i)} = t_{ij}F^{(i)}$ for any $t \in t_{ij}F^{(i)}$ [19–21].

group G, $[G : F^{(i)}] = n_G : n_F$, where n_G and n_F are the orders of G and $F^{(i)}$, respectively [20]. Applying successively all left cosets of (3.6) to the domain $\mathbf{P}^{(i)}$ we get all domains of the class $G\mathbf{P}^{(i)}$:

$$G\mathbf{P}^{(i)} = eF^{(i)}\mathbf{P}^{(i)} + t_{i2}F^{(i)}\mathbf{P}^{(i)} + \ldots + t_{iq}F^{(i)}\mathbf{P}^{(i)} = \\ = \mathbf{P}^{(i)} + t_{i2}\mathbf{P}^{(i)} + \ldots + t_{iq}\mathbf{P}^{(i)}. \tag{3.7}$$

The equation (3.7) defines a *one-to-one correspondence between the domains* $G\mathbf{P}^{(i)}$ *and the set of left cosets of* $F^{(i)}$ *in* G. From this relation we deduce the following

Theorem I. The number q of distinct domains which can form at a parametric transition from G to $F^{(i)}$ equals the number of the left cosets in the resolution

$$G = F^{(i)} + t_{i2}F^{(i)} + \ldots + t_{iq}F^{(i)}, \tag{3.8}$$

i.e., q equals the index of $F^{(i)}$ in G,

$$q = [G : F^{(i)}]. \tag{3.9}$$

For finite group G,

$$q = n_G : n_F \tag{3.10}$$

where n_G and n_F are orders of G and $F^{(i)}$, respectively.

There exist n_F elements of G which transform the domain $\mathbf{P}^{(i)}$ into the domain $\mathbf{P}^{(j)}$ $(j = 1, \ldots, q)$. These elements are comprised in the left coset $t_{ij}F^{(i)}$ of the resolution (3.8). All q domains can be found by applying to $\mathbf{P}^{(i)}$ representatives of all distinct left cosets of the resolution (3.8).

Any parametric transition is accompanied by reduction of symmetry; hence, according to (3.9) or (3.10), there is always $q > 1$. Thus *at any parametric phase transition the splitting of the low symmetry phase into domains may occur.*

Let us note that any element $g \in G$ transforms a domain from $G\mathbf{P}^{(i)}$ in another domain of the same class. The application of g on $G\mathbf{P}^{(i)}$ results, therefore, in a permutation of elements in $G\mathbf{P}^{(i)}$, i.e. the *class is invariant under* G. This means that a poly-domain aggregate in which all domains of $G\mathbf{P}^{(i)}$ appear with the same probability has, in average, the symmetry G of the high symmetry phase[13]). This statement can be utilized for constructing the group G of the high symmetry phase (which is sometimes unaccessible or unknown) from the domain structure of the low symmetry phase.

So far we have considered proper domains only. Sometimes, however, it is difficult to detect the transition parameter though improper parameters can be observed. Then the notion of improper domains is useful. Under an *improper domain* we understand

[13]) Zheludev and Shuvalov [1] and also Ascher [7] reached the same conclusion for ferroelectric transitions. Ascher, moreover, pointed out the connection with the Goldstone theory of broken symmetries.

the state of the low symmetry phase described by an improper parameter $\boldsymbol{l}^{(i)}$. The class of crystallographically equivalent improper parameters, i.e. $G\boldsymbol{l}^{(i)}$, will represent possible improper domains of the low symmetry phase.

All results of the Section can be applied to improper domains if we substitute the isotropy group $G_{\boldsymbol{l}^{(i)}}$ for $F^{(i)}$. Thus, for example, the decomposition of the class $G\boldsymbol{l}^{(i)}$ reads (cf. Eq. (3.7)):

$$G\boldsymbol{l}^{(i)} = eG_{\boldsymbol{l}^{(i)}}\boldsymbol{l}^{(i)} + g_{i2}G_{\boldsymbol{l}^{(i)}}\boldsymbol{l}^{(i)} + \ldots + \tag{3.11}$$

$$+ g_{iq_l}G_{\boldsymbol{l}^{(i)}}\boldsymbol{l}^{(i)} = \boldsymbol{l}^{(i)} + g_{i2}\boldsymbol{l}^{(i)} + \ldots + g_{iq_l}\boldsymbol{l}^{(i)} ,$$

and the number q_l of improper domains is

$$q_l = \left[G : G_{\boldsymbol{l}^{(i)}}\right] . \tag{3.12}$$

The isotropy group $G_{\boldsymbol{l}^{(i)}}$ is a proper supergroup of $F^{(i)}$, $F^{(i)} \subset G_{\boldsymbol{l}^{(i)}} \subseteq G$, hence *the number q_l of improper domains is always less than the number q of proper domains,*

$$q_l < q . \tag{3.13}$$

On the other hand, the equality

$$q_l = q \tag{3.14}$$

holds if, and only if,

$$G_{\boldsymbol{l}^{(i)}} = F^{(i)} . \tag{3.15}$$

Then $\boldsymbol{l}^{(i)}$ should be treated as a "symmetrically proper" transition parameter.

Another consequence follows from (3.12). If one can observe a property described by the parameter $\boldsymbol{l}^{(i)}$ then a necessary condition for the detection of the domain structure is

$$G_{\boldsymbol{l}^{(i)}} \subset G . \tag{3.16}$$

If, on the other hand,

$$G_{\boldsymbol{l}^{(i)}} = G \tag{3.17}$$

domains are masked and cannot be detected by this method.

4. CRYSTALLOGRAPHICALLY EQUIVALENT LOW SYMMETRY PHASES AND THEIR DEGENERACY

We have shown that at the parametric phase transition domains from the class $G\boldsymbol{P}^{(i)}$ may appear. To every domain $\boldsymbol{P}^{(j)}$ from $G\boldsymbol{P}^{(i)}$ corresponds an isotropy group $G_{\boldsymbol{P}^{(j)}} = F^{(j)}$ which describes the associated low symmetry phase. For deducing all these low symmetry phases we utilize the following statement [5, 8]:

If $t_{ij} \in G$ transforms $\boldsymbol{P}^{(i)}$ into $\boldsymbol{P}^{(j)}$,

$$\boldsymbol{P}^{(j)} = t_{ij}\boldsymbol{P}^{(i)}, \quad t_{ij} \in G, \tag{4.1}$$

then corresponding groups of low symmetry phases are conjugate under the element t_{ij}^{-1},

$$F^{(j)} = t_{ij}F^{(i)}t_{ij}^{-1}, \quad t_{ij} \in G. \tag{4.2}$$

(We adopt the definition of conjugate subgroups given in [19–21]).

We shall call two *groups* $F^{(j)}$ and $F^{(i)}$ *crystallographically equivalent with respect to* G if an element $t_{ij} \in G$ exists such that (4.2) is fulfilled. The relation of crystallographical equivalence can, again, be used for dividing the set of all subgroups of G into disjoint *classes of crystallographically equivalent subgroups.* We shall denote such a class by $GF^{(i)}$. Obviously, the class $GF^{(i)}$ can be generated by exposing the representative $F^{(i)}$ to all transformations (4.2), and any element of $GF^{(i)}$ can be chosen as the representative[14]). Clearly, all isotropy groups corresponding to all domains of $G\boldsymbol{P}^{(i)}$ form the class $GF^{(i)}$. Since all conjugate subgroups have the same order we see that Eq. (3.9) yields the same number q of domains for any group of the class $G\boldsymbol{P}^{(i)}$.

We shall call the number m of crystallographically equivalent subgroups in $GF^{(i)}$ the *multiplicity of* $F^{(i)}$ *in* G [7]. To find this number we have to realize that all elements of G which do not change $F^{(i)}$ constitute a subgroup of G called the *normalizer of* $F^{(i)}$ *in* G [19–21]. We shall denote this normalizer by $G_{F(i)}$ since it is equivalent of the isotropy group of $F^{(i)}$ in G. Now using the same reasoning as in the proof of the *Theorem I*, but replacing the parameter $\boldsymbol{P}^{(i)}$ by $F^{(i)}$, Eq. (3.1) by (4.2) and $F^{(i)}$ by $G_{F(i)}$, we arrive at the following

Theorem II. The number m of crystallographically equivalent low symmetry phases equals the number of left cosets in the resolution

$$G = G_{F(i)} + h_{i2}G_{F(i)} + \ldots + h_{im}G_{F(i)}, \tag{4.3}$$

that is

$$m = [G : G_{F(i)}] \tag{4.4}$$

where $G_{F(i)}$ is the normalizer of $F^{(i)}$ in G. For finite G,

$$m = n_G : n_{G_F} \tag{4.5}$$

where n_{G_F} is the order of $G_{F(i)}$.

There exist n_{G_F} elements in G which transform the group $F^{(i)}$ into a crystallographically equivalent group $F^{(j)}$. The inverses of these elements constitute the left coset $h_{ij}G_{F(i)}$ of the resolution (4.3). All m crystallographically equivalent low symmetry groups can be found as conjugates of $F^{(i)}$ where the transforming elements are inverses of the representatives of all distinct left cosets of the resolution (4.3).

[14]) We can say that, according to (4.2), the group G operates on the set of its subgroups by "inverse" conjugation. Then $GF^{(i)}$ can, again, be interpreted as an orbit of $F^{(i)}$ in G.

Let us now turn to the fact that, generally, several distinct domains from the class $GP^{(i)}$ may possess one common isotropy group. We shall call the number d of domains from $GP^{(i)}$ with the same isotropy group the *degeneracy of the low symmetry phase.*

Theorem III. The number d of domains with the same group $F^{(i)}$ of the low symmetry phase equals the number of left cosets in the resolution

$$G_{F(i)} = F^{(i)} + l_{i2}F^{(i)} + \ldots + l_{id}F^{(i)} \tag{4.6}$$

i.e., d equals the index of $F^{(i)}$ in $G_{F(i)}$,

$$d = \left[G_{F(i)} : F^{(i)}\right]. \tag{4.7}$$

For finite $G_{F(i)}$,

$$d = n_{G_F} : n_F . \tag{4.8}$$

All domains with the same isotropy group $F^{(i)}$ can be found by experiencing on $P^{(i)}$ successively representatives of all distinct left cosets of the resolution (4.6).

The number of domains q, the multiplicity m and the degeneracy d are related by the equation

$$q = md . \tag{4.9}$$

The proof of the first part of the *Theorem* can be performed in the same way as that of *Theorem I.* Instead of G we consider only those elements of G which do not change $F^{(i)}$, i.e. the group $G_{F(i)}$. Eq. (4.9) follows from Eqs. (3.9), (4.4), (4.7) and from the theorem on index multiplication (for $F^{(i)} \subseteq G_{F(i)} \subseteq G$ it holds $\left[G : F^{(i)}\right] = \left[G : G_{F(i)}\right] . \left[G_{F(i)} : F^{(i)}\right]$ [20]).

We can infer from *Theorem III* that the low symmetry phase is non-degenerate ($d = 1$) if, and only if,

$$F^{(i)} = G_{F(i)} . \tag{4.10}$$

Then to each low symmetry phase from the class $GF^{(i)}$ there corresponds just one domain in the class $GP^{(i)}$, and vice versa. In this case, domains can be faithfully represented by associated groups of the low symmetry phases.

Comparing (3.8) and (4.6) we see that the normalizer $G_{F(i)}$ is identical with the union of d left cosets of (3.8) associated with d domains compatible with $F^{(i)}$.

We turn now to improper domains. Substituting $G_{I(i)}$ for $G_{F(i)}$ in *Theorem III* we get the number d_I of proper domains which are compatible with the improper domain $I^{(i)}$ (i.e., the *degeneracy of the improper domain* $I^{(i)}$):

$$d_I = \left[G_{I(i)} : F^{(i)}\right]. \tag{4.11}$$

The degeneracy d_I and the total number q_I of improper domains are related by the equation

$$q = d_I q_I . \tag{4.12}$$

We may note the striking similarity of *Theorems I–III*. In fact, these *Theorems* are just various "crystallographical versions" of the following algebraic statement: Let G be a group which operates on a set $\mathscr{S}$ (see footnote [6]). Then the orbit $G\boldsymbol{s}$ can be mapped onto the set of all left cosets of the isotropy group $G_{\boldsymbol{s}}$ ($\boldsymbol{s} \in \mathscr{S}$) in G [15]. This mapping follows from the decomposition

$$G\boldsymbol{s} = (eG_{\boldsymbol{s}})\,\boldsymbol{s} + (g_2 G_{\boldsymbol{s}})\,\boldsymbol{s} + \ldots + (g_q G_{\boldsymbol{s}})\,\boldsymbol{s} = \tag{4.13}$$

$$= \boldsymbol{s} + g_2\boldsymbol{s} + \ldots + g_q\boldsymbol{s} = \boldsymbol{s}_1 + \boldsymbol{s}_2 + \ldots + \boldsymbol{s}_q$$

which relates the elements of $G\boldsymbol{s}$, $\boldsymbol{s}_k = g_k\boldsymbol{s}$, with their "coset images" $g_k G_{\boldsymbol{s}}$ ($k = 1, 2, \ldots, q$). The order q of the orbit $G\boldsymbol{s}$ is

$$q = [G : G_{\boldsymbol{s}}]\,. \tag{4.14}$$

5. DOMAIN PAIRS AND THEIR CLASSIFICATION

The simplest object on which the mutual relations between domains can be studied is a pair of domains. First, we shall investigate an *ordered pair*, which consists of the first domain $\boldsymbol{P}^{(i)}$ and the second domain $\boldsymbol{P}^{(j)}$ of the same class $G\boldsymbol{P}^{(i)}$, and will be denoted by $(\boldsymbol{P}^{(i)}, \boldsymbol{P}^{(j)})$.[15]) For a given ordered pair there exists at least one element t_{ij} such that

$$\boldsymbol{P}^{(j)} = t_{ij}\boldsymbol{P}^{(i)}\,, \quad t_{ij} \in G\,. \tag{5.1}$$

Any element of G which transforms the first domain $\boldsymbol{P}^{(i)}$ into the second domain $\boldsymbol{P}^{(j)}$ will be referred to as a *twinning operation*[16]) *of the ordered pair* $(\boldsymbol{P}^{(i)}, \boldsymbol{P}^{(j)})$. The set of all twinning operations (5.1) will be called the *twinning complex of the ordered pair* $(\boldsymbol{P}^{(i)}, \boldsymbol{P}^{(j)})$ and will be denoted by T_{ij}. From the *Theorem I* it follows immediately that the twinning complex T_{ij} contains n_F twinning operations which constitute one left coset of $F^{(i)}$,

$$T_{ij} = t_{ij}F^{(i)}\,, \quad t_{ij} \in G\,, \tag{5.2}$$

where t_{ij} is any twinning operation of $(\boldsymbol{P}^{(i)}, \boldsymbol{P}^{(j)})$, and $F^{(i)}$ is the isotropy group of the first domain $\boldsymbol{P}^{(i)}$.

---

[15]) A twin (see footnote 2)) can be formed from an ordered pair $(\boldsymbol{P}^{(i)}, \boldsymbol{P}^{(j)})$ only if a coherent coexistence of domains $\boldsymbol{P}^{(i)}$ and $\boldsymbol{P}^{(j)}$ is possible. This condition may not be fulfilled for all ordered pairs [9].

[16]) F-operation in Aizu's terminology [4, 5]. We stress that the twinning operation of an ordered pair may not coincide with the twinning operation of the corresponding twin since, in some cases, a small additional rotation is needed to bring domains of an ordered pair into a mutual contact along a coherent stress-free domain wall [9]. Then the twinning operations of an ordered pair should be treated as *pseudo-twinning operations* of the corresponding twin.

The *isotropy group* $F^{(ij)}$ *of the ordered pair* $(\boldsymbol{P}^{(i)}, \boldsymbol{P}^{(j)})$ consists of elements common to the isotropy groups $F^{(i)}$ and $F^{(j)}$ of the first and second domains, respectively,

$$F^{(ij)} = F^{(i)} \cap F^{(j)} \tag{5.3}$$

where $\cap$ denotes the set-theoretic intersection.

Two *ordered pairs* $(\boldsymbol{P}^{(i)}, \boldsymbol{P}^{(j)})$ and $(\boldsymbol{P}^{(k)}, \boldsymbol{P}^{(l)})$ are said to be *crystallographically equivalent with respect to* G, $(\boldsymbol{P}^{(i)}, \boldsymbol{P}^{(j)}) \overset{G}{\sim} (\boldsymbol{P}^{(k)}, \boldsymbol{P}^{(l)})$, if an element $g \in G$ exists such that

$$(g\boldsymbol{P}^{(i)}, g\boldsymbol{P}^{(j)}) = (\boldsymbol{P}^{(k)}, \boldsymbol{P}^{(l)}), \quad g \in G. \tag{5.4}$$

The twinning complexes T_{kl}, T_{ij} *of crystallographically equivalent pairs* (5.4) *are conjugate under the inverse of the element* g *which relates the equivalent pairs,*

$$T_{kl} = gT_{ij}g^{-1}, \quad g \in G. \tag{5.5}$$

Proof: Let $t_{ij} \in T_{ij}$; then $\boldsymbol{P}^{(l)} = g\boldsymbol{P}^{(j)} = gt_{ij}\boldsymbol{P}^{(i)} = gt_{ij}g^{-1}\boldsymbol{P}^{(k)}$, hence $gt_{ij}g^{-1} \in T_{kl}$. On the other hand, any element $t_{kl} \in T_{kl}$ can be written in the form $t_{kl} = gt'_{ij}g^{-1}$ where $t'_{ij} \in T_{ij}$: $t_{kl} = g(g^{-1}t_{kl}g)\,g^{-1} = gt'_{ij}g^{-1}$; $t'_{ij}\boldsymbol{P}^{(i)} = g^{-1}t_{kl}g\boldsymbol{P}^{(i)} = g^{-1}t_{kl}\boldsymbol{P}^{(k)} = g^{-1}\boldsymbol{P}^{(l)} = \boldsymbol{P}^{(j)}$, hence $t'_{ij} \in T_{ij}$.

The isotropy groups $F^{(kl)}$, $F^{(ij)}$ *of the crystallographically equivalent pairs* (5.4) *are* also *conjugate under the inverse of* g,

$$F^{(kl)} = gF^{(ij)}g^{-1} \tag{5.6}$$

since from Eqs. (5.4), (4.1) and (4.2) it follows that $F^{(kl)} = (gF^{(i)}g^{-1}) \cap (gF^{(j)}g^{-1}) = g(F^{(i)} \cap F^{(j)})\,g^{-1} = gF^{(ij)}g^{-1}$.

The change of the order in an ordered pair will be called *transposition* and will be denoted by the superscript t:

$$(\boldsymbol{P}^{(i)}, \boldsymbol{P}^{(j)})^t = (\boldsymbol{P}^{(j)}, \boldsymbol{P}^{(i)}). \tag{5.7}$$

The twinning complex T_{ji} *of the transposed pair* $(\boldsymbol{P}^{(i)}, \boldsymbol{P}^{(j)})^t$ *equals the inverse of the twinning complex* T_{ij} *of the original ordered pair* $(\boldsymbol{P}^{(i)}, \boldsymbol{P}^{(j)})$,

$$T_{ji} = T_{ij}^{-1} = (t_{ij}F^{(i)})^{-1} = F^{(i)}t_{ij}^{-1}, \tag{5.8}$$

since all elements of T_{ij}^{-1} transform $\boldsymbol{P}^{(j)}$ into $\boldsymbol{P}^{(i)}$, $T_{ij}^{-1}\boldsymbol{P}^{(j)} = F^{(i)}t_{ij}^{-1}\boldsymbol{P}^{(j)} = F^{(i)}\boldsymbol{P}^{(i)} = \boldsymbol{P}^{(i)}$, and the set T_{ij}^{-1} contains n_F elements and thus forms, according to *Theorem I*, the entire twinning complex T_{ji}.

We turn now to the *classification of ordered pairs*. Often, single twinning operation (e.g., a mirror, the inversion) is used for labeling an ordered pair (a twin). We could hardly justify this in our approach, for all n_F twinning operations of T_{ij} have, crystallographically, equal rights to be chosen as representatives. Therefore, we put forward a simple distinction based on the comparison of the ordered pair with the associated transposed pair. An ordered pair crystallographically equivalent with the transposed

pair,

$$(\boldsymbol{P}^{(i)}, \boldsymbol{P}^{(j)})^t \overset{G}{\sim} (\boldsymbol{P}^{(i)}, \boldsymbol{P}^{(j)}), \tag{5.9}$$

will be referred to as an *ambivalent pair*. The pairs $(\boldsymbol{P}^{(i)}, \boldsymbol{P}^{(j)})^t$ and $(\boldsymbol{P}^{(i)}, \boldsymbol{P}^{(j)})$ which are not crystallographically equivalent will be called *complementary polar pairs*.

This classification can be restated in terms of the twinning complexes. According to (5.4) and (5.9) a necessary and sufficient condition for a pair $(\boldsymbol{P}^{(i)}, \boldsymbol{P}^{(j)})$ to be ambivalent is the existence of an element a_{ij} such that

$$a_{ij}\boldsymbol{P}^{(i)} = \boldsymbol{P}^{(j)} \quad \text{and} \quad a_{ij}\boldsymbol{P}^{(j)} = \boldsymbol{P}^{(i)}, \quad a_{ij} \in G. \tag{5.10}$$

The element a_{ij} must be a twinning operation of $(\boldsymbol{P}^{(i)}, \boldsymbol{P}^{(j)})$ and also a twinning operation of $(\boldsymbol{P}^{(i)}, \boldsymbol{P}^{(j)})^t$. Thus

$$a_{ij} \in T_{ij} \cap T_{ij}^{-1}. \tag{5.11}$$

Another equivalent condition follows from (5.10): $\boldsymbol{P}^{(i)} = a_{ij}\boldsymbol{P}^{(j)} = a_{ij}^2\boldsymbol{P}^{(i)}$, hence $a_{ij}^2 \in F^{(i)}$. Similarly, $\boldsymbol{P}^{(j)} = a_{ij}\boldsymbol{P}^{(i)} = a_{ij}^2\boldsymbol{P}^{(j)}$, hence $a_{ij}^2 \in F^{(j)}$. Therefore,

$$a_{ij}^2 \in F^{(i)} \cap F^{(j)} = F^{(ij)}, \quad a_{ij} \in T_{ij}. \tag{5.12}$$

Conversely, if (5.12) holds then $a_{ij}\boldsymbol{P}^{(j)} = a_{ij}a_{ij}\boldsymbol{P}^{(i)} = \boldsymbol{P}^{(i)}$, i.e. $a_{ij} \in T_{jl}$ and (5.11) is satisfied.

If, specifically, $T_{ij} = T_{ji} = T_{ij}^{-1}$, then $T_{ij} = a_{ij}F^{(i)} = T_{ij}^{-1} = F^{(i)}a_{ij}^{-1}$, and $a_{ij}F^{(i)} = a_{ij}^{-1}F^{(i)}$ for each $a_{ij} \in T_{ij}$. Therefore $a_{ij}F^{(i)} = F^{(i)}a_{ij}$ for all $a_{ij} \in T_{ij}$, so that $T_{ij} \subset G_{F^{(i)}}$ and, according to *Theorem III*, $F^{(i)} = F^{(j)} = F^{(ij)}$.

If no element a_{ij} fulfilling (5.10) (or any equivalent condition) exists then $(\boldsymbol{P}^{(i)}, \boldsymbol{P}^{(j)})$ is a polar pair, and vice versa. If, moreover, T_{ij}^{-1} forms an entire left coset disjoint with T_{ij}, i.e. if $T_{ij}^{-1} = t_{ik}F^{(i)}$, $k \neq j$, then $(t_{ij}F^{(i)})^{-1} = F^{(i)}t_{ij}^{-1} = t_{ik}F^{(i)} = t_{ij}^{-1}F^{(i)}$ since $t_{ij}^{-1} \in t_{ik}F^{(i)}$ and t_{ij}^{-1} can, therefore, be taken as a representative of $t_{ik}F^{(i)}$. Thus all elements of T_{ij}^{-1}, and also of T_{ij}, commute with $F^{(i)}$. Further, t_{ik} brings $\boldsymbol{P}^{(i)}$ into $\boldsymbol{P}^{(k)}$ and $\boldsymbol{P}^{(j)}$ into $\boldsymbol{P}^{(i)}$, so that $(\boldsymbol{P}^{(j)}, \boldsymbol{P}^{(i)})$ and $(\boldsymbol{P}^{(i)}, \boldsymbol{P}^{(k)})$ are crystallographically equivalent ordered pairs.

Theorem IV. An ordered pair $(\boldsymbol{P}^{(i)}, \boldsymbol{P}^{(j)})$ is ambivalent if, and only if, either of the following equivalent relations holds

$$\emptyset \subset T_{ij} \cap T_{ij}^{-1}, \tag{5.13}$$

$$a_{ij}^2 \in F^{(ij)}, \quad \text{for some} \quad a_{ij} \in T_{ij}. \tag{5.14}$$

If, specifically,

$$T_{ij} = T_{ij}^{-1} \tag{5.15}$$

then all elements of T_{ij} satisfy (5.14), commute with $F^{(i)}$, and

$$F^{(ij)} = F^{(i)} = F^{(j)}. \tag{5.16}$$

An ordered pair $(\boldsymbol{P}^{(i)}, \boldsymbol{P}^{(j)})$ is polar if, and only if, either of the following conditions is fulfilled

$$T_{ij} \cap T_{ij}^{-1} = \emptyset , \tag{5.17}$$

$$t_{ij}^2 \text{ non} \in F^{(ij)} , \quad \text{for all} \quad t_{ij} \in T_{ij} . \tag{5.18}$$

If, specifically, T_{ij}^{-1} constitutes a left coset disjoint with T_{ij},

$$T_{ij}^{-1} = t_{ik} F^{(i)} , \quad k \neq j , \tag{5.19}$$

then all elements of T_{ij} and of $T_{ij}^{-1} = T_{ik}$ commute with $F^{(i)}$. Further,

$$F^{(ij)} = F^{(i)} = F^{(j)} = F^{(k)} = F^{(ik)} \tag{5.20}$$

and

$$(\boldsymbol{P}^{(j)}, \boldsymbol{P}^{(i)}) \overset{G}{\sim} (\boldsymbol{P}^{(i)}, \boldsymbol{P}^{(k)}) . \tag{5.21}$$

Simple rules follow immediately from *Theorem IV*. Thus, for example, to any twinning complex containing the inversion, a mirror or a two-fold axis, there corresponds an ambivalent ordered pair. The twinning complex of a polar pair contains no element of order 2.

Finally, we mention briefly unordered domain pairs. Under an *unordered pair* a set of two domains is meant irrespectively of their order. The unordered pair of domains $\boldsymbol{P}^{(i)}$ and $\boldsymbol{P}^{(j)}$ will be denoted by $\langle \boldsymbol{P}^{(i)}, \boldsymbol{P}^{(j)} \rangle$. Obviously, the ordered pair $(\boldsymbol{P}^{(i)}, \boldsymbol{P}^{(j)})$ and its transpose $(\boldsymbol{P}^{(j)}, \boldsymbol{P}^{(i)})$ correspond to the same unordered pair $\langle \boldsymbol{P}^{(i)}, \boldsymbol{P}^{(j)} \rangle$. Two unordered pairs $\langle \boldsymbol{P}^{(i)}, \boldsymbol{P}^{(j)} \rangle$ and $\langle \boldsymbol{P}^{(k)}, \boldsymbol{P}^{(l)} \rangle$ are said to be crystallographically equivalent with respect to G, $\langle \boldsymbol{P}^{(k)}, \boldsymbol{P}^{(l)} \rangle \overset{G}{\sim} \langle \boldsymbol{P}^{(i)}, \boldsymbol{P}^{(j)} \rangle$, if $g \in G$ exists such that either

$$g\boldsymbol{P}^{(i)} = \boldsymbol{P}^{(k)} \quad \text{and} \quad g\boldsymbol{P}^{(j)} = \boldsymbol{P}^{(l)} \tag{5.22}$$

or

$$g\boldsymbol{P}^{(j)} = \boldsymbol{P}^{(k)} \quad \text{and} \quad g\boldsymbol{P}^{(i)} = \boldsymbol{P}^{(l)} .$$

Obviously, all results of this Section can be applied to improper domains; we just substitute the normalizer $G_{(1)}$ for the symmetry group $F^{(i)}$.

6. CLASSES OF CRYSTALLOGRAPHICALLY EQUIVALENT DOMAIN PAIRS

From q domains of the class $G\boldsymbol{P}^{(i)}$ one can form q^2 ordered pairs and $\frac{1}{2}q(q+1)$ unordered pairs. The relation of crystallographical equivalence of domain pairs satisfies three requirements of an equivalence relation and divides, therefore, these sets of pairs into disjoint *classes of domain pairs crystallographically equivalent with respect to G*. A class of crystallographically equivalent ordered pairs will be denoted by $G(\boldsymbol{P}^{(i)}, \boldsymbol{P}^{(j)})$ and the class of crystallographically equivalent unordered pairs

by $G\langle \boldsymbol{P}^{(i)}, \boldsymbol{P}^{(j)}\rangle$ where $(\boldsymbol{P}^{(i)}, \boldsymbol{P}^{(j)})$ and $\langle \boldsymbol{P}^{(i)}, \boldsymbol{P}^{(j)}\rangle$ are representatives of classes[17]), respectively. The entire class can be generated by applying all operations from G to both domains of the representative. Classes can, again, be interpreted as orbits and any pair from the class can be taken as its representative.

The significance of the classes is clear. When studying the crystallographical properties of domain pairs we may confine our attention to the set of crystallographically non-equivalent pairs only. Such a set can be formed by taking one representative of each class. We find now a procedure for constructing the representatives of all classes.

Notice first that in every class $G(\boldsymbol{P}^{(k)}, \boldsymbol{P}^{(l)})$ an ordered pair $(\boldsymbol{P}^{(i)}, \boldsymbol{P}^{(j)})$ can be found such that its first domain is a chosen domain $\boldsymbol{P}^{(i)}$ since an element h must exist in G such that $h\boldsymbol{P}^{(k)} = \boldsymbol{P}^{(i)}$, so that $(\boldsymbol{P}^{(k)}, \boldsymbol{P}^{(l)}) \overset{G}{\sim} (h\boldsymbol{P}^{(k)}, h\boldsymbol{P}^{(l)}) = (\boldsymbol{P}^{(i)}, h\boldsymbol{P}^{(l)})$. A class of crystallographically ordered pairs may contain several ordered pairs with the first domain $\boldsymbol{P}^{(i)}$. Two crystallographically equivalent ordered pairs with the same first domain $\boldsymbol{P}^{(i)}$ can be related by elements of $F^{(i)}$ only, so that

$$(6.1) \qquad \text{if} \quad (\boldsymbol{P}^{(i)}, \boldsymbol{P}^{(j)}) \overset{G}{\sim} (\boldsymbol{P}^{(i)}, \boldsymbol{P}^{(l)}) \quad \text{then} \quad \boldsymbol{P}^{(j)} \overset{F^{(i)}}{\sim} \boldsymbol{P}^{(l)} .$$

Second domains of all ordered pairs with fixed first domain $\boldsymbol{P}^{(i)}$ form, therefore, the class $F^{(i)}\boldsymbol{P}^{(j)}$.

The class $G\boldsymbol{P}^{(i)}$ can be resolved into disjoint classes of domains crystallographically equivalent with respect to $F^{(i)}$:

$$(6.2) \qquad G\boldsymbol{P}^{(i)} = \boldsymbol{P}^{(i)} + F^{(i)}\boldsymbol{P}^{(j)} + \ldots + F^{(i)}\boldsymbol{P}^{(r)} .$$

To any class of crystallographically equivalent ordered pairs with the first domain $\boldsymbol{P}^{(i)}$ there corresponds in the resolution (6.2) just one class of domains crystallographically equivalent with respect to $F^{(i)}$, and vice versa. The disjoint subsets of (6.2) can be constructed by making use of the following relation

$$(6.3) \qquad F^{(i)}\boldsymbol{P}^{(k)} = F^{(i)}t_{ik}\boldsymbol{P}^{(i)} = F^{(i)}t_{ik}F^{(i)}\boldsymbol{P}^{(i)} .$$

As $t_{ik}F^{(i)}$ comprises all elements of G which transform $\boldsymbol{P}^{(i)}$ into $\boldsymbol{P}^{(k)}$ we realize that the set $F^{(i)}t_{ik}F^{(i)}$ contains all elements of G which generate the entire class $F^{(i)}\boldsymbol{P}^{(k)}$ from $\boldsymbol{P}^{(i)}$. The set $F^{(i)}t_{ik}F^{(i)}$ si called a double coset of $F^{(i)}$ in G [18]). A group G can be decomposed into set-theoretic sum of disjoint double cosets [19–21]:

$$(6.4) \qquad G = F^{(i)}eF^{(i)} + F^{(i)}t_{i2}F^{(i)} + \ldots + F^{(i)}t_{ir}F^{(i)} .$$

The resolution (6.2) can, therefore, be written in the following way

$$(6.5) \qquad G\boldsymbol{P}^{(i)} = F^{(i)}eF^{(i)}\boldsymbol{P}^{(i)} + F^{(i)}t_{i2}F^{(i)}\boldsymbol{P}^{(i)} + \ldots + F^{(i)}t_{ir}F^{(i)}\boldsymbol{P}^{(i)} .$$

[17]) Henceforth "class" means class of domain pairs crystallographically equivalent with respect to the group G of the high symmetry phase. The indifferent expression "domain pair" will indicate that the statement holds for ordered pairs and, separately, also for unordered pairs.

[18]) Generally, the *double coset* FgH is the set of all products fgh where g is a fixed element of

This relation states a *one-to-one correspondence between the classes of ordered domain pairs and the double cosets* of $F^{(i)}$ *in* G. Specifically, the number r of crystallographically equivalent classes of ordered pairs equals the number of distinct double cosets in the resolution (6.4). Notice that the number r includes the trivial class which consists of the trivial pairs $(\boldsymbol{P}^{(j)}, \boldsymbol{P}^{(j)})$, $j = 1, 2, \ldots, q$.

Now we shall demonstrate that a class always consists of ordered pairs of the same type. From the definition of the crystallographical equivalence it follows that if two ordered pairs are crystallographically equivalent then the corresponding transposed pairs are also crystallographically equivalent. To every class there corresponds a class of transposed pairs. Since the classes are disjoint we infer that two classes formed by mutually transposed pairs are either identical or disjoint. In the former case, the class consists of ambivalent pairs only and will be referred to as an *ambivalent class*; in the latter case, two disjoint classes of mutually transposed pairs will be called *complementary polar classes*.

We show how the type of a class can be inferred from the properties of the associated double coset. We notice first that the set of inverse elements of $F^{(i)}t_{ij}F^{(i)}$ forms again a double coset, $(F^{(i)}t_{ij}F^{(i)})^{-1} = F^{(i)}t_{ij}^{-1}F^{(i)}$, which is either identical or disjoint with the double coset $F^{(i)}t_{ij}F^{(i)}$. The double coset which is its own inverse, will be referred to as an *ambivalent double coset*[19]). If a double coset is disjoint with its inverse, we shall call $F^{(i)}t_{ij}F^{(i)}$ and $(F^{(i)}t_{ij}F^{(i)})^{-1}$ *complementary polar double cosets*.

Furthermore, the right coset $F^{(i)}t_{ij}$ contains representatives of all left cosets in a double coset $F^{(i)}t_{ij}F^{(i)}$. Since $(t_{ij}F^{(i)})^{-1} = F^{(i)}t_{ij}^{-1}$, *the inverse coset* $(t_{ij}F^{(i)})^{-1}$ *contains representatives of all left cosets of the inverse double coset* $F^{(i)}t_{ij}^{-1}F^{(i)}$. *If a twinning complex* $t_{ij}F^{(i)}$ *belongs to an ambivalent double coset then* $(t_{ij}F^{(i)})^{-1}$ *contains representatives of all left cosets in* $F^{(i)}t_{ij}F^{(i)}$, i.e. a representative of $t_{ij}F^{(i)}$ as well. Thus $t_{ij}F^{(i)}$ and $(t_{ij}F^{(i)})^{-1}$ have at least one common element and, according to *Theorem IV*, the corresponding pair $(\boldsymbol{P}^{(i)}, \boldsymbol{P}^{(j)})$ is ambivalent. Conversely, if $(\boldsymbol{P}^{(i)}, \boldsymbol{P}^{(j)})$ is an ambivalent pair then, according to *Theorem IV*, an element a_{ij} can be found such that

$$a_{ij} \in t_{ij}F^{(i)} \subset F^{(i)}t_{ij}F^{(i)}, \tag{6.6}$$

and, simultaneously

$$a_{ij} \in F^{(i)}t_{ij}^{-1} \subset F^{(i)}t_{ij}^{-1}F^{(i)}. \tag{6.7}$$

Hence the corresponding double coset is ambivalent. If, on the other hand, $t_{ij}F^{(i)}$ belongs to a polar double coset then no element a_{ij} satisfying (6.6) and (6.7) exists and, consequently, $(\boldsymbol{P}^{(i)}, \boldsymbol{P}^{(j)})$ is a polar pair. Finally, if $t_{ij}F^{(i)}$ has no common element with $F^{(i)}t_{ij}^{-1}$ then $F^{(i)}t_{ij}F^{(i)}$ must be a polar double coset.

---

the group G, and f, h run over all elements of subgroups F and H, respectively ($F \subseteq G$, $H \subseteq G$) [19–21]. In our case, $F = H$. It holds $Fg'F = FgF$ for any $g' \in FgF$.

[19]) In analogy with ambivalent conjugation classes [19].

If, specifically, $(t_{ij}F^{(i)})^{-1}$ constitutes a left coset (i.e. if (5.15) or (5.19) holds) then $t_{ij}F^{(i)} \subset G_{F^{(i)}}$ and the double coset consists of one left coset only,

$$F^{(i)}t_{ij}F^{(i)} = t_{ij}F^{(i)} . \tag{6.8}$$

Conversely, if (6.8) holds then $t_{ij}F^{(i)} \subset G_{F^{(i)}}$ (see Theorem 66 of Speiser [21]), so that $(t_{ij}F^{(i)})^{-1} = (F^{(i)}t_{ij})^{-1} = t_{ij}^{-1}F^{(i)} = t_{ik}F^{(i)}$, i.e. the inverse coset forms again a left coset which must be either identical or disjoint with $t_{ij}F^{(i)}$. Due to *Theorem III* there are just d left cosets of this kind in the resolution (3.8).

Before summarizing the main results of this Section we mention briefly the *classes of unordered domain pairs*. The relation $\overset{G}{\sim}$ divides the set of all unordered pairs into disjoint classes. To each ambivalent class of ordered pairs there corresponds one class of unordered pairs, whereas to two complementary classes of ordered pairs there corresponds one class of unordered pairs. This correspondence enables us to utilize the results obtained for classes of ordered pairs also for the classes of unordered pairs.

Theorem V. The number r of classes of crystallographically equivalent ordered pairs equals the number of double cosets in the decomposition

$$G = F^{(i)}eF^{(i)} + F^{(i)}t_{i2}F^{(i)} + \ldots + F^{(i)}t_{ir}F^{(i)} . \tag{6.9}$$

The representative of the j-th class of ordered pairs can be found in the form

$$(\boldsymbol{P}^{(i)}, t_{ij}\boldsymbol{P}^{(i)}) \tag{6.10}$$

where t_{ij} is a representative of the j-th double coset of the resolution (6.9). A one-to-one correspondence exists between ambivalent classes of ordered pairs and ambivalent double cosets of the decomposition (6.9), and between complementary polar classes of ordered pairs and complementary polar double cosets of (6.9).

There exist d distinct classes of ordered pairs represented by the ordered pairs $(\boldsymbol{P}^{(i)}, \boldsymbol{P}^{(k)})$ the components of which have the common isotropy group

$$F^{(i)} = F^{(k)} = F^{(ik)} \tag{6.11}$$

(d is the degeneracy of $F^{(i)}$). Corresponding double cosets, and only these double cosets, consist of one left coset,

$$F^{(i)}t_{ik}F^{(i)} = t_{ik}F^{(i)} . \tag{6.12}$$

The inverses of these, and only of these, double cosets form left cosets,

$$(t_{ik}F^{(i)})^{-1} = t_{im}F^{(i)} , \quad t_{im} \in G , \tag{6.13}$$

and the union of these cosets constitutes the normalizer $G_{F^{(i)}}$.

The number s of the classes of crystallographically equivalent unordered pairs equals

$$s = a + \tfrac{1}{2}c \tag{6.14}$$

where a and c are numbers of ambivalent and complementary double cosets in (6.9), respectively. The representatives of all classes of unordered pairs can be found in the form

$$\langle \boldsymbol{P}^{(i)}, t_{il}\boldsymbol{P}^{(i)} \rangle \tag{6.15}$$

where t_{il} runs over representatives of all ambivalent double cosets and over either of the representatives of each pair of complementary polar double cosets in (6.9).

We may note that no simple explicit formula analogous to (3.9) exists for the number of classes of ordered or unordered pairs. In some cases, however, the following consideration may be effective. The number p_{ij} of left cosets in $F^{(i)}t_{ij}F^{(i)}$ is (see Theorem 1.7.1. of Hall [20])

$$p_{ij} = \left[t_{ij}^{-1}F^{(i)}t_{ij} : F^{(i)} \cap t_{ij}^{-1}F^{(i)}t_{ij}\right] = \left[F^{(i)} : F^{(ij)}\right]. \tag{6.16}$$

Applying this expression to the resolution (6.9) we obtain the relation

$$q = \left[F^{(i)} : F^{(i)}\right] + \ldots + \left[F^{(i)} : F^{(ij)}\right] + \ldots \tag{6.17}$$

where $F^{(ij)}, \ldots$ are the isotropy groups of the representative ordered pairs (6.10). Obviously, the number of terms on the right side of the Eq. (6.17) equals the number of classes. Just d of these terms equal unity. If, specifically, all $F^{(ij)}$ in remaining terms have equal order then

$$r = d + (q - d)/\left[F^{(i)} : F^{(i,ij)}\right]. \tag{6.18}$$

7. APPLICATIONS

In order to illustrate possible use of general results we discuss two examples: First, we analyse the domain structure of the monoclinic phase of WO_3, and, second, we derive special properties of domain structures for transitions where the group F is an invariant subgroup of the group G.

1. *Tungsten trioxide*, WO_3, has at room temperature the point group symmetry $F = 2/m$ and above 740 °C the symmetry $4/mmm$ [22]. The only common supergroup of these groups is $m3m$ which can be, therefore, treated as the symmetry group G of the high symmetry "mother phase". The number q of domains which can appear in the monoclinic phase is $q = n_G : n_F = 48 : 4 = 12$. We may choose $F^{(1)} = 2_x/m$ The left coset decomposition of $m3m$ with respect to $2_x/m$ can be performed easily using the multiplication table of $m3m$ [23]. The j-th row in Table 1 contains

Table 1

Decomposition of $m3m$ into left and double cosets of $2_x/m$.

Left cosets (twinning complexes)						Associated domains	
T_{1j}	$t_{1j}\,2_x/m$				type	$P^{(j)}$	orientation
T_{11}	1	$\bar{1}$	2_x	m_x	ambiv.	$P^{(1)}$	$\|0UV\|$
T_{12}	m_y	2_y	m_z	2_z	ambiv.	$P^{(2)}$	$\|0\bar{U}V\|$
T_{13}	m_b	2_b	m_a	2_a	ambiv.	$P^{(3)}$	$\|0VU\|$
T_{14}	$\bar{4}_x^3$	4_x^3	$\bar{4}_x$	4_x	ambiv.	$P^{(4)}$	$\|0\bar{V}U\|$
T_{15}	m_f	2_f	$\bar{4}_z^3$	4_z^3	ambiv.	$P^{(5)}$	$\|U0V\|$
T_{16}	m_e	2_e	$\bar{4}_z$	4_z	ambiv.	$P^{(6)}$	$\|\bar{U}0V\|$
T_{17}	m_d	2_d	$\bar{4}_y$	4_y	ambiv.	$P^{(7)}$	$\|VU0\|$
T_{18}	m_c	2_c	$\bar{4}_y^3$	4_y^3	ambiv.	$P^{(8)}$	$\|\bar{V}U0\|$
T_{19}	3_δ	$\bar{3}_\delta$	3_γ	$\bar{3}_\gamma$	polar	$P^{(9)}$	$\|V0U\|$
$T_{1,10}$	3_β	$\bar{3}_\beta$	3_α	$\bar{3}_\alpha$	polar	$P^{(10)}$	$\|V0\bar{U}\|$
$T_{1,11}$	3_δ^2	$\bar{3}_\delta^2$	3_β^2	$\bar{3}_\beta^2$	polar	$P^{(11)}$	$\|UV0\|$
$T_{1,12}$	3_γ^2	$\bar{3}_\gamma^2$	3_α^2	$\bar{3}_\alpha^2$	polar	$P^{(12)}$	$\|U\bar{V}0\|$

Notation [25]: $x = [100]$, $y = [010]$, $z = [001]$, $a = [011]$, $b = [0\bar{1}1]$, $c = [101]$, $d = [10\bar{1}]$, $e = [110]$, $f = [\bar{1}10]$, $\alpha = [1\bar{1}\bar{1}]$, $\beta = [\bar{1}1\bar{1}]$, $\gamma = [\bar{1}\bar{1}1]$, $\delta = [111]$.

Table 2

Decomposition of $m3m$ into left cosets of $4_x/mmm$.

Left cosets of $4_x/mmm$	Associated subgroups $F^{(j)}$	Domains stable under $F^{(j)}$
$1\ \ 4_x\ \ 2_x\ \ 4_x^3\ \ m_y\ \ m_z\ \ m_a\ \ m_b$	$2_x/m$	$P^{(1)}, P^{(2)}, P^{(3)}, P^{(4)}$
$\bar{1}\ \ \bar{4}_x\ \ m_x\ \ \bar{4}_x^3\ \ 2_y\ \ 2_z\ \ 2_a\ \ 2_b$		
$m_f\ \ \bar{3}_\beta\ \ \bar{4}_z^3\ \ \bar{3}_\alpha\ \ 4_z\ \ 2_e\ \ 3_\gamma\ \ 3_\delta$	$2_z/m$	$P^{(5)}, P^{(6)}, P^{(9)}, P^{(10)}$
$2_f\ \ 3_\beta\ \ 4_z^3\ \ 3_\alpha\ \ \bar{4}_z\ \ m_e\ \ \bar{3}_\gamma\ \ \bar{3}_\delta$		
$m_d\ \ \bar{3}_\alpha^2\ \ \bar{4}_y\ \ \bar{3}_\gamma^2\ \ 2_c\ \ 4_y^3\ \ 3_\beta^2\ \ 3_\delta^2$	$2_y/m$	$P^{(7)}, P^{(8)}, P^{(11)}, P^{(12)}$
$2_d\ \ 3_\alpha^2\ \ 4_y\ \ 3_\gamma^2\ \ m_c\ \ \bar{4}_y^3\ \ \bar{3}_\beta^2\ \ \bar{3}_\delta^2$		

the twinning complex T_{ij} of the ordered pair $(P^{(1)}, P^{(j)})$, $j = 1, 2, \ldots, 12$. Each of the first four cosets equals its inverse, hence their union provides the normalizer $G_{F^{(1)}} = 4_x/mmm$. The multiplicity of the low symmetry phase is $m = n_G : n_{G_F} = 48 : 16 =$

$= 3$ and the degeneracy $d = n_{G_F} : n_F = 16 : 4 = 4$, i.e. each of three crystallographically equivalent low symmetry phases leaves four domains invariant. The decomposition of $m3m$ into left cosets of $4_x/mmm$ is given in Table 2. Each element of the first row leaves $2_x/m$ unchanged, each inverse element of the second row transforms $2_x/m$ into $2_z/m$, and each inverse element of the third row transforms $2_x/m$ into $2_y/m$. Comparing Tables 1 and 2 we can verify that each left coset of $4_x/mmm$ consists of three left cosets of $2_x/m$; domains associated with these three cosets are stable under the same low symmetry group.

Classification of the ordered domain pairs can be performed by inspecting the twinning complexes and their inverses. Thus we find that $(\boldsymbol{P}^{(1)}, \boldsymbol{P}^{(j)})$ are ambivalent pairs for $j = 1, 2, \ldots, 8$ (check that (5.14) is fulfilled), and polar pairs for $j = 9, 10, 11, 12$. Since $F^{(1j)} = \bar{1}$ for $j = 5, 6, \ldots, 12$, the number of left cosets in double cosets $F^{(1)}t_{ij}F^{(1)}$ for $j > 4$ equals $\left[F^{(1)} : F^{(15)}\right] = 2$, and the number of classes is $r = 4 + (12 - 4)/2 = 8$. Left cosets can be assembled into double cosets by making use of the fact that the inverse coset $(t_{1j}F^{(1)})^{-1}$ contains representatives of all left cosets of the inverse double coset $F^{(1)}t_{ij}^{-1}F^{(1)}$. In Table 1 left cosets constituting one double coset are presented within one solid frame, complementary polar double cosets are marked by additional dashed frame. We see that there exist 6 classes of ambivalent ordered pairs (the representatives of these classes are $(\boldsymbol{P}^{(1)}, \boldsymbol{P}^{(j)})$, $j = 1, 2, 3, 4, 5, 7$) and 2 complementary polar classes (the representatives are $(\boldsymbol{P}^{(1)}\, \boldsymbol{P}^{(j)})$, $j = 9, 11$). Thus, from possible 144 ordered pairs and 78 possible unordered pairs we need to consider only 8 crystallographically non-equivalent ordered pairs and 7 crystallographically non-equivalent unordered pairs.

We notice that the whole analysis can be performed without specifying the transition parameter which is needed only for the exact domain characterization. It can be shown that a symmetric second order tensor $e_{ij}^{(1)}$ with $e_{12}^{(1)} = e_{23}^{(1)} = 0$ and all other components non-zero and unequal (in the standard coordinate system of $m3m$) induces the symmetry reduction from $m3m$ to $2_x/m$ and provides us, therefore, with a transition parameter $(G_{e^{(1)}} = 2_x/m = F^{(1)})$. The monoclinic phase can be treated as a "macroscopically full (proper)" ferroelastic phase [5]. Then, within the macroscopic approach, the spatial orientation of a domain can conveniently be represented by a straight line directed along the principal axis of the tensor $e^{(i)}$ which lies in the mirror plane m of the corresponding low symmetry group [24]. These characteristic directions $|UVW|$ are also given in Table 1.

2. Some of the general results obtained in previous Sections are particularly simple if *the symmetry group F of the low symmetry phase is an invariant subgroup of the symmetry group G of the high symmetry phase*, i.e. if it holds [19–21]:

$$Fg = gF \quad \text{for all} \quad g \in G. \tag{7.1}$$

Then

(i) there exists only one low symmetry phase which leaves invariant all q domain of $G\boldsymbol{P}^{(i)}$ (from (7.1) it follows that $G_F = G$);

(ii) the number r of classes of crystallographically equivalent ordered pairs equals the number q of domains:

$$r = q \tag{7.2}$$

(due to (7.1) all double cosets are identical with the left cosets of F in G).

(iii) the twinning complexes form a factor group G/F provided the coset multiplication is defined in the usual manner [19–21]:

$$T_{ij}T_{ik} = t_{ij}Ft_{ik}F = (t_{ij}t_{ik})\,F\,. \tag{7.3}$$

The condition (7.1) is fulfilled in two important cases: if G is a commutative group, and if F has index 2. In the latter case there exist two domains $\boldsymbol{P}^{(1)}$, $\boldsymbol{P}^{(2)}$ and one symmetry phase F which preserves both domains. There are two classes of crystallographically equivalent ordered pairs which can be represented by the pairs $(\boldsymbol{P}^{(1)}, \boldsymbol{P}^{(1)})$ and $(\boldsymbol{P}^{(1)}, \boldsymbol{P}^{(2)})$ and one symmetry phase F which stabilizes both domains. The twinning complex T_{12} contains all elements of G which do not belong to F. The factor group G/F has the order 2 and its elements are F and T_{12}. The defining relation of G/F is $(T_{12})^2 = F$, hence $T_{12}^{-1} = T_{12}$, and the non-trivial pairs are ambivalent.

Table 3

Decomposition of 622 into left cosets of 32.

Left cosets of 32		Domains
T_{11}	$1 \quad 3 \quad 3^2 \quad 2_1 \quad 2_3 \quad 2_5$	+
T_{12}	$6 \quad 6^3 \quad 6^5 \quad 2_4 \quad 2_6 \quad 2_2$	−

One may verify all these relations on the Dauphiné twinning in α-quartz. At about 573 °C the β-phase (symmetry 622) transforms into α-phase (symmetry 32). Corresponding resolution of $G = 622$ into left cosets of $F = 32$ is given in Table 3. Domains can, conventionally, be designated + or −, e.g. according to the sign of the d_{122} component of the piezoelectric coefficient.

The author is grateful to Dr. V. Dvořák and to Dr. F. Kroupa for critical comments on the manuscript.

Received 26. 4. 1972.

References

[1] Zheludev I. S., Shuvalov L. A.: Kristallografiya *1* (1956), 681.
[2] Shuvalov L. A.: J. Phys. Soc. Japan *28*, Supplement (1970), 38.
[3] Zheludev I. S.: *in* Solid State Physics. Edited by H. Ehrenreich, F. Seitz, D. Turnbull, Academic Press, New York 1971, Vol. 26, p. 429.
[4] Aizu K.: J. Phys. Soc. Japan *27* (1969), 387.
[5] Aizu K.: Phys. Rev. *B 2* (1970), 754.
[6] Ascher E.: Helv. Phys. Acta *39* (1966), 466.
[7] Ascher E.: Group-theoretical Considerations on Ferroelectric Phase Transitions and Polarisation Reversals, Lecture Notes, Battelle Institute, Geneva 1967; Chem. Phys. Letters *1* (1967), 69.
[8] Indenbom V. L.: *in* Physics of Imperfect Crystals, Proc. of the School held in Telavi, Tbilisi 1966, Vol. I, p. 5.
[9] Kroupa F., Janovec V.: to be published.
[10] Dvořák V.: J. Phys. Soc. Japan *28*, Supplement (1970), 252.
[11] Landau L., Lifshitz E. M.: Statistical Physics. Addison-Wesley, New York 1958, Ch. 14.
[12] Ascher E.: Physics Letters *20* (1966), 352.
[13] Tisza L.: Ann. Phys. (N.Y.) *13* (1961), 1.
[14] Gränicher H., Müller K. A.: Materials Research Bulletin *6* (1971), 977.
[15] Lang S.: Algebra. Addison-Wesley, Reading, Mass. 1965, Ch. I, § 5.
[16] Birman J. L.: *in* Proc. of the Symposium on Ferroelectricity. Edited by E. F. Weller, Elsevier Publ. Co, New York 1967, p. 20.
[17] Devonshire A. F.: Phil. Mag. *40* (1949), 1040; ibid. *42* (1951), 1065.
[18] Levanyuk A. P., Sannikov D. G.: Zh. eksper. teor. Fiz. *60* (1971), 1109.
[19] Jansen L., Boon M.: Theory of Finite Groups. North-Holland Publ. Co., Amsterdam 1967.
[20] Hall M.: The Theory of Groups. The Macmillan Co., New York 1959.
[21] Speiser A.: Theorie der Gruppen von endlicher Ordnung. J. Springer, Berlin 1937.
[22] Känzig W.: *in* Solid State Physics. Edited by F. Seitz, D. Turnbull, Academic Press, New York 1957, Vol. 4, p. 1.
[23] Kovalev O. V.: Irreducible Representations of the Space Groups. Gordon and Breach, New York 1965.
[24] Fousek J.: private communication.
[25] Ascher E.: Properties of Shubnikov Point Groups (Part 1). Report from Battelle Institute, Geneva.

Ferroelectrics
1976, Vol. 12, pp. 43–53

Printed in Great Brita

A SYMMETRY APPROACH TO DOMAIN STRUCTURES

VÁCLAV JANOVEC†

Swiss Federal Institute of Technology (ETH), Laboratory of Solid State Physics, CH-8049 Zürich, Switzerland

(Received September 22, 1975)

Whereas the symmetry of the order parameter is specified by operations preserved at the transition, domains are determined by lost symmetry operations. The number and the relations between domains and domain pairs can be found by grouping the lost operations into left and double cosets. Different types of domains, rotational (e.g., ferroelectric, ferroelastic) and translational ones, are related to maximal subgroups retaining a characteristic domain property. The interface between domains is treated as a two-dimensional residue of the parent phase and is described by two-sided plane groups. The existence, orientation and charge of coherent stress-free domain walls between ferroelastic domains can also be determined from left coset decompositions. Junctions and interactions of antiphase boundaries, domain walls and imperfect dislocations are considered. Annihilation of antiphase boundaries by moving domain walls, the creation of antiphase boundaries by reacting domain walls and the selective interactions of dislocations with antiphase boundaries and domain walls are demonstrated on the example of gadolinium molybdate. Goldstone modes as a dynamical counterpart of domain structures in systems described by continuous symmetry groups are briefly mentioned.

INTRODUCTION

Domain formation (transformation twinning) is a direct consequence of the symmetry lowering at the phase transition. In the past, two different types of domain structures have been studied separately: Macroscopic rotation domains (mainly in ferroelectrics, ferromagnetics and ferroelastics) and antiphase translation domains (in alloys). Only recently both types of domains and interactions between domain walls, antiphase boundaries and dislocations have been observed in gadolinium molybdate[1–5] and in some other materials.[6,7] Rotation and translation domains can appear simultaneously at any transition in which both the point group symmetry and the translation symmetry decrease.[6,8–11] The complexity of these structures has not yet been fully revealed and appreciated. In this paper we try to domenstrate how simple symmetry considerations can help in deciphering domain structures in such cases.

1 DOMAINS AND DOMAIN PAIRS

Number of Domains, Symmetry Relations Between Domains

In proper ferroelectrics a vector can be attached to each domain. Counting the number of crystallographically equivalent directions one can find the number of ferroelectric domains.[12–14] Many alloys have relatively simple structures so that the antiphase domains can be directly visualized and enumerated.[15] These simple methods fail, however, in many other more complicated phase transitions, especially when both point and translation symmetry change. Then an algebraic treatment appears to be a more reliable guide.[16–19] It is independent on our limited abilities to visualize symmetry relations in space and makes it possible to exploit simple theorems of the group theory.

To demonstrate the essence of this approach let us consider an orthorhombic proper ferroelectric phase of perovskites.[20] Twelve different directions of the spontaneous polarization along the face diagonals characterizing twelve possible domains are listed in the third column of Table I. The second column contains all 48 symmetry operations of the cubic parent point group $G = m3m$. They are divided in such a manner that in the jth row all operations are assembled that transform the first domain [110] into the jth one. Four operations in the first row retain the polarization of the first domain and constitute the group $F = 2_{xy}mm$ of the orthorhombic phase. For any other domain there exist always four operations that produce this domain from the first one. This division of the group G into disjoint subsets consisting of the same number of operations as

† Permanent address: Institute of Physics, Czechosl. Acad. Sci., Na Slovance 2, 180 40 Prague 8, Czechoslovakia.

TABLE I

Decomposition of $m3m$ into left and double cosets of $2_{xy}mm$

j	Left cosets				$\frac{\mathbf{P}^{(j)}}{\lvert\mathbf{P}^{(j)}\rvert}$	Spont. deform.	$\measuredangle\, \mathbf{P}_1\mathbf{P}_j$	f-elast. DW's
1	1	2_{xy}	$m_{\bar{x}y}$	m_z	[110]	$u^{(I)}$	0°	
2	$\bar{1}$	m_{xy}	$2_{\bar{x}y}$	2_z	[$\bar{1}\bar{1}$0]	$u^{(I)}$	180°	W_∞
3	2_x	4_z^3	$\bar{4}_z$	m_y	[1$\bar{1}$0]	$u^{(II)}$	90°	W_eW
6	2_y	4_z	$\bar{4}_z^3$	m_x	[$\bar{1}$10]	$u^{(II)}$		
4	2_{xy}	3_x	$\bar{3}_z$	$\bar{4}_y$	[0$\bar{1}$1]	$u^{(III)}$	120°	WS_e
7	$2_{\bar{x}z}$	3_y	$\bar{3}$	$\bar{4}_y^3$	[0$\bar{1}\bar{1}$]	$u^{(IV)}$		
8	2_{yz}	3_y^2	$\bar{3}_z^5$	$\bar{4}_x^3$	[$\bar{1}$01]	$u^{(V)}$		
9	$2_{\bar{y}z}$	3_x^2	$\bar{3}^5$	$\bar{4}_x$	[$\bar{1}$0$\bar{1}$]	$u^{(VI)}$		
5	m_{xz}	$\bar{3}_x$	3_z	4_y	[01$\bar{1}$]	$u^{(III)}$	60°	W_eS
10	$m_{\bar{x}z}$	$\bar{3}_y$	3	4_y^3	[011]	$u^{(IV)}$		
11	m_{yz}	$\bar{3}_y^5$	3_z^2	4_x^3	[10$\bar{1}$]	$u^{(V)}$		
12	$m_{\bar{y}z}$	3_x^5	3^2	4_x	[101]	$u^{(VI)}$		

Notation: Subscripts indicate orientation of axes in the standard coordinate system of the cubic system; at diads zero components are omitted, at triads only positive components are given (e.g. 3_x, 3 mean rotations along the 3-fold axes in the direction [1$\bar{1}\bar{1}$] and [111], respectively). $\mathbf{P}^{(j)}/\lvert\mathbf{P}^{(j)}\rvert$ denote direction of the spontaneous polarization in the jth ferroelectric domain. Latin superscripts signify different tensors of spontaneous deformation. Left cosets constituting one double coset are assembled within two horizontal solid lines. Subscript e denotes a charged wall. Walls without subscript are neutral.

the subgroup F is known as the decomposition of G into left cosets of the subgroup F:[21]

$$G = F + g_2F + \cdots + g_qF. \qquad (1)$$

The number q of left cosets in the decomposition (1) is called the index of F in G and is denoted by $[G:F]$. Within point groups $q = n_G : n_F$, where n_G, n_F are numbers of operations in G and F, respectively. We can say, therefore, that the number of domains equals the index of F in G and that all operations from G that transform the first domain into the jth one constitute just the g_jF left coset. These statements enable us to determine the number of domains and their symmetry relations without considering the order parameter at all. This point can be appreciated when the order parameter has a non-vectorial character as the following example shows.

Gadolinium molybdate (GMO) changes its symmetry from the tetragonal $G = P\bar{4}2_1m$ to the orthorhombic improper ferroelectric $F = Pba2$.[22] The order parameter transforms according to a two-dimensional representation[23] to which no vector or tensor can be attached. We shall, therefore, represent domains by sets of equivalent positions in the common net of

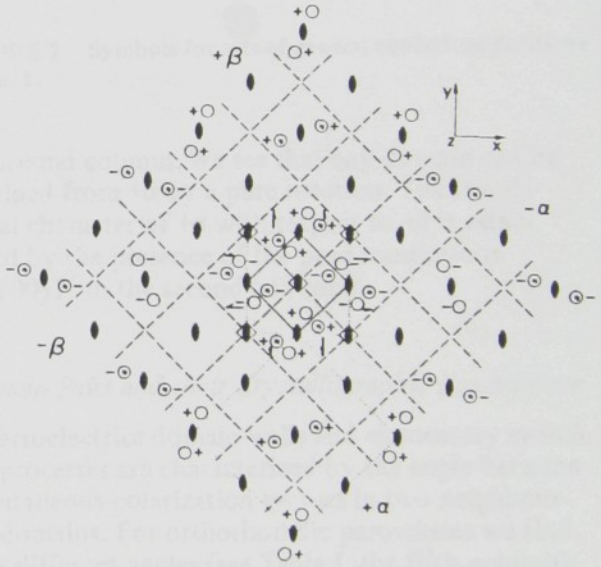

FIGURE 1 Symmetry elements and general equivalent positions of the tetragonal paraelectric space group $P\bar{4}2_1m$ (given in the centre of the figure) and of the orthorhombic improper ferroelectric group $Pba2$ (background net) of gadolinium molybdate. Symbols $+\alpha$, $-\alpha$, $+\beta$, $-\beta$ denote different distributions of equivalent positions in $Pba2$ structure and correspond to four different domains. Primitive unit cells in $P\bar{4}2_1m$ and in $+\alpha$ and $+\beta$ domains are shown with dotted lines.

TABLE II

Decomposition of $P\bar{4}2_1m$ into left and double cosets of $Pba2$

Left cosets				Domain	$\frac{P_z}{\lvert P_z \rvert}$
$(E\mid 000)\ T'$	$(4^2\mid 100)\ T'$	$(m_{xy}\mid -\frac{1}{2}\frac{1}{2}0)\ T'$	$(m_{\bar{x}y}\mid \frac{1}{2}\frac{1}{2}0)\ T'$	$+\alpha$	[001]
$(E\mid 100)\ T'$	$(4^2\mid 000)\ T'$	$(m_{xy}\mid \frac{1}{2}\frac{1}{2}0)\ T'$	$(m_{\bar{x}y}\mid \frac{1}{2}-\frac{1}{2}0)\ T'$	$+\beta$	
$(2_x\mid -\frac{1}{2}\frac{1}{2}0)\ T'$	$(2_y\mid \frac{1}{2}\frac{1}{2}0)\ T'$	$(\bar{4}^3\mid 100)\ T'$	$(\bar{4}\mid 000)\ T'$	$-\alpha$	[00$\bar{1}$]
$(2_x\mid \frac{1}{2}\frac{1}{2}0)\ T'$	$(2_y\mid \frac{1}{2}-\frac{1}{2}0)\ T'$	$(\bar{4}^3\mid 000)\ T'$	$(\bar{4}\mid 100)\ T'$	$-\beta$	

Symmetry operations are expressed in Seitz notation[21] with origin at $\bar{4}$; translational parts refer to the primitive translations t_1, t_2, t_3 of the tetragonal group $P\bar{4}2_1m$. The Seitz operators of $Pba2$ have been derived from general equivalent positions given in Ref. 24 by transforming them into the coordinate system of $P\bar{4}2_1m$. Translation group T' of the group $Pba2$ consists of all translations $t' = n_1t_1 + n_2t_2 + n_3t_3$, with $n_1 + n_2$ even, $n_1 - n_2$ even, and n_3 integer. Each left coset constitutes a double coset. Complementary polar double cosets are separated by a dashed line.

symmetry elements of the orthorhombic phase (see Figure 1). Any equivalent position of the tetragonal phase has an equal right to be chosen as the initial point for generating all equivalent positions of the orthorhombic phase. Four different sets of equivalent positions that can be produced are drawn in four corners of the figure and are denoted by $+\alpha$, $-\alpha$, $+\beta$, $-\beta$. They correspond to four possible domains. Any of these sets is invariant with respect to all operations of F, but changes under any operation of G not contained in F. We see that (i) each domain contains either +points or −points (the sign corresponds to the sign of the spontaneous polarization $\mathbf{P}_z$). If we are to change the sign we always have to perform a rotation. We can call, therefore, + or − domains rotation or macroscopic domains. (ii) we can get from $+\alpha$ to $+\beta$ or from $-\alpha$ to $-\beta$ by a pure translation. Therefore, we call $+\alpha$ and $+\beta$, $-\alpha$ and $-\beta$ pairs of translation or antiphase domains.

The equivalent positions in the orthorhombic phase appear always in couples. This enables us to introduce abbreviated symbols for sets of equivalent positions (see Figure 2) which we shall use in a later discussion.

In the algebraic approach we decompose the space group $P\bar{4}2_1m$ into left cosets of $Pba2$ (see Table II). Although both groups consist of an infinite number of operations we get four left cosets. To each of them there corresponds one domain. The first coset assembles again all operations leaving the first $+\alpha$ domain invariant, i.e. the group F. Each of the other cosets collects those operations of G that bring $+\alpha$ into another domain the symbol of which is given in

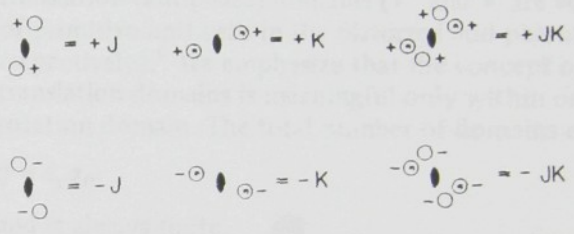

FIGURE 2 Symbols for sets of general equivalent positions in Fig. 1.

the second column. We see that any domain can be obtained from $+\alpha$ by a pure rotation. The translational character of $+\alpha$ with respect to $+\beta$ is established by the presence of the pure translations $(E\mid 100)T'$ in the second left coset.

Domain Pairs and their Crystallographic Equivalence

In ferroelectrics domain walls and elementary switching processes are characterized by the angle between spontaneous polarization vectors in two neighbouring domains. For orthorhombic perovskites we find four different angles (see Table I, the fifth column): 180°, 90°, 120° and 60°. Domain pairs $(\mathbf{P}^{(1)}, \mathbf{P}^{(j)})$ with the same angle are crystallographically equivalent i.e. they can be related by an operation from G. The left cosets corresponding to $\mathbf{P}^{(j)}$'s in all equivalent pairs $(\mathbf{P}^{(1)}, \mathbf{P}^{(j)})$ are collected in Table I within two horizontal lines. They constitute a set called a double coset of F in G[19, 21]

$$G = F + Fg_2F + \cdots + Fg_rF. \qquad (2)$$

Dividing the group G into double cosets of F we thus find the number and representatives of all non-equivalent domain pairs—again without considering the order parameter. (On determining double cosets from the left coset resolution see Ref. 19.)

In Table II each left coset constitutes one double coset. Hence for GMO we have three classes of non-equivalent domain pairs with representative pairs $(+\alpha, +\beta)$, $(+\alpha, -\beta)$, and $(+\alpha, -\beta)$.

Generally, a double coset Fg_jF is either identical with its inverse $Fg_j^{-1}F$ or has with it no common operation. We call the former an ambivalent double coset; a corresponding domain pair $(\mathbf{P}^{(1)}, \mathbf{P}^{(j)})$ is equivalent with the transposed pair $(\mathbf{P}^{(j)}, \mathbf{P}^{(1)})$. In the latter case we call Fg_jF and $Fg_j^{-1}F$ complementary polar double cosets; corresponding pairs $(\mathbf{P}^{(1)}, \mathbf{P}^{(j)})$ and $(\mathbf{P}^{(j)}, \mathbf{P}^{(1)})$ are then crystallographically non-equivalent.[19] All double cosets in Table I and the second double coset in Table II are ambivalent. The third and the fourth rows in Table II are complementary polar double cosets. Domain pairs $(+\alpha, -\alpha)$ and $(+\alpha, -\beta)$ are therefore non-equivalent with $(-\alpha, +\alpha)$ and $(-\beta, +\alpha)$, respectively. Physical consequences of this non-equivalence will become clear in Section 3.

Domain Degeneracy

In the example of the orthorhombic perovskites one can observe besides ferroelectric domains ferroelastic domains as well. The latter are determined by spontaneous deformations which are given in an abbreviated form in the fourth column of Table I. We count six ferroelastic domains. The first one, $u^{(1)}$, is preserved by eight operations which form a group $G_u = m_{xy}mm$ (the "stabilizer" of $u^{(1)}$ in G). All other ferroelestic domains can be derived from the decomposition

$$G = G_u + g_2 G_u + \cdots + g_{q_u} G_u. \tag{3}$$

The index $[G : G_u]$ determines the number q_u of ferroelastic domains.

From Table I it follows that the first ferroelastic domain $u^{(1)}$ can contain two ferroelectric domains $\mathbf{P}^{(1)}$ and $\mathbf{P}^{(2)}$. The corresponding coset decomposition is

$$G_u = F + h_2 F, \quad h_2 \in G_u. \tag{4}$$

When we put (4) into (3) we see that each left coset of G_u consists of two left cosets of F, i.e. each ferroelastic domain can contain two ferroelectric domains.[25] We shall call the number $d_u = [G_u : F]$ the degeneracy of ferroelastic domains. For total number q of domains we get

$$q = d_u q_u. \tag{5}$$

GMO provides us with another example of degeneracy (see Table II): The stabilizer G_P of the spontaneous polarization is the group $Cmm2$ which consists of two first left cosets of F.[2] Hence we have two ferroelectric domains which are two times translationally degenerate.

This is just a particular case of a general rule. The Hermann theorem[18, 26] guarantees that we can always find a group Z (it is the maximal equitranslation subgroup of G for which $F \subseteq Z \subseteq G$) which stabilizes a typical macroscopic property appearing in the distorted phase. The index $q_0 = [G : Z]$ determines the number of rotation (macroscopic) domains and equals $n_G^- : n_F^-$ where n_G^-, n_F^- are numbers of operations in point groups isogonal with G and F, respectively. Each rotation domain can further split into

$$d_t = [Z : F] = V' : V \tag{6}$$

translation (antiphase) domains (V' and V are volumes of primitive unit cells in the distorted and parent phases respectively).[6] We emphasize that the concept of translation domains is meaningful only within one rotation domain. The total number of domains equals

$$q = d_t q_0 \tag{7}$$

and is always finite.

The last conclusion is a consequence of the fact that crystallographic space groups are infinite but discrete. In systems described by continuous symmetry groups, the group of the ordered phase may have an infinite index. In this case the concept of domains and domain boundaries loses its sense since the typical parameter describing the ordered phase may appear with equal chance in an infinite number of variants. The anisotropy vanishes and gapless excitations, known as Goldstone modes,[27] can appear in the ordered phase. Their characteristic feature is that they restore the symmetry of the parent phase. Transitions in liquid crystals provide examples of such a behaviour.[28]

2 DOMAIN BOUNDARIES

Domain Interface and its Symmetry

Two domains meet along a domain boundary (DB). Since a DB is a composition plane of a transformation twin[29] we shall treat it in a manner similar to that used in the crystallography of twinning.

Crystallographical considerations have revealed that in many growth twins the twin interface (called boundary structure) has a structure of a polymorphic (real or hypothetical) modification of the individual crystal.[30-32] This can be substantiated by an energy minimum requirement: The excess surface energy of the boundary is a result of small deviations of atom positions within the interface from their normal positions in the bulk. When the interface has a structure which is shared by both twin individuals, then the average deviations are relatively small and the surface energy is also relatively low. The consideration can be formalized by treating the interface as a thin slice the symmetry of which can be described in terms of two-sided plane groups.[33,34] This slice, when considered alone, has elements in its plane symmetry that are not present in a corresponding plane section of the crystal individual. These extra symmetry operations are possible twin operations.[31]

Applying this approach to domain structures we may treat each plane in the parent phase which lowers its plane symmetry at the transition as a potential domain interface. (We are neglecting spontaneous deformations in this consideration.) In other words, we treat the interface between two domains as a two-dimensional residue of the parent phase in the distorted phase. A certain plane with descending symmetry can, however, represent a possible interface of several domain pairs. This can be seen from the following consideration.

Let G_s and F_s be the symmetries of a certain plane in the parent phase and in the first domain of the distorted phase, respectively. Then all lost operations belonging to G_s but not to F_s transform the first domain on one side of the plane into another domain on the other side. Every left coset in the resolution

$$G_s = F_s + w_2 F_s + \cdots + w_s F_s \qquad (8)$$

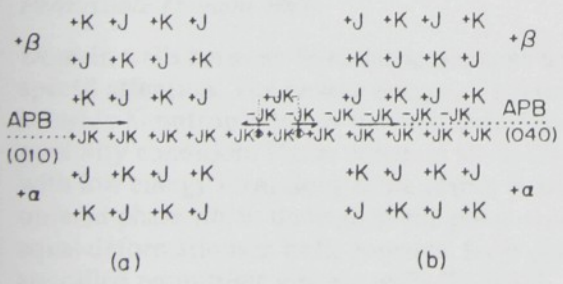

FIGURE 3 Antiphase boundaries in gadolinium molybdate depicted by abbreviated equivalent position sets (see Figures 1 and 2). (a) Antiphase boundary (010). (b) Antiphase boundary (040). The structure of the tetragonal paraelectric phase is sketched in the centre of the figure.

produces a different twin with the same first domain, the same interface but with an unlike second domain.

We see, therefore, that we have to differentiate between domain interface and DB: The latter carries some information about the relation between domains on both sides of the boundary (we distinguish, e.g., 90° and 180° domain boundaries) whereas the former may not. Symmetrically, the domain interface is described by a plane group G_s but DB is specified by a left coset of the plane group F_s. Operations of this coset transform the first domain of a pair into its second domain leaving the interface unchanged.

A domain pair $(\mathbf{P}^{(1)}, \mathbf{P}^{(j)})$ can be classified as a translational (rotational) one if the corresponding left coset $g_j F$ contains (does not contain) a pure translation. Accordingly, we can distinguish two types of DB's: an antiphase boundary (APB) bridging domains in a translational pair and a domain wall (DW) separating domains in a rotational pair.

We shall illustrate the above considerations on the GMO example. As seen from Figure 1 the plane (010) in the orthorhombic structure contains two-fold axes 4_z^2, 2_z and translations $\mathbf{t}_{13} = n_1\mathbf{t}_1 + n_3\mathbf{t}_3$ and its plane symmetry is $G_s = p\,121$ (in the International notation) or $(\mathbf{t}_1 : \mathbf{t}_3)\cdot 2$ (in the Shubnikov-Koptsik noncoordinate notation[34]). At the transition the four-fold axes disappear and the translational symmetry reduces to $\mathbf{t}'_{13} = 2n_1\mathbf{t}_1 + n_3\mathbf{t}_3$, $F_s = p121$ $(2\mathbf{t}_1 : \mathbf{t}_3)\cdot 2$. The plane forms an interface of an APB which is shown in Figure 3a. The plane (040) contains two-fold screw axes (see Figure 1) and its symmetry

TABLE III

Decomposition of the plane group $p12_11$ $(\mathbf{t}_3 : \mathbf{t}_1)\cdot 2_1$ into left and double cosets of $p1$ $(\mathbf{t}_3 : 2\mathbf{t}_1)\cdot 1$

Left cosets		
Origin on 2_{1x}	Origin at $\bar{4}$	Domain
$(E \mid 000)\ T'_{13}$	$(E \mid 000)\ T'_{13}$	$+\alpha$
$(E \mid 100)\ T'_{13}$	$(E \mid 100)\ T'_{13}$	$+\beta$
$(2_x \mid -\frac{1}{2}00)\ T'_{13}$	$(2_x \mid -\frac{1}{2}\frac{1}{2}0)\ T'_{13}$	$-\alpha$
$(2_x \mid \frac{1}{2}00)\ T'_{13}$	$(2_x \mid \frac{1}{2}\frac{1}{2}0)\ T'_{13}$	$-\beta$

Seitz operators are related to primitive translations $\mathbf{t}_1$, $\mathbf{t}_2$, $\mathbf{t}_3$ of $P\bar{4}2_1m$. The translation group T' of $p12_11$ consists of all translations $\mathbf{t}' = 2n_1\mathbf{t}_1 + n_3\mathbf{t}_3$. Origin on 2_{1x} is displaced by $\mathbf{t}_0 = (0\frac{1}{4}0)$ from the origin at $\bar{4}$.

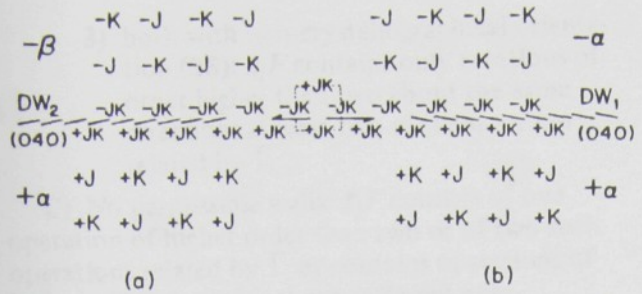

FIGURE 4 Two crystallographically non-equivalent 180° (040) domain walls DW_1 and DW_2 in gadolinium molybdate.

lowers from $G_s = p12_11\ (\mathbf{t}_3 : \mathbf{t}_1) \cdot 2_1$ to $F_s = p1\ (\mathbf{t}_3 : 2\mathbf{t}_1) \cdot 1$. From the decomposition (8), given in Table III we infer that an interface with the same symmetry can form either an APB (see Figure 3b) or two 180° DW's shown in Figure 4. These two DW's are crystallographically non-equivalent since the corresponding left cosets belong to two different complementary polar double cosets. All possible DB's with the same orientation can, therefore, be in GMO divided into three classes of non-equivalent DB's given in Table IV. This conclusion contrasts with Ref. 2

TABLE IV

Equivalent domain boundaries in GMO

Equivalent DB's				Label
$(+\alpha \mid +\beta)$	$(+\beta \mid +\alpha)$	$(-\alpha \mid -\beta)$	$(-\beta \mid -\alpha)$	APB
$(+\alpha \mid -\alpha)$	$(+\beta \mid -\beta)$	$(-\alpha \mid +\beta)$	$(-\beta \mid +\alpha)$	DW_1
$(+\alpha \mid -\beta)$	$(+\beta \mid -\alpha)$	$(-\alpha \mid +\alpha)$	$(-\beta \mid +\beta)$	DW_2

where all 180° DW's are treated as crystallographically equivalent.

Permissible Domain Walls

Domain walls between ferroelastic domains need special attention. The surface energy of these DW's is highly anisotropic due to the mechanical compatibility condition. Planar coherent stress-free DW's with low energy form along those planes in the disordered phase which undergo at the phase transition equal deformations in both domains. Such planes are called permissible domain walls (PDW).[35]

Let us consider a domain pair $(1, j)$ with spontaneous deformations $u^{(1)}$ and $u^{(j)}$. Depending on scalar invariats

$$I_2 = \begin{vmatrix} D_{11} & D_{12} \\ D_{12} & D_{22} \end{vmatrix} + \begin{vmatrix} D_{11} & D_{13} \\ D_{13} & D_{33} \end{vmatrix} + \begin{vmatrix} D_{22} & D_{23} \\ D_{23} & D_{33} \end{vmatrix},$$

$$I_3 = \det D$$

of the difference tensor $D = u^{(j)} - u^{(1)}$ three cases can occur:[36, 37]

A) $I_2 = I_3 = 0$. Both domains in the pair have identical deformations and can meet along a DW of arbitrary orientation (twinning without change of form).[32] We shall denote these walls by W_∞.

B) $I_2 \neq 0, I_3 = 0$. Two mutually perpendicular PDW's exist. Two twins can be formed from domains (1) and (j) but additional rotations are always necessa which bring domains into mutual contact along the PDW. The PDW's have either a fixed orientation with respect to the parent phase (W-walls) or a non-crystallographic orientation (S-walls).

C) $I_3 \neq 0$. No PDW exists. Domain can meet only along stressed or non-coherent DW's.

The existence and orientation of PDW's can be determined by a direct calculation.[35-41] In this way PDW's in all proper ferroelectrics[39] and proper ferroelastics[41] have been found. It turns out, however, that all information except the explicit orientation of the S-wall can be inferred directly from the left cosets g_jF using the following necessary and sufficient conditions:

A) Twinning without change of form (W_∞): g_jF contains either the inversion $\bar{1}$, or two non-perpendicular diads†, or more than two diads of different directions, or a diad and rotation of higher order about the same direction as the diad.

B) Two perpendicular permissible domain walls
   1) both with fixed orientation (WW): g_jF contains just two perpendicular diads (for $F = 4, \bar{4}, 4/m, 3, \bar{3}$ left coset g_jH_F, where H_F is the holosymmetric point group of F, must be considered instead of g_jF). PDW's are perpendicular to the diads;
   2) one with fixed, the other one with non-crystallographical orientation (WS): g_jF contains only one diad but no rotations about an axis parallel to this diad (for $F = 4, \bar{4}, 4/m, 3, \bar{3}$ left coset g_jH_F must be taken instead of g_jF). The W-wall is perpendicular to the diad.

† The term diad signifies here a two-fold rotation axis or a two-fold inversion axis, i.e. a mirror plane with a normal parallel to the diad.

3) both with non-crystallographical orientation (SS): $g_j F$ contains only rotations of order higher than two about the same direction; at least two of them are not related by $\bar{1}$.

C) No permissible walls: $g_j F$ consists of one operation of higher order than two or of two such operations related by $\bar{1}$, or contains operations of higher order than two about different axes.

We see that PDW's with fixed orientation are connected with planes the symmetry of which decreases at the transition (the perpendicular diad disappears) in contrast to S-walls where such a plane does not exist. It can be, therefore, expected that W-walls have lower energy than the S-walls.

The conditions given above enable a quick search for all symmetry changes at which a certain type of PDW's occurs. Thus, e.g., scanning of all left coset resolutions[43] reveals that S-walls are the only possible PDW's in species 4-2, $\bar{4}$-2, $4/m$-2/m, 6-2, $\bar{6}$-m, and $6/m$-2/m. No PDW's exist at all in species 23-222, $m3$-mmm, 3-1, and $\bar{3}$-$\bar{1}$. In these cases the energy of DW's is expected to be high; if it is comparable with the surface energy of the crystal, parting along the DW can occur.[30, 32] An example is provided by $Tl_2Cd_2(SO_4)_3$ (with $G = 23$ and orthorhombic ferroelastic phase with $F = 222$) where cracks along a stressed DW have been observed in the orthorhombic phase.[44]

Domain Wall Charge

In ferroelectric phases DW's can carry a surface charge which, if not compensated, increases the energy of the wall. The walls can be either charged or neutral depending on their orientation. For two perpendicular PDW's the charge can be determined from the left coset, since

1) if one PDW is charged the other is neutral,[35, 39]

2) electrically charged walls can be generated by a mirror plane whereas the neutral walls by a two-fold axis. (For the discussion of the magnetic charge see Ref. 37.)

Combining these rules we infer, e.g., that a WW_e combination (subscript e denotes an electrically charged wall) is possible only if the left coset contains just one two-fold axis and one perpendicular mirror plane; if two perpendicular two-fold axes are present then both DW's must be neutral (spontaneous polarization, if it exists, is parallel to the PDW's intersection—see, e.g., Table II).

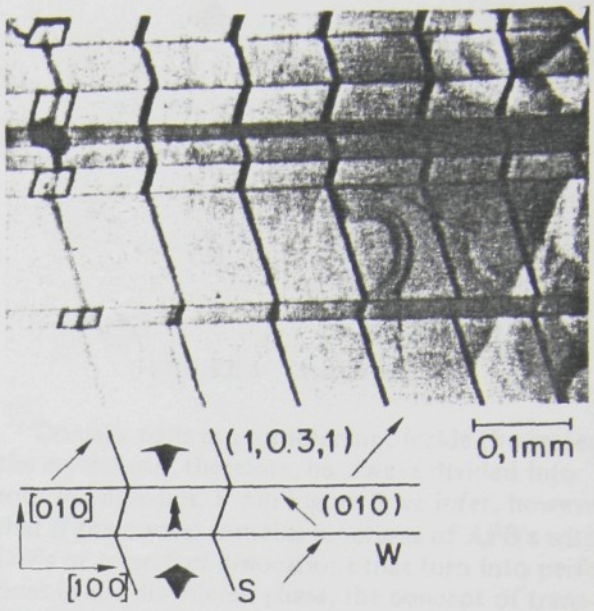

FIGURE 5 Crystallographical 90° W-walls and non-crystallographical 60° S-walls observed on the (001) plane of an orthorhombic $KNbO_3$ crystal by Wiesendanger.[45] The arrows ↗, ↖, ↑ and ↓ signify [110], [$\bar{1}$10], [011], and [01$\bar{1}$] directions of the spontaneous polarization, respectively.

To illustrate the statements of the last two paragraphs we take again the example of orthorhombic perovskites. From the left coset resolution in Table I we can immediately read out the number, type, orientation and charge of DW's (see the last column of the Table). We see that neutral 90° (100), 120° (110) W-walls and 60° (lkl) S-walls have the highest chance to appear. Domain walls observed in the orthorhombic phase of $KNbO_3$ agree with this prediction (see Ref. 45 and Figure 5).

3 INTERACTIONS BETWEEN DOMAIN WALLS, ANTIPHASE BOUNDARIES AND DISLOCATIONS

Junctions of Domain Walls, Antiphase Boundaries and Dislocations[2]

The basic geometrical properties of APB's have been well established in alloys: APB's can form closed loops, may end on the crystal surface or can termin on imperfect dislocations.[15, 46] If rotation domains are available, APB's may also terminate on DW's as illustrated in Figure 6. Here GMO lattice contains a edge dislocation D which is imperfect in the distort phase since the Burgers vector **b** is not equal to any allowed translation in this phase. The dislocation

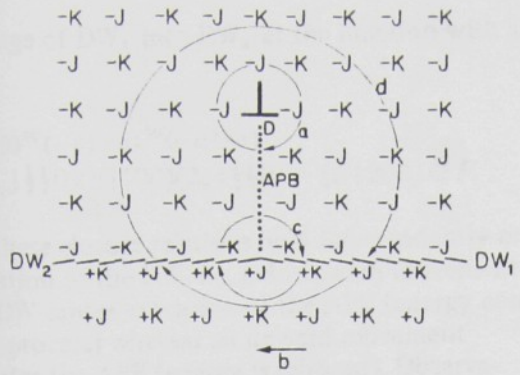

FIGURE 6 A sketch of an antiphase boundary (vertical dotted line) terminating at an imperfect edge dislocation D and at the 180° domain wall (horizontal broken lines) in gadolinium molybdate. At the junction the DW_2 wall changes into the DW_1 one. The interface structure of the antiphase boundary and of the domain walls is not shown.

turns into a perfect one in the parent phase, since **b** becomes identical with the primitive translation $\mathbf{t}_1$. A translation mismatch terminating on the dislocation is an APB. This boundary joins in its lower part a DW. From the drawing we see that at the junction DW_2 changes into a non-equivalent DW_1.

A real domain structure of GMO revealed by etching technique is reproduced in Figure 7.[1] We see APB's forming irregular non-intersecting closed loops, terminating on dislocations or on DW's. Similar results were obtained also by other authors.[2,3]

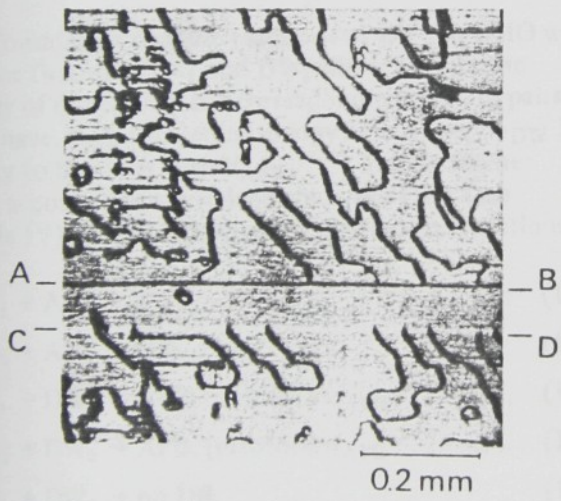

FIGURE 7 Photomicrograph of an etched *c* surface of the gadolinium molybdate crystal taken in reflected light by Barkley and Jeitschko.[1] The conic pits mark dislocations exiting the surface, the straight line grooves along A–B and C–D correspond to 180° domain walls and curved trench-like pits are antiphase boundaries. In the area ABCD with positive surface charge no antiphase boundaries were revealed due to a relatively fast etching of this region.

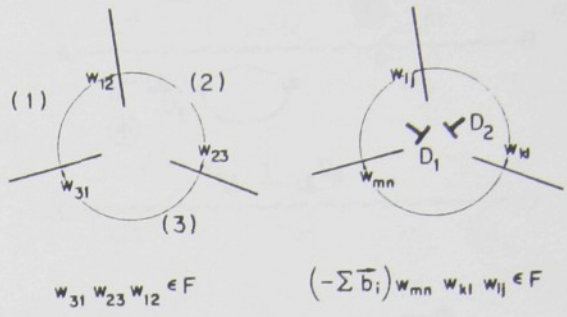

FIGURE 8 Closure relations.

Domain walls cannot interrupt inside the material; the crystal can, therefore, be always divided into rotation domains. From Figure 6 we infer, however, that if the crystal contains junctions of APB's with DW's or imperfect dislocations that turn into perfect ones in the disordered phase, the concept of translation domains loses its sense.

For discussing different types of one-dimensional junctions a simple device, which we shall call closure relation, is useful. Let us consider first a perfect crystal in which we draw a closed circuit that intersects DB's between domains (see the left part of Figure 8). The corresponding twinning operations w_{12}, w_{23}, w_{31} fulfil the relation $w_{31} w_{23} w_{12} \in F$. It expresses the fact that transformations corresponding to all successive intersections of the loop with DB's bring us to a position equivalent to the point of departure. When the crystal contains dislocations D_1, D_2, . . . we make the closed loop in the "good" parts of the crystal (see the right part of Figure 8). Though domains may not be uniquely determined in this case, DB's and corresponding operations w_{ij}, w_{kl}, w_{mn} are well defined. The successive application of these operations brings us to a point which is removed from a position equivalent to the starting point by negative sum of the Burgers vectors of all dislocations enclosed inside the loop. Then the closure relation can be written in the form

$$\left(-\sum_i \mathbf{b}_i\right) w_{mn} w_{kl} w_{ij} \in F. \tag{9}$$

Applying (9) to GMO we can infer, e.g., that the mismatch caused by an imperfect dislocation with $\mathbf{b} = (E \mid 100)$ can be accommodated either by an APB with $w_{(+\alpha \mid +\beta)} = (E \mid 100)$, since $(E \mid 100)(E \mid 100) = (E \mid 200) \in F$ (loop *a* in Figure 6), or by two non-equivalent DW's with $w_{(+\alpha \mid -\beta)} = (2_x \mid \frac{1}{2}\frac{1}{2}0)$ and $w_{(-\alpha \mid +\alpha)} = w_{(+\alpha \mid -\beta)} = (2_x \mid \frac{1}{2}\frac{1}{2}0)$, since for the loop *d* in Figure 6 it holds $(E \mid 100)(2_x \mid \frac{1}{2}\frac{1}{2}0)(2_x \mid \frac{1}{2}\frac{1}{2}0) = (E \mid 200) \in F$ (we use the same Seitz symbols as in Table II). The closure relation for the loop *c* requires

the change of DW_1 into DW_2 at the junction with an APB:

$$W_{(+\alpha|-\beta)}W_{(-\beta|-\alpha)}W_{(-\alpha|+\alpha)} = (2_x|\tfrac{1}{2}\tfrac{1}{2}0)(E|100)(2_x|\tfrac{1}{2}\tfrac{1}{2}0) = (E|200) \in F.$$

All these closure relations hold independently on the position of the DW, i.e. a downward movement of the DW causes extension of the APB (energy consuming process) whereas an upward movement annihilates the APB (energy is released). Observations[1,2] agree with this conclusion. The creation and annihilation of APB's by moving DW's is probably responsible for a well defined threshold field and the linear dependence of the wall velocity on applied field in GMO.[47]

Domain Boundary Reactions

Suppose we have two parallel DB's $(1|j)$ and $(j|k)$ which are close together. They will merge into a single boundary $(1|k)$ if the sum of the surface energies $\sigma_{1j} + \sigma_{jk}$ exceeds the energy σ_{1k} of the resulting DB. If, on the contrary, $\sigma_{1j} + \sigma_{jk} < \sigma_{1k}$ then DB $(1|k)$ would be unstable and would dissociate into separate $(1|j)$ and $(j|k)$ DB's. Formally, the reaction can be written in the form[2]

$$(1|j) + (j|k) = (1|k). \qquad (10)$$

Considering possible reactions of DB's in GMO we notice first that DW_1 and DW_2 differ only in the order of domains in the corresponding domain pairs and have, therefore, equal energy. The energy σ_{DW} is likely to be lower than σ_{APB}.[42,48] Taking further into account the equivalence between DB's (see Table IV) we get the following exothermal reactions:

$$DW_1 + APB \rightarrow DW_2, \qquad (11)$$

$$DW_2 + APB \rightarrow DW_1, \qquad (12)$$

$$DW_1 + DW_1 \rightarrow APB, \text{ (provided } \sigma_{APB} < 2\sigma_{DW}), \qquad (13)$$

$$DW_2 + DW_2 \rightarrow APB, \text{ (provided } \sigma_{APB} < 2\sigma_{DW}), \qquad (14)$$

$$DW_1 + DW_2 \rightarrow \text{no DB}, \qquad (15)$$

$$APB + APB \rightarrow \text{no DB}. \qquad (16)$$

We see that a DW changes into its non-equivalent counterpart when it reacts with an APB. Unlike in the macroscopic approach, when two 180° DW's meet they may not disappear but may form an APB.

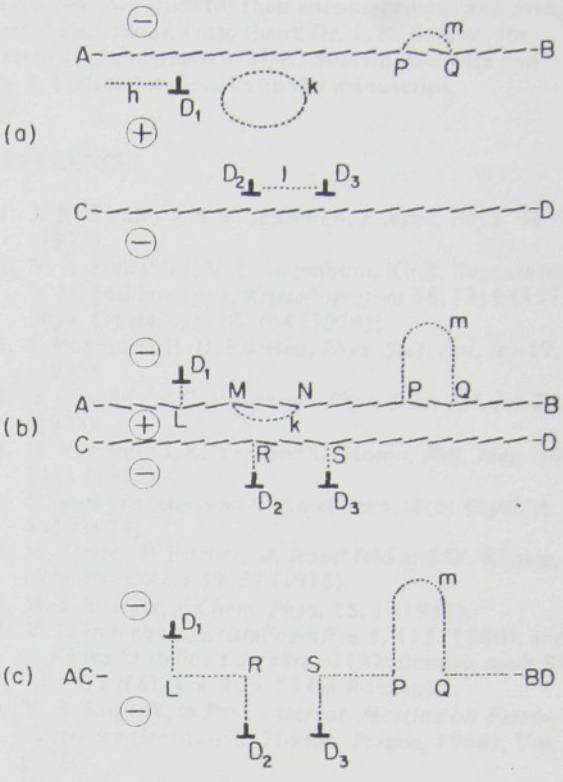

FIGURE 9 Rearrangement of APB pattern by moving domain walls in gadolinium molybdate. D_1, D_2, D_3 are imperfect dislocations, A–B and C–D 180° domain walls; Antiphase boundaries are shown with dotted lines. (a), (b) and (c) show subsequent changes in the APB structure caused by moving domain walls which finally meet along AC–BD.

Only the non-equivalent DW_1 and DW_2 annihilate each other completely†.

The reactions (11)–(16) explain profound changes in the APB pattern caused by moving and interacting DW's. In Figure 9a APB *h* terminates on a dislocation D_1, forms a closed loop *k* and connects dislocations D_2 and D_3. DW changes its character at the junctions P and Q with APB semiloop *m*. In (b) domain walls A–B and C–D have moved towards each other. The loop *k* is partially erased, APB's *h* and *l* have disappeared, but new ones have connected dislocations with DW's. In (c) two DW's have met along AC–BD. In sections RS, PQ walls DW_1 and DW_2 annihilate each other completely; in sections LR, SP DW's of the same type

† Meleshina *et al.*[2] assume that the reaction of a DW and an APB cannot go to completion and treat the "composite boundary" $(+\alpha|+\beta) + (+\beta|-\alpha)$ as a non-equivalent counterpart of the single $(+\alpha|-\alpha)$ DW. Such a composite boundary would, however, be an unstable formation due to an exothermal character of reaction (12). The observed unwillingness of DW to merge with a parallel APB[1] might suggest a large activation energy of the reaction.

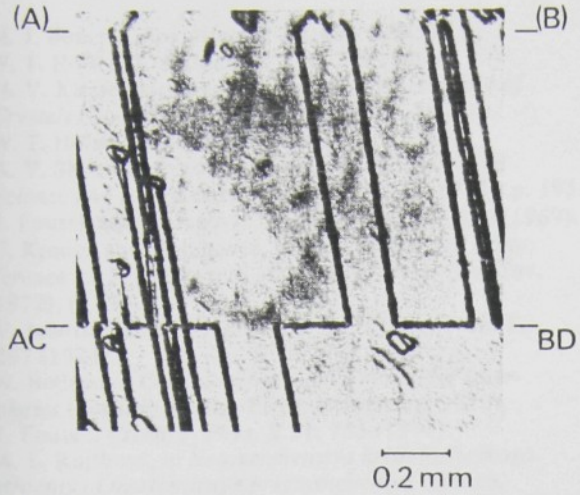

FIGURE 10 Antiphase boundary pattern after encountering two parallel domain walls as observed on the *c* surface of gadolinium molybdate (by courtesy of Barkley and Jeitschko).[1] Two domain walls originally at (A)–(B) and (C)–(D) (below the lower edge—not seen on the photograph) moved towards each other until they have met along AC–BD.

react and produce APB's. The final APB pattern fulfils all geometrical requirements on APB's. Notice that if the DW C–D in (a) would have been of opposite type then the final APB pattern would be different: D_2, D_3 would be interconnected via RS by an APB, there would be no APB's along LR and SP, etc.

Figure 10 shows the APB pattern after encountering two DW's in a real GMO crystal.[1] The similarity between Figures 9c and 10 is evident. The fact that both APB formation and complete annihilation are observed along a line where two 180° DW have met exemplifies the existence of two crystallographically non-equivalent DW's in GMO. Comparing Figures 7 and 10 (taken on two different crystals) we also clearly see the changes in the APB distribution caused by moving and reacting DW's.

In conclusion we note that the translation degeneracy of rotation domains and interactions between DW's, APB's, and dislocations similar to those discussed for GMO are expected to occur in all antiferrodistortive phases. It is just a question of finding suitable experimental techniques which would make them visible and accessible to further examination.

ACKNOWLEDGEMENTS

I am grateful to Prof. W. Känzig and Prof. H. Gränicher for their hospitality at the Solid State Laboratory of the ETH Zürich where this paper was prepared, and further to Prof. R. Blinc, Prof. F. Laves, Dr. E. Wiesendanger, Dr. M. Ziegler and other colleagues for their encouragement and many useful discussions. I also thank Dr. J. R. Barkley for excellent photographs of GMO domain structure and Dr. J. Fousek for remarks on the manuscript.

REFERENCES

1. J. R. Barkley and W. Jeitschko, *J. Appl. Phys.* **44**, 938 (1973).
2. V. A. Meleshina, V. L. Indenbom, Kh.S. Bagdasarov and T. M. Polkhovskaya, *Kristallografiya* **18**, 1218 (1973) [*Sov. Phys. Crystallogr.* **18**, 764 (1974)].
3. J. Bohm and H. D. Kürsten, *Phys. Stat. Sol. (a)* **19**, 179 (1973).
4. B. Capelle and C. Malgrange, *Phys. Stat. Sol. (a)* **20**, K 5 (1973).
5. N. Yamamoto, K. Yagi and G. Honjo, *Phil. Mag.* **30**, 1161 (1974).
6. G. Van Tendeloo and S. Amelinckx, *Acta Cryst. A* **30**, 431 (1974).
7. M. Ziegler, P. Fischer, M. Rosenfeld and W. Känzig, *Helv. Phys. Acta* **49**, 57 (1976).
8. M. J. Buerger, *J. Chem. Phys.* **15**, 1 (1947).
9. V. L. Indenbom, *Kristallografiya* **5**, 115 (1960), and in *Fizika kristallov s defektami* (Akademiya nauk SSSR, Telavi, 1966), Vol. 1, p. 55 (in Russian).
10. V. A. Koptsik, in *Proc. Internat. Meeting on Ferroelectricity* (Institute of Physics, Prague, 1966), Vol. II, p. 20.
11. E. Ascher, *J. Phys. Soc. Japan* **28**, Supplement, 7 (1970).
12. I. S. Zheludev and L. A. Shuvalov, *Kristallografiya* **1**, 681 (1956).
13. L. A. Shuvalov, *J. Phys. Soc. Japan* **28**, Supplement, 38 (1970).
14. I. S. Zheludev, in *Solid State Physics*, edited by H. Ehrenreich, F. Seitz and D. Turnbull (Academic Press, New York, 1971), Vol. 26, p. 429.
15. M. J. Marcinkowski, in *Electron Microscopy and Strength of Crystals*, edited by G. Thomas and J. Washburn (J. Wiley, New York, 1963), p. 334.
16. A. Cimino and G. S. Parry, *Il Nuovo Cimento* **19**, 971 (1961).
17. K. Aizu, *Phys. Rev.* B 2, 754 (1970).
18. E. Ascher, in *Les Transitions de Phase*, 13^e Cours de Perfectionnement de l'Association Vaudoise des Chercheurs en Physique, 1971, p. 133.
19. V. Janovec, *Czech. J. Phys. B* **22**, 974 (1972).
20. F. Jona and G. Shirane, *Ferroelectric Crystals* (Pergamon Press, Oxford, 1962), p. 110.
21. C. J. Bradley and A. P. Cracknell, *The Mathematical Theory of Symmetry in Solids* (Clarendon Press, Oxford, 1972).
22. W. Jeitschko, *Naturwissenschaften* 57, 544 (1970), and *Acta Cryst. B* **28**, 60 (1972).
23. V. Dvořák, *Phys. Stat. Sol. (b)* **45**, 147 (1971).
24. *International Tables for X-ray Crystallography* (Kynoch Press, Birmingham, 1965) Vol. I.
25. K. Aizu, *J. Phys. Soc. Japan* **32**, 1287 (1972).
26. C. Hermann, *Z. Kristallogr.* **69**, 250 (1928).
27. T. Schneider and P. F. Meier, *Physica* **69**, 521 (1973).
28. V. Janovec, to be published.
29. P. Gray, *The Crystalline State* (Oliver and Boyd, Edinburgh, 1972), p. 335.

30. M. J. Buerger, *Am. Mineral.* **30**, 469 (1945).
31. W. T. Holser, *Z. Kristallogr.* **110**, 249 (1958).
32. M. V. Klassen-Neklyudova, *Mechanical Twinning of Crystals* (Consultant Bureau, New York, 1964).
33. W. T. Holser, *Z. Kristallogr.* **110**, 266 (1958).
34. A. V. Shubnikov and V. A. Koptsik, *Symmetry in Science and Art* (Plenum Press, New York, 1974), p. 195.
35. J. Fousek and V. Janovec, *J. Appl. Phys.* **40**, 135 (1969).
36. F. Kroupa and V. Janovec, In *Proc. of the 3rd Conference on High Strength Martensitic Steels* (Havířov, 1972), p. 133.
37. V. Janovec and L. A. Shuvalov, *Int. J. Magnetism* **5**, 297 (1974).
38. W. Bollmann, *Crystal Defects and Crystalline Interphases* (Springer Verlag, Berlin-Heidelberg, 1970).
39. J. Fousek, *Czech. J. Phys. B* **21**, 955 (1971).
40. A. L. Rojtburd, in *Nesovershenstva kristallicheskogo stroeniya i martensitnye prevrashcheniya* (Nauka, Moskva, 1972), p. 7 (in Russian).
41. J. Sapriel, *Phys. Rev. B* **12**, 5128 (1975) and these Proceedings.
42. L. L. Boyer and J. R. Hardy, *Solid State Commun.* **11**, 555 (1972).
43. V. Janovec and E. Dvořáková, *Subgroups of Crystallographic Point Groups: Conjugation, Normalizers, Left and Double Coset Decompositions* (Report V-FZU 75/1 of the Institute of Physics, Prague, 1974). Available on request.
44. B. Březina dna M. Glogarová, *Phys. Stat. Sol. (a)* **11**, K39 (1972).
45. E. Wiesendanger, *Czech. J. Phys. B* **23**, 91 (1973).
46. J. W. Christian, *The Theory of Transformations in Metals and Alloys* (Pergamon Press, Oxford, 1965).
47. A. Kumada, *Phys. Letters A* **30**, 186 (1969).
48. A. Fousková and J. Fousek, *Phys. Stat. Sol. (a)* **32**, 213 (1975).

Ferroelectrics, 1981, Vol. 35, pp. 105–110
0015-0193/81/3501-0105/$06.50/0

SYMMETRY AND STRUCTURE OF DOMAIN WALLS

VÁCLAV JANOVEC
Inst.of Physics, Czech.Acad.Sci., Na Slovance 2, 18040 Prague, Czechoslovakia

Abstract Symmetries of domain pairs and domain twins are described by black & white space and layer groups, resp. Domain walls (DW´s) are represented by paths in order parameter space which determine their structure and symmetry. Symmetry aspects of phase transitions of DW´s, lattice pinning of DW´s and some properties of DW lattices in incommensurate phases are discussed.

Domain wall (DW) is a slice of structure that accommodates structures of two neighboring domains. It is a defect of incomplete symmetry reduction that can be conveniently discussed in symmetry terms. We shall use ammonium fluoroberyllate (AFB) in commensurate and incommensurate phases for illustration of our exposition.

SINGLE DOMAIN STATES, DOMAIN PAIRS AND TWIN LAWS

A commensurate distorted phase, formed from a parent phase of symmetry G, can be realized in homogeneous single domain states D_i with symmetry groups F_i, $i = 1,2,\ldots n$. For AFB $G = Pnam$, $n = 4$, $F_1 = F_3 = -Pn2_1a$ (with spontaneous polarization $P_y < 0$), $F_2 = F_4 = +Pn2_1a$ ($P_y > 0$) and cell doubling along x (Fig. 1).

Simplest non-homogeneous state is a domain twin consisting of domains D_i, D_j and a DW denoted W_{ij}. DW is inseparable from the twin, namely DW symmetry is that of th twin. Basic twin characteristic, the twin law, specifies relation between structures of D_i and D_j and can be determined e.g., by optical or X-ray methods. Symmetrically, it is described by a group J_{ij} of symmetry operations (SO´s) of G that bring a domai pair, consisting of D_i and D_j extended into entire space, into coincidence with itself. J_{ij} assembles SO´s $F_i \cap F_j = F_{ij}$ that retain both D_i and D_j , and SO´s, e.g., i'_{ij}, that transform D_i into D_j and, simultaneously, D_j into D_i (exchange of D_i and D_j results in an indistinguishable domain pair):

$$J_{ij} = F_{ij} + i'_{ij}F_{ij} = F_{ij} + I'_{ij} \quad . \tag{1}$$

J_{ij} can be treated as a black & white space group.[1,2] This description,which is a generalization of designating twin laws of merohedry and reticular merohedry by black & white point groups[3] enables one to classify domain pairs. E.g., if F_{ij} is a polar group and J_{ij} is non-polar the domain pair is ferroelectric (in AFB $F_{12} = P11a$, $J_{12} = +P11(2/a)$), if J_{ij} is based on a black & white Bravais lattice[1] domain pair is translational (antiphase) one ($J_{13} = P'n2_1a$ in AFB). J_{ij} allows also to classify domain pairs in Friedel´s nomenclature[4] and establish relation between domain twins and twins of classical crystallography: with the exception of cubic reticular merohedry all types of triperiodic twins can be found between domain pairs and can be treated as resulting from (hypothetical) phase transitions. On the other hand, some types of domain pairs, e.g., translational or with $I'_{ij} = 0$, which have not been considered in classical twinning, occur in domain structures.

TWIN WITH ZERO THICKNESS DOMAIN WALL

consists of a planar DW of zero thickness, W^o_{ij}, placed at x =0, a domain D_i occupy half-space $x < 0$ and domain D_j filling up half-space $x > 0$. We shall consider only twins with coherent DW's. This condition is fulfilled in non-ferroelastic domain pairs for any orientation of W^o_{ij}. For most of ferroelastic domain pairs there are two perpendicular orientations of coherent W^o_{ij}.[5,6]

Symmetry group T^o_{ij} of the twin (and W^o_{ij}) is a layer group[2,7] since SO's of the twin must preserve a two-dimensional net common to lattices of D_i and D_j and translations along x are not allowed. T^o_{ij} consists of a plane group X^o_{ij} that leaves D_i, and sign x unchanged, and of complex Y^o_{ij} that exchanges D_i, D_j and, simultaneously, half-space $x < 0$ and $x > 0$:

$$T^o_{ij} = X^o_{ij} + Y^o_{ij} = X^o_{ij} + \underline{t}'_{ij} X^o_{ij} \quad , \tag{2}$$

where $\underline{t}'_{ij} \in Y^o_{ij}$. T^o_{ij} can be interpreted as a black & white layer group.[8]

A sectional layer (plane) group $\bar{K}$ ($\vec{\bar{K}}$) of a space group K assembles SO's of K that leave a chosen plane (and its normal) invariant.[7] Relation between T^o_{ij} and the sectional layer group $\bar{J}_{ij}$ along W^o_{ij} is revealed by decomposition

$$\bar{J}_{ij} = \vec{\bar{F}}_{ij} + \underline{t}'_{ij}\vec{\bar{F}}_{ij} + \underline{r}_{ij}\vec{\bar{F}}_{ij} + \underline{s}'_{ij}\vec{\bar{F}}_{ij} = T^o_{ij} + R^o_{ij} \quad , \tag{3}$$

where $\underline{r}_{ij}$ exchanges half-spaces but leaves D_i, D_j invariant whereas $\underline{s}'_{ij}$ exchanges D_i, D_j but preserves sign x. R^o_{ij} changes the twin into the inverse twin in which $x < 0$ half-space is occupied by D_j and $x > 0$ by D_i . $\vec{\bar{F}}_{ij} = X^o_{ij}$. $\bar{J}_{ij}$ expresses symmetry of DW central structure that accommodates D_i and D_j. For $F_i = F_j$, $\bar{G} \geqslant \bar{J}_{ij} > \bar{F}_i$, i.e., DW is a failure to accomplis complete symmetry reduction in a plane. Conversely, each plan that lowers its sectional layer symmetry at the transition i a potential DW.

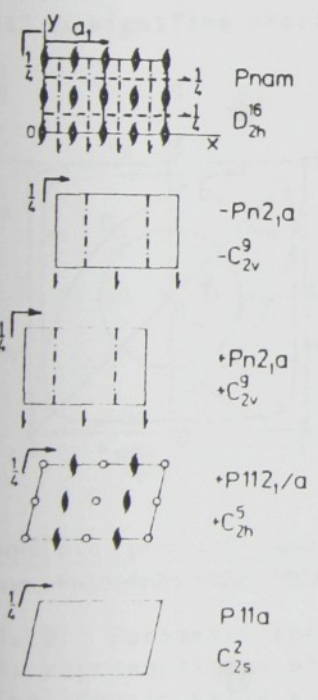

FIG. 1 Symmetries of distorted structures in AFB

We discriminate symmetric ($Y^o_{ij} \neq 0$) and asymmetric ($Y^o_{ij} = 0$), invertible ($R^o_{ij} \neq 0$) and non-invertible ($R^o_{ij} = 0$) twins. A non-invertible twin, e.g., a charged ferroelectric DW, is not crystallographically equivalent with inverted twin in particular they possess different DW energies, $\mathcal{E}_{ij} \neq \mathcal{E}_{ji}$.

Groups $\bar{J}_{ij}$, T^{o}_{ij} depend on the orientation and position of W^{o}_{ij} in the structure D_i since SO's t_{ij} and r_{ij} are available in special positions only. The DW energy changes, therefore, with position and this is the reason of lattice pinning and activation energy of DW's.[9] For ferroelectric W^{o}_{12} in AFB we get $\bar{J}_{12} = T^{o}_{12} = p\bar{1}'$, $pll2_1'$ or pl for W^{o}_{12} at position 0, $a_1/2$, elsewhere, resp. This twin is non-invertible, $\varepsilon_{12} \neq \varepsilon_{21}$! For antiphase boundary (APB) W^{o}_{13} is $\bar{J}_{13} = pn2_1m$ at $a_1/4$ or $3a_1/4$ and and $\bar{J}_{13} = 11m$ elsewhere; $T^{o}_{13} = pn'll$, $pl2_1'1$ and pl at $a_1/4, 3a_1/4$ and elsewhere, resp. Twin is invertible. Ferroelectric DW's in gadolinium molybdate provide an example of asymmetric DW's.[10]

FINITE THICKNESS DOMAIN WALLS: SYMMETRY, STRUCTURE AND PHASE TRANSITIONS

Structure of a DW of finite thickness can be conveniently discussed in the space of order parameter which has for AFB two components p and q[11] (Fig. 2). Single domain states are represented by points 1,2,3,4, and a smoothly varying structure of a DW, bridging domain D_i with D_j, by an oriented path connecting point i with j. To each position x in real space there corresponds a point p(x),q(x) on the path (homotopy mapping) which describes the local structure in DW. The rate of the structure change with position can be expressed by function

$$h(x) = \left((dp/dx)^2 + (dq/dx)^2 \right)^{1/2} . \qquad (4)$$

Small h signifies nearly homogeneous "inside domain" region whereas maximum h corresponds to DW centre.

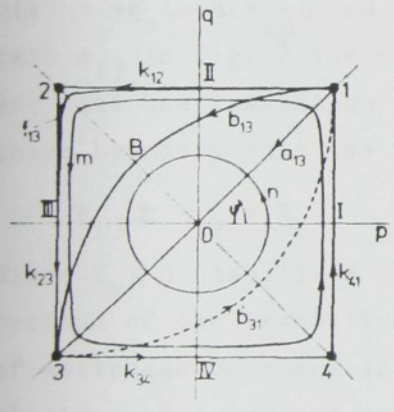

p=q=0	p=q	p=-q	p=0	q=0	p,q
Pnam	-Pn2$_1$a	+Pn2$_1$a	-P11$2_1$/a	-P11$2_1$/a	P11a

FIG. 2 Parameter space of AFB: representation of domains, domain walls and incommensurate structures. Local symmetries.

To each point of p,q space there corresponds certain symmetry $E_m(p,q)$ of homogeneous distorted structure (Fig. 2 below). E_m are just the epikernels[12] of the representation inducing the phase transition. The local symmetry at position x in DW can be described by three-dimensional space group $E_m(p(x),q(x))$ only if h(x) is small. At positions with high h the local symmetry should be described by the sectional layer group $\bar{E}_m(p(x),q(x))$.

The actual structure of a DW can be determined from the condition of minimum energy This task can be, however, accomplished for $n > 2$ only in special cases. Thus for the ferroelectric DW W_{12} the solution $p(x) = -p_o \tanh x/d$, $q(x) = q_o$ (path k_{12} in Fig. 2), with d characterizing DW thickness, has

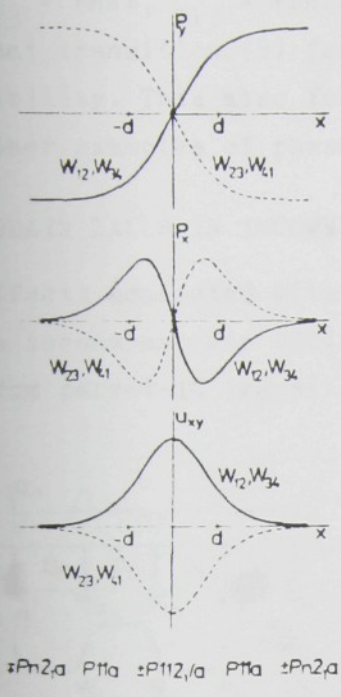

FIG. 3 Structure of ferroelectric domain walls

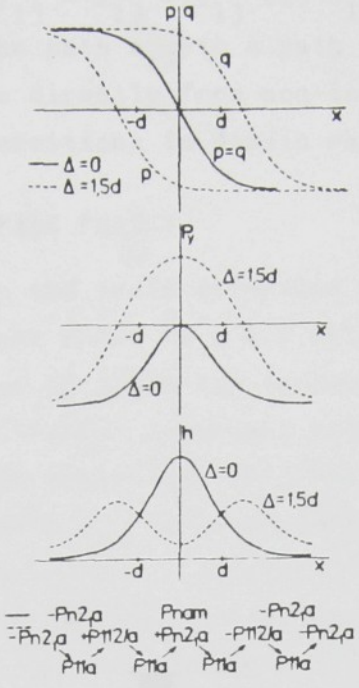

FIG. 4 Structure of an antiphase boundary

been found.[13] Relations $P_y \sim pq$, $P_x \sim pq(p^2 - q^2)$, $u_{xy} \sim (p^2 - q^2)$ yield spatial variations of polarization components and shear deformation u_{xy} (Fig. 3). We see that the main features of these dependences follow directly from the sequence of local symmetries. Inequality $\varepsilon_{12} \neq \varepsilon_{21}$ is caused by Lifshitz invariant which has not been considered in above solutions. It can be justified in the approximation of constant amplitude $p^2 + q^2$.[14]

Fig. 4 illustrates the situation in antiphase boundary W_1 for which the solution[13]

$$p(x) = -p_o \tanh(x + \Delta)/d ,$$

$q(x) = -q_o \tanh(x - \Delta)/d$ has been utilized. Solution with $\Delta = 0$ is associated with path a_{13} in Fig. 2 whereas $\Delta = 1{,}5$ d corresponds to path f_{13}. From h(x) we clearly see that the transition from path a_{13} to f_{13} represents a dissociation of one antiphase boundary into two ferroelectric DW's:

$$W_{13} \rightleftarrows W_{12} + W_{23} \quad . \tag{5}$$

Since $E_y < 0$ stabilizes path a_{13} and $E_y > 0$ favores paths of type f_{13} or b_{13} the direction of the transition (5) can be controlled by electric field. Both splitting of antiphase boundary into two ferroelectric DW's [15] and association of two ferroelectric DW's into an antiphase boundary in electric field [16,17] have been observed in gadolinium molybdate.

Global symmetry T^e_{ij} of DW W^e_{ij} with path e consists of SO's that transform the entire DW (twin) into itself. T^e_{ij} is a layer group of the same structure as T^o_{ij} (see Eq.(2)) though $T^e_{ij} \leq T^o_{ij}$, since T^e_{ij} must, in addition, preserve the path e. Group J_{ij} is replaced by symmetry C^e_{ij} of DW central structure determined by a point of e stable under T^e_{ij} (e.g., points II and B on k_{12} and b_{13}, resp.). Invertibility of W^e_{ij} is determined by C^e_{ij}. For the ferroelectric W_{12} in AFB $C^k_{12} = +P112'_1/a = J_{12}$,

$T_{12}^{k} = T_{12}^{o} = \bar{C}_{12}^{k}$, W_{12}^{k} is non-invertible. For antiphase boundary W_{13} we get $C_{13}^{a} = Pnam$, $C_{13}^{b} = +Pn2_1a$, $T_{13}^{a} = T_{13}^{b} = T_{13}^{o}$ but $\bar{C}_{13}^{b} = T_{13}^{b} < \bar{C}_{13}^{a} = \bar{J}_{13}$. This means that transition (5) from the path a_{13} to a path b_{13} is accompanied by lost of invertibility. This also follows directly from non-invertible character of W_{12} and W_{23}. Other examples of phase transitions in domain walls have been discussed elsewhere[18,19].

DOMAIN WALLS IN INCOMMENSURATE PHASES

Effects connected with DW's and their structure have the best chance to be observed in incommensurate (IC) phases where DW's are relatively thick and numerous. Far enough from parent-IC transition an IC phase can be considered as a lattice of DW's.[14] Lifshitz invariant reduces in the IC phase the energy of ferroelectric DW's but not of antiphase boundaries (for path a_{13} is Lifshitz invariant inactive). Antiphase boundaries are, therefore, excluded from participation in the DW lattice. Due to non-invertible character of ferroelectric DW's either sequence α with increasing indices (anticlockwise sense of representative loops m or n of IC phase in Fig. 2) or β with decreasing indices (clockwise sense of representative loops) is realized (Fig. 5). Average value of any spontaneous quantity taken over the lattice period L is zero, hence the macroscopic symmetry of this regular phase is that of the parent phase (mmm for AFB).

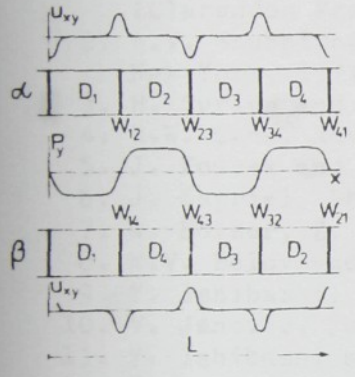

FIG. 5 Lattice of domain walls in the incommensurate phase of AFB.

Electric field $E_y < 0$ shifts W_{12} towards W_{23} and W_{34} towards W_{41} enhancing thus relative volume of odd domains with $P_y < 0$ on the expense of even domains with $P_y > 0$ and, simultaneously, increasing the period L ($L \to \infty$ for $E_y = E_c$). For high enough fields (but lower than E_c) one can visualize a situation where ferroelectric DW's associate into antiphase boundaries forming thus a lattice of antiphase boundaries with domains of the same polarity. Possibility of such an arrangement has been confirmed by calculations in constant amplitude approximation.[20] When the field is switched off antiphase boundaries dissociate in ferroelectric DW's which tend to restore the original DW configuration. Since DW's can be pinned in some intermediate positions the average polarization remains non-zero and the macroscopic symmetry is m2m. This provides an alternative explanation of hystereses loops observed in IC phases.[21]

A shear stress $\sigma_{xy} > 0$ favores central structure of W_{12} and W_{34} and depresses that of W_{23} and W_{41} (sequence α). For high σ_{xy} one can envisage a situation when

favored central structures II and IV turn into domains D_{II}, D_{IV} separated by antiphase boundaries $W_{II\ IV}$, $W_{IV\ II}$. After removing σ_{xy} the original structure may no fully recover leaving the average $u_{xy} \neq 0$ and macroscopic symmetry 112/m. This migh explain observed hystereses of the quadrupole moment component q_{xy} and anomalies of q_{xy}/σ_{xy}.[22]

ACKNOWLEDGEMENTS

The author expresses sincere thanks to V. Dvořák, O. Hudák, J. Petzelt and Z. Zikmund for many useful discussions and permission to quote some of unpublished result

REFERENCES

1. C.J. Bradley and A.P. Cracknell, The Mathematical Theory of Symmetry in Solids (Clarendon Press, Oxford, 1972).
2. A.V. Shubnikov and V.A. Kopcik, Symmetry in Science and Art (Plenum Press, New York, 1974).
3. H. Curien and Y. Le Corre, Bull. Soc. franc. Minér. Crist., 81, 126 (1958).
4. R.W. Cahn, Advances in Physics, 3, 363 (1954).
5. J. Fousek and V. Janovec, J. Appl. Phys., 40, 135 (1969).
6. J. Sapriel, Phys. Rev B, 12, 5128.
7. W. Holser, Z. Kristallogr., 110, 249 (1958).
8. N.V. Belov and T.N. Tarkhova, Kristallografiya, 1, 4 (1956).
9. Y. Ishibashi, J. Phys. Soc. Japan, 46, 1254 (1979).
10. V. Janovec, Ferroelectrics, 12, 43 (1976).
11. Y. Ishibashi and V. Dvořák, J. Phys. Soc. Japan, 44, 32 (1978).
12. E. Ascher, J.Phys. C: Solid State Phys., 10, 1365 (1977).
13. Y. Ishibashi and V. Dvořák, J. Phys. Soc. Japan, 41, 1650 (1976).
14. A.D. Bruce, R.A. Cowley and A.F. Murray, J. Phys. C: Solid State Phys., 11, 3591(1978).
15. N. Yamamoto, K. Yagi and G. Honjo, phys. stat. sol.(a) 62, 657 (1980).
16. J.R. Barkley and W. Jeitschko, J. Appl. Phys., 44, 938 (1973).
17. V.A. Meleshina, V.L. Indenbom, Kh.S. Bagdasarov and T.M. Polkhovskaya, Kristallografiya, 18, 1218 (1973).
18. J. Lajzerowicz and J.J. Niez, in Solitons and Condensed Matter Physics, Editors A.R. Bishop and T. Schneider (Springer, Berlin,1978), p. 195.
19. J. Lajzerowicz and J.J. Niez, J. Physique Lett., 40, L-165 (1979).
20. O. Hudák, submitted to J. Phys. C: Solid State Phys.
21. K. Hamano, Y. Ikeda, T. Fujimoto, K. Ema and S. Hirotsu, J. Phys. Soc. Japan, 49, 2278 (1980).
22. V.V. Gladkij, S.N. Kallayev, V.A. Kirikov and L.A. Shuvalov, Ferroelectrics, 26, 813 (1980).

Ferroelectrics, 1986, Vol. 66, pp. 169–187
0015-0193/86/6604-0169/$20.00/0

PERFECT DOMAIN TEXTURES OF INCOMMENSURATE PHASES

V. JANOVEC and V. DVOŘÁK

Institute of Physics, Czechoslovak Academy of Sciences, Prague 8, Na Slovance 2, 180 40, Czechoslovakia

(*Received March 18, 1985*)

Domain textures of typical incommensurate phases are constructed as regular domain structures formed by equivalent domain walls of minimum negative energy. Structures with two or three modulation waves can form several stripe textures and textures periodic in two or three directions. Equivalent textures can coexist as textural blocks. Symmetry properties of perfect domain textures are discussed.

I INTRODUCTION

An incommensurate structure[1,2] often appears as an intermediate phase in the phase sequence commensurate (C)—incommensurate (I)—parent (P) phase observed at heating. Usually, the C phase can be described by an order parameter η specifying the structural difference between C and P phases. The C structure can be always built up in several equivalent orientations and/or positions. These equivalent C structures, which we shall call domain states (DS's) have the same energy but different values of η. Different DS's can coexist forming a domain structure with η taking DS values in relatively large areas (domains) separated by relatively narrow transient regions (walls) with a steep change of η.

The I phase is a spatially modulated structure that can be described by periodically varying η. Just below the P–I transition this modulation is usually almost sinusoidal. On cooling, the modulation wave length increases and the form of the modulation changes so that regions with structures close to DS are expanding and regions with intermediate structures are shrinking. If the intermediate regions become much smaller than the modulation period the I structure can be viewed as a regular domain structure in which almost commensurate regions are identified with C domains and the transient regions (discommensurations) with walls. This structure, which we shall call a *domain texture*[3] *of the* I *phase* (DTI), allows to visualize and treat complicated situations, e.g., I structures modulated in several directions, defects in I structures, textural transitions, etc.

In this contribution we confine ourselves to the determination of possible topologically different forms of perfect domain textures in typical I systems. To illustrate symmetry properties of walls we include a trivial example (sodium nitrite) and in two cases (krypton monolayer on graphite, quartz) recover well known results. Our consideration is based mainly on symmetrical and geometrical arguments and is therefore, independent on the model or approximation. First we remind necessary facts about domain structures and then outline the idea of the procedure.

II DOMAIN STRUCTURE OF THE COMMENSURATE PHASE

The appearance of C *domain states* (DS's) is a consequence of symmetry lowering at the P–C transition and different DS's are related by symmetry operations lost at this transition. DS's related by lost translations form *classes of translational* DS's. The DS's from the same class have unit cells of the same orientation and we say that they belong to the same *orientational state*. DS's belonging to the same orientational state have the same macroscopic properties whereas DS's belonging to different orientational states differ in some spontaneous tensor components.

The number of orientational states equals $n_0 = n_P : n_C$, where n_P and n_C are orders of the point groups of the P and C phases, resp. and the number of translational DS's within each orientational state is $d_t = N_C : N_P$, where N_C and N_P are numbers of molecules in the primitive unit cell of the C and P phase, resp. The total number n of DS's equals

$$n = n_0 d_t = (n_P : n_C)(N_C : N_P) \tag{1}$$

and can be, therefore, determined from the symmetry groups of the P and C phases.[4,5]

A DS will be labelled A_a, where A signifies the orientational state and the subscript a (translational index) denotes the translational DS within A. We shall use integers for labelling, $A = 1, 2, \ldots, n_0$, $a = 1, 2, \ldots, d_t$. If possible the same translational index is used for DS's related by point group operations. In the order parameter space the DS's are represented by points.

A C *domain* is a DS restricted to a certain region demarcated by the surface or by walls. A planar *domain wall* (W) is specified by domain A_a on the negative side and by domain B_b on the positive side of the wall normal $\mathbf{n}$ which also determines the orientation of the wall.

We shall use for such wall the symbol $A_a/\mathbf{n}/B_b$ or simply A_a/B_b if the orientation is clear from the context or if it is not significant.

In this abbreviated symbol the domain on the left adheres to the negative end of $\mathbf{n}$ and domain on the right to the positive end of $\mathbf{n}$. The wall carries an energy σ per unit area.

The wall has diperiodic symmetry that can be expressed by a layer group.[6–8] This symmetry and also the wall energy σ depend on the orientation and also on the position of the wall center in the lattice. We shall say that a wall has a symmetrically *prominent orientation* if a small deviation from this orientation is accompanied by lowering of the wall symmetry. The energy σ has an extreme for a prominent orientation. Prominent orientation is thus a necessary condition for a wall to have in equilibrium a fixed crystallographical position.

Two *walls* $A_a/\mathbf{n}_1/B_b$ and $C_c/\mathbf{n}_2/D_d$ are *crystallographically equivalent*, $A_a/\mathbf{n}_1/B_b \simeq C_c/\mathbf{n}_2/B_b$, if there exists such an operation g from the parent group that

$$C_c = gA_a, \qquad D_d = gB_b, \qquad \mathbf{n}_2 = g\mathbf{n}_1. \tag{2}$$

Equivalent walls have the same energy σ and their symmetry groups are conjugate under g. In special cases equivalent walls can have the same wall orientation but differ in adhering domains or can join the same two domains but differ in wall orientation.

We say that the wall $A_a/\mathbf{n}/B_b$ is *reversible* if

$$A_a/\mathbf{n}/B_b \simeq B_b/\mathbf{n}/A_a = A_a/-\mathbf{n}/B_b \tag{3}$$

or shortly $A_a/B_b \simeq B_b/A_a$. Then the wall A_a/B_b and the reversed wall B_b/A_a have the same energy σ and the same symmetry. If $A_a/B_b \neq B_b/A_a$, i.e., if (3) does not hold, the wall is called *irreversible*. In this case σ of the reversed wall B_b/A_a is different from that of the original wall A_a/B_b though both have the same symmetry.[8]

In the order parameter space a wall $A_a/\mathbf{n}/B_b$ is represented by an oriented path connecting point A_a with B_b.

III DOMAIN TEXTURES OF INCOMMENSURATE PHASES

In contrast to walls in the C phase which have positive energy σ the walls in the I phase carry negative σ. The equilibrium domain texture of the I phase is determined by competing negative energy of walls tending to increase the density of walls and repulsive interaction between walls trying to increase the wall distance; in I structures modulated in several directions the energy of wall intersections must be also taken into account.[9] With the exception of C phases with two DS's only (sodium nitrite, quartz) the negative contribution to σ is provided by the Lifshitz invariant.[1]

An ideal DTI is composed from walls with minimum negative energy σ. Up to rare exceptions (see the example of sodium nitrite) walls with equal σ are crystallographically equivalent. Our basic assumption is that possible DTI's are just different regular domain patterns that can be formed from all equivalent walls with minimum energy. To find all possible types of DTI we perform the following steps:

(i) Find all DS's and their representative points in the order parameter space.

(ii) Find a wall W^- with minimum negative σ. This is a difficult variational task which we replace by the following reasoning: Starting from a chosen DS, say 1_1, we look for the nearest DS to which Lifshitz invariant "drives" the representative point in the order parameter space. Simultaneously we examine for which orientation is the contribution from Lifshitz invariant the largest.

(iii) Find all walls that are crystallographically equivalent with W^- (e.g., by applying all symmetry operations of the P phase on W^-).

(iv) From these walls construct a regular pattern which represents a possible DTI.

(v) If this texture does not contain all DS's and all equivalent walls W^- construct another DTI starting with one of the missing equivalent walls.

Now we apply this procedure to concrete examples.

IV EXAMPLES OF DOMAIN TEXTURES OF INCOMMENSURATE PHASES

1) Structures Modulated in One Direction

Sodium nitrite. Represents the simplest conceivable case. The symmetry group of the P phase is Immm (D_{2h}^{25}) and that of the C phase Im2m (C_{2v}^{20}). Both P and C

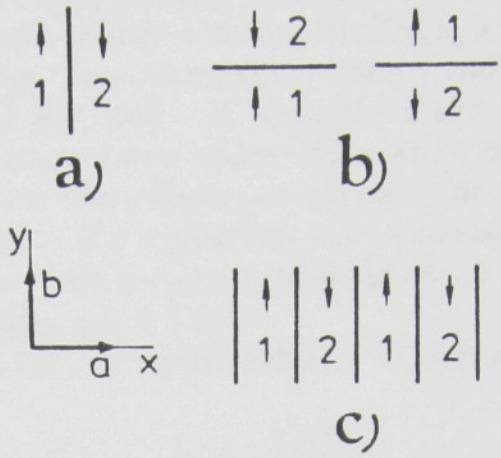

FIGURE 1 Domain walls and stripe texture of sodium nitrite. a) reversible domain walls, b) irreversible domain walls, c) stripe texture.

phases have two molecules in the unit cell, hence there are just two orientational states 1, 2 that can be associated with spontaneous polarization $+P_s$, $-P_s$, resp.

The order parameter has one real component (spontaneous polarization). There is no Lifshitz invariant which would determine the orientation of a wall with negative energy and the domain sequence in this wall. We can, therefore, discuss only the symmetry properties of walls with different orientations and consider their ability to form domain textures. It is easy to corroborate that the wall 1/2 has three prominent orientations with wall normals [100], [001] and [010] (e.g., for [100] orientation the mirror (001) and the 2-fold axis along [001] are the symmetry elements of the wall—see Figure 1a). Moreover, the walls with [100] and [001] orientations are reversible since the 2-fold axis along these normals transforms the wall 1/2 into an equivalent wall 2/1. Due to this property we can form a regular sequence of parallel equivalent walls. This type of DTI called a *stripe texture*—which corresponds to I modulation in $NaNO_2$—is depicted in Figure 1c. The wall 1/2 with [010] orientation is irreversible since there is no operation available that would transform 1/2 into 2/1 (see Figure 1b). Although these two walls are not equivalent (one carries positive and the other negative charge) they have the same energy since free energy density is invariant with respect to space inversion. Equivalent walls with noncrystallographical orientation are not parallel and do not allow to form a stripe texture.

No direct experimental evidence of DTI in $NaNO_2$ is available. In the C phase, however, the etching technique and X-ray topography have revealed a layered domain structure of the [100] orientation with fluctuating distances between parallel and rather thick walls.[10]

Similar conclusions hold for thiourea with Pnma and $P2_1ma$ symmetries of P and C phases, resp.

Rubidium tetrachlorzincate. Many crystals with general formula A_2BX_4 exhibit I phases. The common symmetry of the P phase is Pnma (D_{2h}^{16}), the C phase has polar orthorhombic structure of the C_{2v}^{9} symmetry with unit cell d_t times enlarged along the **a** direction. Thus, e.g., $d_t = 2$ for $(NH_4)_2BeF_4$, $d_t = 3$ for Rb_2ZnCl_4 and

K_2SeO_4, $d_t = 5$ for $[N(CH_3)_4]_2ZnCl_4$. Since the domain texture of $(NH_4)_2BeF_4$ has been already analyzed[6] we shall consider Rb_2ZnCl_4 as an example. Its C phase has the space group $Pn2_1a$. Two orientational states 1 and 2 can be associated with spontaneous polarization $+P_s$ and $-P_s$ along the b axes. There are three translational DS's in each orientational state and six DS's can be labelled $1_1, 1_2, 1_3, 2_1, 2_2, 2_3$.

The order parameter has two complex conjugate components $Q = r\exp(i\varphi)$, Q^* that transform according to the irreducible representation with the wave vector $\mathbf{k} = \frac{1}{3}\mathbf{a}^*$. The values of the phase φ corresponding to all DS's as well as the symmetry relations between DS's are given in Table I.

The existence of the I phase is connected with Lifshitz invariant

$$\Lambda = \lambda r^2 \frac{\partial \varphi}{\partial x} \tag{4}$$

with x along **a**. If we suppose $\lambda < 0$ then Λ provides the largest negative contribution for walls with the normal $\mathbf{n} = [100]$ and with a positive increment in φ. From Table I we find six equivalent walls with paths fulfilling this condition

$$1_1/2_3 \simeq 2_3/1_2 \simeq 1_2/2_1 \simeq 2_1/1_3 \simeq 1_3/2_2 \simeq 2_2/1_1. \tag{5}$$

All these walls are obviously irreversible ferroelectric walls since the Lifshitz invariant (4) is not invariant with respect to $x \to -x$. By repeating the wall sequence (5) one can form a regular layered domain structure that represents the I phase. This stripe texture is sketched in Figure 2a. It is not possible to construct from the set (5) any other sequence of walls that could be regularly repeated, hence there exists just one possible stripe texture of this kind.

A closer analysis (similar to that performed for $(NH_4)_2BeF_4$[6]) of the wall symmetry shows that $\mathbf{n} = [100]$ is not a prominent orientation for the single wall $1_1/2_3$. The orientation corresponding to minimal wall energy is rotated away from this crystallographic direction (this is caused by anisotropy of quadratic terms in spatial derivatives of φ). Crystallographically equivalent walls are then not parallel (see Figure 2b) and cannot form a perfect stripe texture. We also notice that the inclined walls are charged. A stripe structure composed from inclined parallel walls would contain non-equivalent walls (see Figure 2c). Applying to this structure the lost 2-fold screw axis along x we get an equivalent stripe structure in which each

TABLE I

Rubidium tetrachlorzincate: Domain states A_a and their representation in the order parameter space $Q = r\exp(i\varphi)$. The operation g (given in the Seitz symbol related to the basis vectors of the P phase) relates A_a with the domain state 1_1, $A_a = g1_1$. P_s is the spontaneous polarization along b axis

A	1_1	1_2	1_3	2_1	2_2	2_3
g	$(1\|000)$	$(1\|100)$	$(1\|200)$	$\left(m_y\|0\frac{1}{2}0\right)$	$\left(m_y\|1\frac{1}{2}0\right)$	$\left(m_y\|2\frac{1}{2}0\right)$
φ	$\pi/6$	$5\pi/6$	$9\pi/6$	$7\pi/6$	$11\pi/6$	$3\pi/6$
P_s	+	+	+	−	−	−

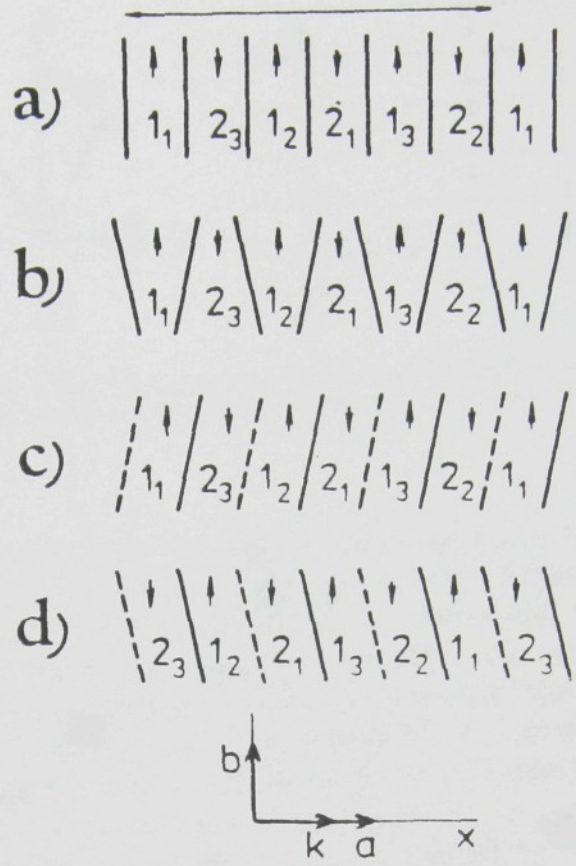

FIGURE 2 Stripe textures in rubidium tetrachlorzincate. a) sequence of equivalent walls perpendicular to [100] direction, b) sequence of equivalent walls with inclined orientation, c), d) sequences of parallel inclined walls; solid and dashed walls are not equivalent. **a**, **b** are basic vectors of the P phase.

wall appears shifted and with opposite inclination (see Figure 2d). These two structures have equal energy, hence the stripe texture with walls normal to [100] direction has extreme (minimal or maximal) energy. We see that whereas the individual wall has an inclined orientation the walls in a regular collection may prefer a crystallographic orientation. This collective feature is conditioned by perfect regularity of the stripe texture so that walls in non-regular structures may exhibit a tendency to behave as singular walls.

Other crystals from the A_2BX_4 family would form similar stripe textures only the number of walls in the elementary sequence will be different.

No direct observation of DTI in A_2BX_4 type crystals is available. In $(NH_4)_2BeF_4$ the scanning electron microscopy has visualized few degrees below the I–C transition a layered domain structure with ferroelectric walls perpendicular to **a**.[11] This is likely to be a relic of the striped DTI.

Barium manganese fluoride. The P phase has orthorhombic symmetry $Cmc2_1$ (C_{2v}^{12}). The symmetry of the C phase is unknown since the I phase persists till very low temperatures. The I phase is described by two waves with vectors

$$\mathbf{k}_1 = \tfrac{1}{2}\mathbf{a}^* + \mu\mathbf{c}^*, \qquad \mathbf{k}_2 = \tfrac{1}{2}\mathbf{b}^* + \mu\mathbf{c}^*, \tag{6}$$

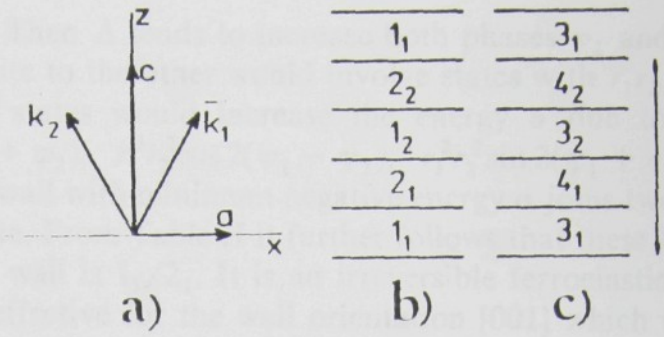

FIGURE 3 Domain textures in barium manganese fluoride. a) projection of wave vectors $\mathbf{k}_1, \mathbf{k}_2$ on xz-plane; a and c are vectors of the conventional orthorhombic unit cell. b), c) two possible stripe textures.

where $\mathbf{a}^*, \mathbf{b}^*, \mathbf{c}^*$ are vectors of the reciprocal lattice and $\mu \cong 0,39$[12], i.e., the wave vectors have a common I component along the **c** axis (see Figure 3a). Measurements under hydrostatic pressure yield $\mu \simeq 0.403$,[13] we, therefore, take as the simplest lock-in value $\mu = 1/2$. From the symmetry of the order parameter with $\mathbf{k}_1, \mathbf{k}_2$ ($\mu = 1/2$) describing the P–C phase transition and the fact that the unit cell volume (incommensurate modulation neglected) is doubled[14] it is easy to show that the C phase would have the lowest triclinic symmetry P1 (C_1^1). There are four orientational states that differ in spontaneous strain components e_{12}, e_{13}, e_{23} and each orientational state can be realized in two DS's that are related by lost translation **c**. We have eight DS's: $1_1, 1_2, 2_1, 2_2, 3_1, 3_2, 4_1, 4_2$.

The order parameter has two complex components $Q_1 = r_1 \exp(i\varphi_1)$, $Q_2 = r_2 \exp(i\varphi_2)$ with $r_1 = r_2 = r$ but only one non-zero amplitude, i.e., the C phase is a single state associated with one wave only. The values of the order parameter and spontaneous strain components for all DS's are given in Table II.

The Lifshitz invariant is

$$\Lambda = \lambda\left(r_1^2 \frac{\partial \varphi_1}{\partial z} + r_2^2 \frac{\partial \varphi_2}{\partial z}\right). \tag{7}$$

TABLE II

Barium manganese fluoride: Domain states A_a and their representation in the order parameter space $r_1 \exp(i\varphi_1)$, $r_2 \exp(i\varphi_2)$. Operation g (Seitz symbols in the P phase) relates A_a to domain state 1_1. e_{12}, e_{13}, e_{23} are spontaneous shear deformations

A_a	1_1	1_2	2_1	2_2	3_1	3_2	4_1	4_2
g	$(1\|000)$	$(1\|001)$	$\left(2_z\|00\frac{1}{2}\right)$	$\left(2_z\|00\frac{3}{2}\right)$	$(m_x\|000)$	$(m_x\|001)$	$\left(m_y\|00\frac{1}{2}\right)$	$\left(m_y\|00\frac{3}{2}\right)$
r_1	r	r	r	r	0	0	0	0
φ_1	φ	$\varphi + \pi$	$\varphi + \pi/2$	$\varphi + 3\pi/2$				
r_2	0	0	0	0	r	r	r	r
φ_2					φ	$\varphi + \pi$	$\varphi + \pi/2$	$\varphi + 3\pi/2$
e_{12}	+	+	+	+	−	−	−	−
e_{13}	+	+	−	−	−	−	+	+
e_{23}	+	+	−	−	+	+	−	−

We choose $\lambda < 0$. Then Λ tends to increase both phases φ_1 and φ_2. The transition from one single state to the other would involve states with $r_1 r_2 \neq 0$ inside the wall and these double states would increase the energy σ due to mixed terms like $r_1^2 r_2^2$, $r_1^2 r_2^2 \cos 2(\varphi_1 + \varphi_2)$, $r_1^2 r_2^2 \cos 2(\varphi_1 - \varphi_2)$, $r_1^2 r_2^2 \sin 2(\varphi_1 + \varphi_2)$, etc. We infer, therefore, that the wall with minimum negative energy σ joins two DS's belonging to the same single state. From Table II it further follows that these DS's differ in phase by $\pi/2$. One such wall is $1_1/2_1$. It is an irreversible ferroelastic wall. The Lifshitz invariant is most effective for the wall orientation [001] which is not a prominent one. However, this orientation assures a stress-free coherence of the ferroelastic wall since the shears e_{13}, e_{23} break the 2-fold axis.[5] The elastic energy of the wall is minimal for this orientation and we shall, therefore further consider walls with $\mathbf{n} = [001]$.

Applying on $1_1/2_1$ operations of the P phase we get eight equivalent walls

$$1_1/2_1 \simeq 2_1/1_2 \simeq 1_2/2_2 \simeq 2_2/1_1$$

$$\simeq 3_1/4_1 \simeq 4_1/3_2 \simeq 3_2/4_2 \simeq 4_2/3_1. \qquad (8)$$

From these walls it is possible to form two stripe textures sketched in Figure 3b, c. These stripe textures can coexist in equilibrium and form *textural blocks*. From Table II it follows that they exhibit monoclinic macroscopic symmetry 2 since shears e_{13} and e_{23} cancel in average and blocks appear as ferroelastic domains differing in sign of the spontaneous deformation e_{12}. Such "domains" (textural blocks) meet coherently without stresses along either (100) or (010) "walls" (block boundaries) which are crystallographically nonequivalent.

These conclusions agree with γ-diffractometry measurements which disclosed macroscopic ferroelastic "domains" that were discriminated by opposite sign of the e_{12} shear deformation.[15] From this observation it also follows that these domains join along boundaries with (010) orientation.

2) *Structures Modulated in Two Directions*

Barium sodium niobate (BSN) is a representative of the tungsten-bronze-oxide family. The symmetry of the P phase is P4bm (C_{4v}^2) and that of the C phase Bbm2 (C_{2v}^{16}) with four times more formula units in the primitive unit cell. Two orientational states differ in the sign of the spontaneous deformation e_{12}. There are eight DS's $1_1, 1_2, 1_3, 1_4, 2_1, 2_2, 2_3, 2_4$.

The order parameter has two complex components $Q_1 = r_1 \exp(i\varphi_1)$, $Q_2 = r_2 \exp(i\varphi_2)$ that transform according to the irreducible representation with the star[16]

$$\mathbf{k}_+ = \frac{\mathbf{a}^* + \mathbf{b}^*}{4} + \frac{\mathbf{c}^*}{2}, \qquad \mathbf{k}_- = \frac{\mathbf{a}^* - \mathbf{b}^*}{4} + \frac{\mathbf{c}^*}{2}, \qquad -\mathbf{k}_+, -\mathbf{k}_-. \qquad (9)$$

The C phase is a single state,[16] i.e. either r_1 or r_2 equals zero. The correspondence between DS's and order parameter values is given in Table III.

TABLE III

Barium sodium niobate: Domain states A_a and their representation in the order parameter space $r_1\exp(i\varphi_1)$, $r_2\exp(i\varphi_2)$. Operation g transforms domain state 1_1 into A_a, $A_a = g1_1$

A_a	1_1	1_2	1_3	1_4	2_1	2_2	2_3	2_4
g	(1|000)	(1|100)	(1|200)	(1|300)	(4_z|000)	(4_z|100)	(4_z|200)	(4_z|300)
r_1	r	r	r	r	0	0	0	0
φ_1	0	$\pi/2$	π	$3\pi/2$				
r_2	0	0	0	0	r	r	r	r
φ_2					0	$\pi/2$	π	$3\pi/2$

The Lifshitz invariant has the form

$$\Lambda = \frac{\sqrt{2}}{2}\lambda\left[r_1^2\left(\frac{\partial\varphi_1}{\partial x} + \frac{\partial\varphi_1}{\partial y}\right) + r_2^2\left(\frac{\partial\varphi_2}{\partial x} - \frac{\partial\varphi_2}{\partial y}\right)\right]$$

$$= \lambda\left(r_1^2\frac{\partial\varphi_1}{\partial x'} - r_2^2\frac{\partial\varphi_2}{\partial y'}\right) \tag{10}$$

where x, y, x', y' are coordinate axes along [100], [010], [110], [$\bar{1}$10] directions of the P phase (see Figure 4). A wall which joins two DS's belonging to different single states has intermediate structures with $r_1 \neq 0$ and $r_2 \neq 0$ that increase the wall energy due to the term $r_1^2 r_2^2$; the existence of single domain states in the C phase suggests that this term is energetically unfavourable. We infer, therefore, that walls with minimum energy connect DS's from the same single state. Then the Lifshitz invariant will contribute most in walls with a normal [110] or [$\bar{1}$10]; in the former case φ_1 increases in the wall by $\pi/2$ and in the latter case φ_2 decreases by $\pi/2$.

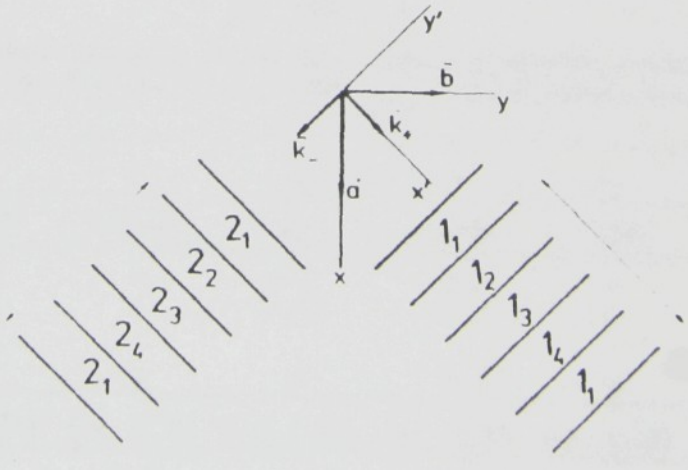

FIGURE 4 Two possible stripe textures in barium sodium niobate. **a**, **b** are basic vectors of the P phase, $\mathbf{k}_-$, $\mathbf{k}_+$ are the projections of the wave vectors on the xy-plane.

From Table III we find equivalent walls:

$$\mathbf{n} = [110]: \quad 1_1/1_2 \simeq 1_2/1_3 \simeq 1_3/1_4 \simeq 1_4/1_1 \tag{11}$$

$$\mathbf{n} = [\bar{1}10]: \quad 2_1/2_4 \simeq 2_4/2_3 \simeq 2_3/2_2 \simeq 2_2/2_1. \tag{12}$$

All these walls have prominent orientations since a perpendicular mirror m is their symmetry element. We notice that the walls (11) join DS's related by translation 3a and W's (12) DS's related by a.

Equivalent walls (11), (12) can form two stripe textures with prominent orientations (see Figure 4). These textures have equal energy and can coexist in equilibrium as textural blocks. Macroscopically these blocks appear as ferroelastic domains differing in the sign of the spontaneous shear e_{12}. The coherent stress-free boundaries between these blocks have two equivalent orientations (100) and (010).

Barium strontium niobate (SBN) belongs also to tungsten-bronze-oxide family with the same P4bm (C_{4v}^2) space group of P phase as BSN. However, the space group of the C phase has not been experimentally determined since the I phase persists till low temperatures. In contradistinction to BSN, the I phase preserves the macroscopic tetragonal symmetry[17] and hence assuming that the order parameter transforms according to the same irreducible representation as in BSN the C state must be a double state with $r_1^2 = r_2^2$. Then it can be shown that the symmetry of the C phase is I4 (C_4^5) with 8 times more formula units in the unit cell than in the P phase. The two orientational states differ in the sign of the spontaneous component d_{123}–d_{213}. There are 16 DS's. The phases φ_1, φ_2 of all DS's can be found in Table IV.

The Lifshitz invariant has the same form (10) as for BSN. The negative contribution from this invariant with $r_1 = r_2$ is slightly higher for wall orientations [100], [010] connected with simultaneous changes of φ_1 and φ_2 than for [110], [$\bar{1}$10] orientations associated with a change in one component only. On the other hand, the contribution of anisotropic terms, like $r_1^4 \cos 4\varphi_1 + r_2^4 \cos 4\varphi_2$, is also higher for the

TABLE IV

Barium strontium niobate: Domain states A_a, their relation (expressed by operation g that transforms 1_1 into A_a, $A_a = g1_1$) and representation in the order parameter space $r_1\exp(i\varphi_1)$, $r_2\exp(i\varphi_2)$. $r_1 = r_2 \neq 0$

A_a	1_1	1_2	1_3	1_4	1_5	1_6	1_7	1_8
g	(1|000)	(1|100)	(1|200)	(1|300)	(1|010)	(1|110)	(1|210)	(1|310)
φ_1	0	$\pi/2$	π	$3\pi/2$	$\pi/2$	π	$3\pi/2$	0
φ_2	0	$\pi/2$	π	$3\pi/2$	$3\pi/2$	0	$\pi/2$	π
A_a	2_1	2_2	2_3	2_4	2_5	2_6	2_7	2_8
g	$(m_x, \|\frac{1}{2}\frac{1}{2}0)$	$(m_x, \|\frac{3}{2}\frac{1}{2}0)$	$(m_x, \|\frac{5}{2}\frac{1}{2}0)$	$(m_x, \|\frac{7}{2}\frac{1}{2}0)$	$(m_x, \|\frac{1}{2}\frac{3}{2}0)$	$(m_x, \|\frac{3}{2}\frac{3}{2}0)$	$(m_x, \|\frac{5}{2}\frac{3}{2}0)$	$(m_x, \|\frac{7}{2}\frac{3}{2}0)$
φ_1	$\pi/2$	π	$3\pi/2$	0	π	$3\pi/2$	0	$\pi/2$
φ_2	0	$\pi/2$	π	$3\pi/2$	$3\pi/2$	0	$\pi/2$	π

first two orientations making thus the preference of these orientations questionable. We shall, therefore, consider both possibilities:

(i) Walls involving the change of both components of the order parameter.

The wall $1_1/1_2$ with $\mathbf{n} = [100]$ gains the largest Lifshitz contribution but this orientation is not a prominent one (mirror and glide planes change the orientational state). It can be shown that the extreme wall energy is obtained for $\mathbf{n}$ rotated about an angle ϵ around the c direction. Applying lost translations we get the following equivalent walls of the same orientation inclined by ϵ from [100]:

$$1_1/1_2 \simeq 1_2/1_3 \simeq 1_3/1_4 \simeq 1_4/1_1$$
$$\simeq 1_5/1_6 \simeq 1_6/1_7 \simeq 1_7/1_8 \simeq 1_8/1_5. \tag{13}$$

Four-fold rotations generate another set of equivalent walls with $\mathbf{n}$ deviated about ϵ from [010] direction:

$$1_1/1_5 \simeq 1_5/1_3 \simeq 1_3/1_7 \simeq 1_7/1_1$$
$$\simeq 1_2/1_6 \simeq 1_6/1_4 \simeq 1_4/1_8 \simeq 1_8/1_2. \tag{14}$$

The mirror planes produce two other sets of equivalent walls with deviation $-\epsilon$

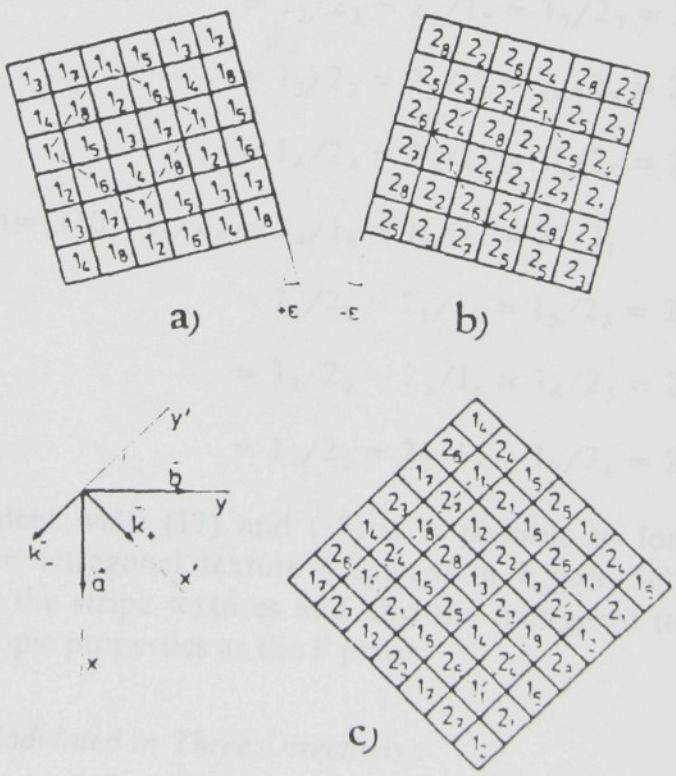

FIGURE 5 Possible tetragonal domain textures in barium strontium niobate formed by a), b) walls with variation in both order parameter components (ϵ measures the deviation from a crystallographic orientation), c) walls with a change in one component. Unit cells of the textures are marked by dashed lines. $\mathbf{a}, \mathbf{b}$ are basic vectors of the P phase, $\mathbf{k}_-, \mathbf{k}_+$ are the wave vectors.

from [100]:

$$2_1/2_2 \simeq 2_2/2_3 \simeq 2_3/2_4 \simeq 2_4/2_1$$
$$\simeq 2_5/2_6 \simeq 2_6/2_7 \simeq 2_7/2_8 \simeq 2_8/2_5, \tag{15}$$

and with deviation $-\epsilon$ from [010]

$$2_1/2_5 \simeq 2_5/2_3 \simeq 2_3/2_7 \simeq 2_7/2_1$$
$$\simeq 2_2/2_6 \simeq 2_6/2_4 \simeq 2_4/2_8 \simeq 2_8/2_2. \tag{16}$$

Each row in (13)–(16) represents an elementary wall sequence of a stripe texture. These textures do not have prominent orientations and can coexist as textural blocks. Only textures belonging to different orientational states could be discriminated macroscopically.

Other structures that can be formed from the equivalent walls (13)–(16) are two tetragonal textures sketched in Figures 5a, b. They have the symmetry p4 and no prominent orientation. Macroscopically they differ in the sign of piezoelectric tensor component d_{123}–d_{213}.

(ii) Walls involving the change of one component of the order parameter.

A wall facilitated by Lifshitz invariant is $1_1/2_1$ with prominent orientation [110] (the mirror in this wall is its symmetry operation). Equivalent walls are:

$$\mathbf{n}=[110]\colon 1_1/2_1 \simeq 2_1/1_6 \simeq 1_6/2_6 \simeq 2_6/1_1$$
$$\simeq 1_2/2_2 \simeq 2_2/1_7 \simeq 1_7/2_7 \simeq 2_7/1_2$$
$$\simeq 1_3/2_3 \simeq 2_3/1_8 \simeq 1_8/2_8 \simeq 2_8/1_3$$
$$\simeq 1_4/2_4 \simeq 2_4/1_5 \simeq 1_5/2_5 \simeq 2_5/1_4. \tag{17}$$

$$\mathbf{n}=[\bar{1}10]\colon 1_1/2_4 \simeq 2_4/1_8 \simeq 1_8/2_7 \simeq 2_7/1_1$$
$$\simeq 1_2/2_1 \simeq 2_1/1_5 \simeq 1_5/2_8 \simeq 2_8/1_2$$
$$\simeq 1_3/2_2 \simeq 2_2/1_6 \simeq 1_6/2_5 \simeq 2_5/1_3$$
$$\simeq 1_4/2_3 \simeq 2_3/1_7 \simeq 1_7/2_6 \simeq 2_6/1_4. \tag{18}$$

From 32 equivalent walls (17) and (18) it is possible to form 8 different stripe textures and one tetragonal texture (depicted in Figure 5c) all with prominent orientations. All the stripe textures and also the tetragonal texture have the same average macroscopic properties as the P phase.

3) Structures Modulated in Three Directions

Quartz and aluminium phosphate. The symmetries of P and C phases are $P6_222$ (D_6^4) and $P3_221$ (D_3^6), unit cells of both phases contain 3 molecules. There are just

two DS's 1, 2 identical with two orientational states that can be associated with plus or minus sign of the spontaneous component d_{111} of the piezoelectric tensor.[18]

The order parameter is a real number and transforms according to the irreducible representation B_1 (at the Γ point) of $P6_222$. Similarly as in $NaNO_2$, there is no Lifshitz invariant and walls W^- result from a Lifshitz-like invariant.[19] The orientation of W^- cannot be predicted from symmetry considerations only. We examine, therefore, textures that can result from W's of three different crystallographical orientations.

(i) W's perpendicular to 2-fold axis 2_y that is lost at the transition, e.g., $n = [01\bar{1}0]$ in hexagonal system. Walls with this orientation are reversible since 2_y transforms $1/01\bar{1}0/2$ into $2/01\bar{1}0/1$ and vice versa. We get six equivalent W's of three orientations

$$\begin{aligned} 1/01\bar{1}0/2 &\simeq 2/01\bar{1}0/1 \\ &\simeq 1/\bar{1}010/2 \simeq 2/\bar{1}010/1 \\ &\simeq 1/1\bar{1}00/2 \simeq 2/1\bar{1}00/1, \end{aligned} \tag{19}$$

from which three stripe textures can be formed (see Figure 6a). We note that 2_x axes in the centres of stripe domains are symmetry elements of the stripe texture. From walls (19) other textures periodical in 3 directions can be constructed: two complementary triangular textures (similar to those depicted in Figure 6b, but with walls

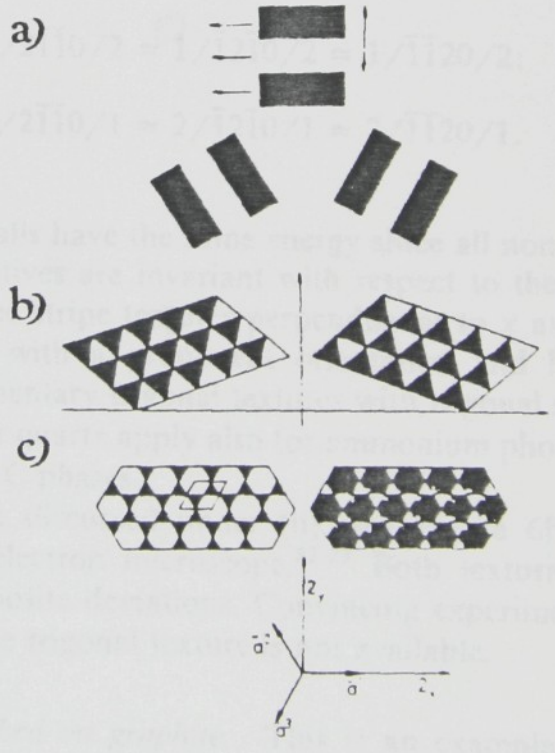

FIGURE 6 Possible domain textures in quartz a) stripe textures with walls perpendicular to lost 2-fol axes, b) two complementary triangular textures in inclined orientations, c) two complementary textur with trigonal symmetry and crystallographic orientation. Black and white domains correspond to doma states 1 and 2, resp. Two-fold axis 2_x is preserved, 2_y lost at the P–C transition.

perpendicular to 2_y axes) with plane symmetry p6 and two complementary trigonal textures (Figure 6c) with plane symmetry p31m.

The stability of these textures should be examined since the orientation $[01\bar{1}0]$ of a single wall is not a prominent one (no 2-fold axis is a symmetry operation of such a wall). Consequently, single wall of minimum energy σ will have a general orientation rotated away from the $[01\bar{1}0]$ one. For simplicity, we shall consider walls parallel to the c axis, i.e.,

(ii) W's with orientation [uvt0]. There are six equivalent walls each with different orientation. Similarly as in Rb_2ZnCl_4, no stripe texture can be formed from these equivalent walls. A stripe texture with a general orientation would have to be built up from non-equivalent parallel walls and it would have no prominent symmetry. Stripe texture considered under (i) has a prominent orientation (due to 2_x axes—see Figure 6a) and, consequently, extremal energy. We cannot, therefore, exclude that the stripe texture with $[01\bar{1}0]$ orientation is stable though the single wall with this orientation is unstable. Two complementary triangular textures with opposite deviations from the crystallographical orientation (see Figure 6b) can be formed from six equivalent walls of general orientation. They have p6 plane symmetry, hence the special crystallographic orientation of these triangular textures considered above is not prominent and a minimum energy will be reached in rotated-away orientations. These conclusions have been obtained already earlier from a careful analysis of the thermodynamic potential of quartz.[19-21]

(iii) W's perpendicular to 2-fold axis 2_x preserved at the transition, e.g. with $\mathbf{n} = [2\bar{1}\bar{1}0]$, have prominent orientation (both perpendicular and parallel 2-fold axis are symmetry operations of the wall). They are two classes of symmetrically equivalent walls:

$$1/2\bar{1}\bar{1}0/2 \simeq 1/\bar{1}2\bar{1}0/2 \simeq 1/\bar{1}\bar{1}20/2;$$

$$2/2\bar{1}\bar{1}0/1 \simeq 2/\bar{1}2\bar{1}0/1 \simeq 2/\bar{1}\bar{1}20/1. \qquad (20)$$

Nevertheless, all these walls have the same energy since all non-homogeneous terms containing spatial derivatives are invariant with respect to the inversion $x \to -x$. Hence one can form three stripe textures perpendicular to x axes, two complementary triangular textures with a prominent orientation and hexagonal symmetry p6mm, and two complementary trigonal textures with trigonal symmetry p3.

All results obtained for quartz apply also for ammonium phosphate with the same symmetries of the P and C phases.

The triangular texture discussed under (ii) (see Figure 6b) has been directly observed in quartz by electron microscope.[22,23] Both textural blocks are clearly visible as areas with opposite deviations. Convincing experimental evidence about the stripe textures and the trigonal texture is not available.

Krypton monolayer adsorbed on graphite. This is an example of I phases in two dimensional systems.[2,24] The P phase has the hexagonal plane symmetry p6mm with basic vectors $\mathbf{a}_h^j$, $j = 1, 2, 3$. The C phase, denoted $\sqrt{3} \times \sqrt{3}$ R 30°, has the same symmetry group but with $\sqrt{3}$ times larger basic vectors $\mathbf{a}_H^j$ rotated away by 30° (see

Figure 7a). The volume of the C unit cell is 3 times larger than that of the P unit cell. Hence there are just 3 translational DS's 1, 2, 3. DS's 2, 3 are obtained from the DS 1 by applying lost translations $\mathbf{a}^1_h$, $2\,\mathbf{a}^1_h$, resp.

The order parameter has three complex components $r_j \exp(i\varphi_j)$, $j = 1, 2, 3$, with equal amplitudes $r_1 = r_2 = r_3 = r$ and equal phases $\varphi_1 = \varphi_2 = \varphi_3 = \varphi$. The phase φ corresponding to DS's 1, 2, 3 equals 0, $2\pi/3$ and $4\pi/3$, resp. The Lifshitz invariant is

$$\Lambda = \lambda r^2 \left(\frac{\partial \varphi_1}{\partial x_1} + \frac{\partial \varphi_2}{\partial x_2} + \frac{\partial \varphi_3}{\partial x_3} \right)$$

$$= \lambda r^2 \left[\frac{\partial \varphi_1}{\partial x_1} - \frac{1}{2} \left(\frac{\partial \varphi_2}{\partial x_1} + \frac{\partial \varphi_3}{\partial x_1} \right) + \frac{\sqrt{3}}{2} \left(\frac{\partial \varphi_2}{\partial y_1} - \frac{\partial \varphi_3}{\partial y_1} \right) \right] \qquad (21)$$

where the x_j axes are parallel to $\mathbf{a}^j_h$ and y_1 to $\mathbf{a}^2_H$. Walls perpendicular to y_1 are energetically unfavourable since an opposite change of φ_2 and φ_3 with constant φ_1 does not drive the representative point from one DS to any other DS. This condition is fulfilled, however, for walls perpendicular to x_1 where Λ yields the largest negative contribution with phase increments $\Delta\varphi_1 = +2\pi/3$, $\Delta\varphi_2 = \Delta\varphi_3 = -4\pi/3$ for $\lambda < 0$. One such a wall connects DS 1 with DS 2 (proceeding in positive x_1 direction) and produces the shift $\mathbf{a}^1_h$ of adjacent structures. This wall is irreversible: the change of the sequence to 2/1 (equivalent to transformation $x \to -x$) turns the negative contribution of Λ into a positive one and the shift created by this wall

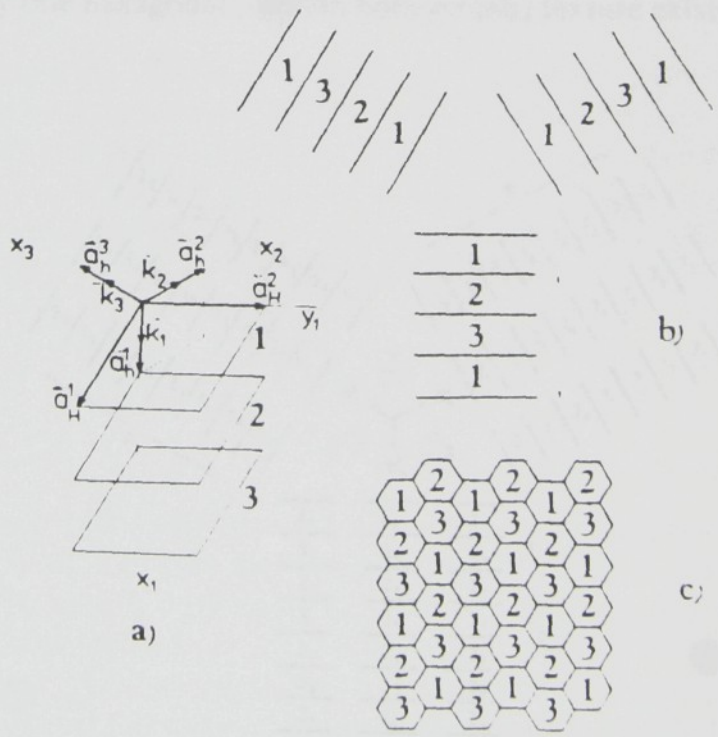

FIGURE 7 On the krypton monolayer on graphite. a) three translational domain states 1, 2, 3; $\mathbf{a}^j_h$, $\mathbf{a}^j_H$ are basic vectors of the P and C phases, resp., $\mathbf{k}_j$ are wave vectors of the modulation, $j = 1, 2, 3$. b) three possible stripe textures, c) hexagonal (honeycomb) texture.

becomes 2 $\mathbf{a}^1_h$. The equivalent walls are

$$1/\mathbf{a}^1_h/2 \simeq 2/\mathbf{a}^1_h/3 \simeq 3/\mathbf{a}^1_h/1$$
$$\simeq 1/\mathbf{a}^2_h/2 \simeq 2/\mathbf{a}^2_h/3 \simeq 3/\mathbf{a}^2_h/1$$
$$\simeq 1/\mathbf{a}^3_h/2 \simeq 2/\mathbf{a}^3_h/3 \simeq 3/\mathbf{a}^3_h/1, \tag{22}$$

where the vectors $\mathbf{a}^j_h$ indicate the direction of the wall normal. All three orientations are prominent and all walls are irreversible.

Each row in (22) represents one stripe texture (see Figure 7b). All nine types of walls form one hexagonal (honeycomb) texture (Figure 7c) which recovers the p6mm symmetry of the P phase though with much larger unit cell. All these textures have prominent orientation and have been thoroughly discussed in many papers (see, e.g. References 2, 24, 25).

2H polytype $TaSe_2$. Represents one of the transition-metal-dichalcogenide layer crystals which exhibits remarkable charge-density-wave phase transitions. The P phase has $P6_3/mmc$ symmetry and the C phase the Cmcm symmetry with tripled periodicity along two hexagonal axes basic vectors. There are three ferroelastic orientational states with different orientations of the C unit cell and for each there exist nine translational DS's; thus in all we have 27 DS's. The analysis of this case will be given elsewhere and here we present only the results. There are 54 equivalent ferroelastic walls with minimum σ from which it is possible to form 9 different stripe textures each with a different elementary wall sequence consisting of 6 walls (see Figure 8). Only one hexagonal (double honeycomb) texture exists (see Figure 9); it is

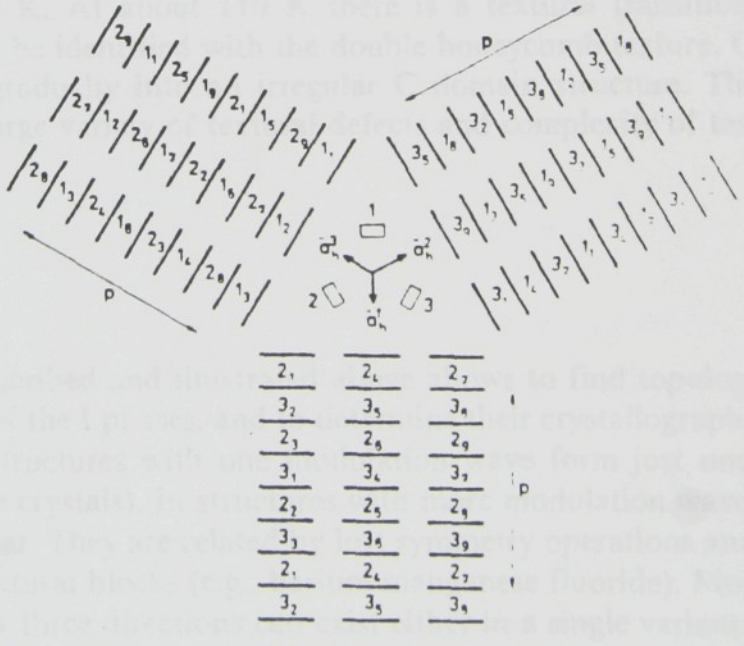

FIGURE 8 Equivalent stripe textures of 2H-$TaSe_2$. $\mathbf{a}^j_h$ ($j = 1, 2, 3$) are basic vectors of the P phase rectangles indicate orientation of conventional C unit cell.

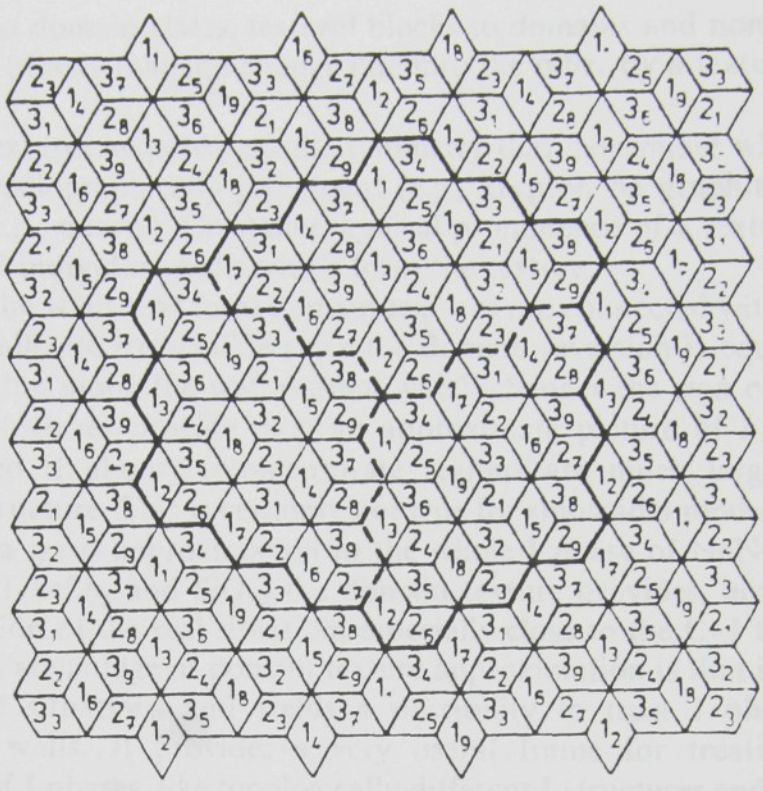

FIGURE 9 Double honeycomb texture in 2H-$TaSe_2$. Dashed (solid) frames mark primitive (conventional) unit cells of the periodic pattern.

a regular repetition of a rhombic unit cell that contains once each of 27 DS's, once each of 54 walls and, in addition, 18 three-fold wall intersections and 9 six-fold intersections.

Domain textures in 2H-$TaSe_2$ have been directly observed by electron microscope.[26,27] Coexisting stripe textures with a sharp contrast are seen only on heating above 90 K. At about 110 K there is a textural transition to a triply I structure that can be identified with the double honeycomb texture. On cooling this texture changes gradually into an irregular C domain structure. The observations have revealed a large variety of textural defects and complexity of textural and C–I transitions.

V SUMMARY

The approach described and illustrated above allows to find topologically different domain textures of the I phases, and to determine their crystallographical orientation and symmetry. Structures with one modulation wave form just one stripe texture (e.g., A_2BX_4 type crystals). In structures with more modulation waves several stripe textures can appear. They are related by lost symmetry operations and can coexist in equilibrium as textural blocks (e.g., barium manganese fluoride). Moreover, textures periodic in two or three directions can exist either in a single variant which recovers the symmetry of the P phase (e.g., Kr monolayer on graphite) or in several equivalent variants forming textural blocks (e.g., in quartz). Equivalent textures are

analogous to domain states, textural blocks to domains and non-equivalent textures to different phases that can change one into the other by a textural transition[3] (e.g., 2H-$TaSe_2$).

Perfect textures acquire periodic symmetry that determines whether their orientation is crystallographically prominent (e.g., krypton on graphite) or non-crystallographical (e.g., quartz). Crystallographical prominence of a texture can be different than that of individual walls which form the texture.

Most of the walls that form domain textures are connected with Lifshitz invariant. All these walls are irreversible since the domain reversion is equivalent to $x \rightarrow -x$ transformation along the wall normal which changes the sign of Lifshitz invariant.

Domain textures provide only an approximate picture of I structures which is substantiated if almost commensurate regions are much larger than regions of changing structure. This is certainly not true for sinusoidal modulation (which seems to be, e.g., a good approximation in the whole I phase of $NaNO_2$). In many cases (e.g., for 2H-$TaSe_2$ and SiO_2) the domain texture provides, however, a reasonable approximation of the real situation, especially close to the C–I transition.

The main advantage of domain texture approximation is that it allows to visualize complicated situations and yields a possibility to treat I phases as systems of interacting walls. It provides a very useful frame for treating the topological properties of I phases, like topologically different I structures and topological defects of these structures. Topological characteristics of these objects are independent of the form of the I modulation and hold, therefore, beyond domain texture approximation.

ACKNOWLEDGMENT

The authors express their thanks to Pierre Saint-Gregoire for a very useful discussion on the incommensurate structure of $BaMnF_4$.

REFERENCES

1. V. Dvořák, in *Modern Trends in the Theory of Condensed Matter*, Eds. A. Pekalski and J. Przystawa (Springer, Berlin, 1980), p. 447.
2. P. Bak, *Rep. Prog. Phys.*, **45**, 587 (1982).
3. W. L. McMillan, preprint (unpublished).
4. G. Van Tendeloo and S. Amelinckx, *Acta Cryst.*, **A30**, 431 (1974).
5. V. Janovec, *Ferroelectrics*, **12**, 43 (1976).
6. V. Janovec, *Ferroelectrics*, **35**, 105 (1981).
7. R. C. Pond and D. S. Vlachavas, *Proc. R. Soc. London*, **A386**, 95 (1983).
8. Z. Zikmund, *Czech. J. Phys.*, **B34**, 932 (1984).
9. P. Bak, in Solitons and Condensed Matter Physics, Eds. A. R. Bishop and T. Schneider (Springer, Berlin, 1978), p. 216.
10. S. Suzuki and M. Takagi, *J. Phys. Soc. Jpn.*, **30**, 188 (1971).
11. A. Röder, C. Scheiding, and H. Maack, *Ferroelectrics*, (Letter Section), **44**, 101 (1982).
12. D. E. Cox, S. M. Shapiro, R. J. Nelmes, T. W. Ryan, H. J. Bleif, R. A. Cowley, M. Eibschütz and H. J. Gruggenheim, *Phys. Rev.*, **B28**, 1640 (1983).
13. P. Saint-Gregoire, N. Barthes, R. Almairac, J. Nouet, J. Y. Jesland, C. Filippini and U. Steigenberger, *Ferroelectrics*, **53**, 307 (1984).
14. V. Dvořák and J. Fousek, *Phys. Stat. Sol. (a)*, **61**, 99 (1980).
15. P. Saint-Gregoire, R. Almairac, A. Freund and J. Y. Gesland, *Ferroelectrics*, this volume.
16. J. Schneck, J. C. Tolédano, C. Joffrin, J. Aubrée, B. Joukoff and A. Gabelotaud, *Phys. Rev.*, **B** 1766 (1982).

17. J. Schneck, J. C. Tolédano, R. Whatmore and F. W. Ainger, *Ferroelectrics*, **36**, 327 (1981).
18. G. Dolino, J. P. Bachheimer, F. Gervais and A. F. Wright, *Bull. Minéral.*, **106**, 267 (1983).
19. T. A. Aslanyan, A. P. Levanyuk, M. Vallade and J. Lajzérowicz, *J. Phys. C: Solid State Phys.*, **16**, 6705 (1983).
20. M. B. Walker, *Phys. Rev.*, **B28**, 6407 (1983).
21. B. Berge, Thesis, Grenoble University (1984).
22. G. Van Tendeloo, J. Van Landuyt and S. Amelinckx, *Phys. Stat. Sol. (a)*, **30**, K11 (1975); **33**, 723 (1976).
23. G. Dolino, J. P. Bachheimer, B. Berge, O. M. E. Zeyen, G. Van Tendeloo, J. Van Landuyt and S. Amelinckx, *J. Physique*, **45**, 901 (1984).
24. J. Villain, in Ordering in Strongly Fluctuating Condensed Matter Systems, Ed. T. Riste (Plenum Press, New York, 1979), p. 221.
25. D. A. House and M. E. Fischer, *Phys. Rev.*, **B29**, 239 (1984).
26. K. K. Fung, S. McKernan, J. W. Steeds and J. A. Wilson, *J. Phys. C: Solid State Phys.*, **14**, 5417 (1981).
27. C. H. Chen, J. M. Gibson, and R. M. Fleming, *Phys. Rev.*, **B26**, 184 (1982).

CHRISTIAN, J. W. (1954). *Acta Cryst.* **7**, 415–416.
JOHNSON, C. A. (1963). *Acta Cryst.* **16**, 490–497.
KAGAN, A. C., UNIKEL', A. P. & FADEEVA, V. I. (1982). *Zavodskaya Laboratoriya*, **48**, 38–46.
KAKINOKI, J. (1967). *Acta Cryst.* **23**, 875–885.
KAKINOKI, J. & KOMURA, Y. (1965). *Acta Cryst.* **19**, 137–147.
LELE, S., ANANTHARAMAN, T. R. & JOHNSON, C. A. (1967). *Phys. Status Solidi*, **20**, 59–68.
LELE, S., PRASAD, B. & ANANTHARAMAN, T. R. (1969). *Acta Cryst.* A**25**, 471–475.
MIRZAEV, D. A. & RUSHITS, C. V. (1976). *Kristallografiya*, **21**, 670–677.
NIKOLIN, B. I. (1984). *Mnogosloynie Structuri i Politipism v Metallicheskih Splavah*. Kiev: Naukova Dumka.
NISHIYAMA, Z., KAKINOKI, J. & KAJIWARA, S. (1965). *J. Phys. Soc. Jpn*, **20**, 1192–1211.
PANDEY, D. & KRISHNA, P. (1981). *Indian J. Pure Appl. Phys.* **19**, 796–802.
PATERSON, M. S. (1952). *J. Appl. Phys.* **23**, 805–811.
RUSHITS, S. V. & MIRZAEV, D. A. (1979). *Kristallografiya*, **24**, 1142–1149.
SEBASTIAN, M. T. & KRISHNA, P. (1987). *Prog. Crystal Growth Charact.* **14**, 103–183.
VERMA, A. R. & KRISHNA, P. (1966). *Polymorphism and Polytypism in Crystals*. New York: John Wiley.
WARREN, B. E. (1969). *X-ray Diffraction*. Reading, MA: Addison-Wesley.
WILSON, A. J. C. (1942). *Proc. R. Soc. London Ser. A*, **180**, 277–285.

SHORT COMMUNICATIONS

Contributions intended for publication under this heading should be expressly so marked; they should not exceed about 1000 *words; they should be forwarded in the usual way to the appropriate Co-editor; they will be published as speedily as possible.*

Acta Cryst. (1989). A**45**, 801–802

The coset and double coset decomposition of the 32 crystallographic point groups.

By V. JANOVEC and E. DVORAKOVA, *Institute of Physics, Czechoslovak Academy of Sciences, POB* 24, *Na Slovance* 2, 18040 *Prague* 8, *Czechoslovakia* and T. R. WIKE* and D. B. LITVIN, *Department of Physics, The Pennsylvania State University, The Berks Campus, PO Box* 7009, *Reading, PA* 19610-6009, *USA*

(*Received* 3 *March* 1989; *accepted* 11 *July* 1989)

Abstract

The coset and double coset decompositions of the 32 crystallographic point groups with respect to each of their subgroups are tabulated.

I. Introduction

The mathematical concept of the coset decomposition of a group with respect to one of its subgroups has wide applications in crystallography and solid-state physics. The points of any crystallographic orbit are in a one-to-one correspondence with the cosets of the coset decomposition of the crystallographic group with respect to the site symmetry group of one of its points (Wondratschek, 1983). Coset decompositions have been applied in the analysis of domains of ferroic crystals using coset decompositions of point groups (Aizu, 1970; Janovec, 1972) and of space groups (Aizu, 1974; Janovec, 1972, 1976). This concept has also been used in the derivation of twin laws for (pseudo-)merohedry (Flack, 1987).

The mathematical concept of the double coset decomposition of a group is less well known and has been used in applications to a lesser extent than the coset decomposition [see Ruch & Klein (1987) and references therein]. The double coset decomposition has been used in a tensorial classification of domain pairs in the case where each domain is characterized by a unique form of a physical property tensor (Janovec, 1972) and in the case where more than a single domain is characterized by a specific form of a physical property tensor (Litvin & Wike, 1989).

In § II we briefly review the definitions of coset and double coset decompositions. Tables of the coset and double coset decompositions of the 32 crystallographic point groups with respect to each of their subgroups are given in § III.

II. Coset and double coset decompositions

For a given group G and subgroup H one writes the left coset decomposition of G with respect to H symbolically as

$$G = H + g_2H + g_3H + \ldots + g_nH$$

where g_iH denotes the subset of elements of G obtained by multiplying each element of the subgroup H from the left by the element g_i of G (Hall, 1959). Each subset of elements g_iH, $i = 1, 2, \ldots, n$, is called a left coset of G with respect to H, and the elements g_i, $i = 1, 2, \ldots, n$, of G are called the left coset representatives of the left coset decomposition of G with respect to H.

The subset of elements of G in each coset of the left coset decomposition of G with respect to H is unique, but the coset representatives are not unique. A coset representative g_i can be replaced by the element g_ih, where h is an arbitrary element of the subgroup H.

For a given group G and subgroup H, one writes the double coset decomposition of G with respect to H symbolically as

$$G = H + Hg_2^{dc}H + Hg_3^{dc}H + \ldots + Hg_m^{dc}H$$

where $Hg_i^{dc}H$ denotes the subset of *distinct* elements of G

* Present address: General Electric Aerospace, PO Box 8048, Philadelphia, PA 19101, USA.

0108-7673/89/110801-02$03.00

Table 1. *The coset and double coset decomposition of* $G = m\bar{3}m$ *with respect to* $H = m_z m_x 2_y$

Each row contains the elements of a single coset. Sets of cosets constituting a single double coset are separated, in general, by a horizontal dashed line, but members of pairs of complementary double cosets are separated by a horizontal dotted line.

1	2_y	m_x	m_z
2_x	2_z	$\bar{1}$	m_y
3^2_{xyz}	3_{xyz}	$\bar{3}_{xyz}$	$\bar{3}^5_{xyz}$
3_{xyz}	3^2_{xyz}	$\bar{3}^5_{xyz}$	$\bar{3}_{xyz}$
3_{xyz}	3^2_{xyz}	$\bar{3}^5_{xyz}$	$\bar{3}^5_{xyz}$
3^2_{xyz}	3^2_{xyz}	$\bar{3}_{xyz}$	$\bar{3}^5_{xyz}$
2_{xy}	4_z	$\bar{4}^3_z$	m_{xy}
4^3_z	2_{xy}	m_{xy}	$\bar{4}_z$
2_{xz}	4^3_y	m_{xz}	$\bar{4}_y$
4_y	2_{xz}	$\bar{4}^3_y$	m_{xz}
2_{yz}	2_{xz}	$\bar{4}_x$	$\bar{4}^3_x$
4^3_x	4_x	m_{yz}	m_{yz}

obtained by multiplying each element of the coset $g_j^{dc}H$ from the left by every element of the subgroup H (Hall, 1959).* Each subset of elements $Hg_j^{dc}H$, $j = 1, 2, \ldots, m$, is called a double coset of G with respect to H, and the elements g_j^{dc}, $j = 1, 2, \ldots, m$, are called the double coset representatives of the double coset decomposition of G with respect to H. By their definition, each double coset consists of a specific number of cosets of the coset decomposition of G with respect to H.

The subset of elements of G in each double coset of the double coset decomposition of G with respect to H is unique, but the double coset representatives are not unique. The double coset representative g_j^{dc} can be replaced by $h'g_j^{dc}h$ where h and h' are arbitrary elements of the subgroup H.

The elements of the two double cosets $Hg_j^{dc}H$ and $H(g_j^{dc})^{-1}H$ are either identical or disjoint. If identical, the double coset $Hg_j^{dc}H$ is called an *ambivalent* double coset and the inverse of each element is contained in the double coset. If disjoint, the two double cosets are called *complementary* double cosets, and the inverse of each element in one of a pair of complementary double cosets is found in the other double coset.

* This definition of a double coset decomposition of a group G with respect to a subgroup H, which we use in this paper, is the special case of the more general definition of a double coset decomposition of a group G with respect to two subgroups H and H' (Hasselbarth, Ruch, Klein & Seligman, 1980) when $H' = H$.

III. Tables of coset and double coset decompositions

Tables of the coset and double coset decomposition of the 32 crystallographic point groups with respect to one of each set of conjugate subgroups were given by Janovec & Dvorakova (1974). These tables are extended here and retabulated in International (Hermann–Mauguin) notation to include all subgroups of the 32 crystallographic point groups. In Table 1 we give an example of these tables,* the coset and double coset decomposition of the point group $G = m\bar{3}m$ with respect to the subgroup $H = m_z m_x 2_y$. Each row contains the elements of a single coset. In general, double cosets are separated by horizontal dashed lines but the members of a pair of complementary double cosets are separated by a horizontal dotted line.

References

Aizu, K. (1970). *Phys. Rev. B*, **2**, 754–772.

Aizu, K. (1974). *J. Phys. Soc. Jpn*, **36**, 1273–1279.

Flack, H. D. (1987). *Acta Cryst.* A**43**, 564–568.

Hall, M. Jr (1959). *The Theory of Groups*. New York: Macmillan.

Hasselbarth, W., Ruch, E., Klein, D. J. & Seligman, T. H. (1980). *J. Math. Phys.* **21**, 951–953.

Janovec, V. (1972). *Czech. J. Phys.* B**22**, 974–994.

Janovec, V. (1976). *Ferroelectrics*, **12**, 43–53.

Janovec, V. & Dvorakova, E. (1974). Rep. V-FZU 75/1. Institute of Physics, Czechoslovak Academy of Sciences, Prague, Czechoslovakia.

Litvin, D. B. & Wike, T. R. (1989). *Ferroelectrics*. In the press.

Ruch, E. & Klein, D. J. (1983). *Theor. Chim. Acta*, **63**, 447–472.

Wondratschek, H. (1983). *International Tables for Crystallography*, Vol. A: *Space-Group Symmetry*, edited by Th. Hahn, § 8. Dordrecht: Reidel. (Present distributor Kluwer Academic Publishers, Dordrecht.)

* The complete tables have been deposited with the British Library Document Supply Centre as Supplementary Publication No. SUP 52108 (485 pp.). Copies may be obtained through The Executive Secretary, International Union of Crystallography, 5 Abbey Square, Chester CH1 2HU, England. A computer program on disk for IBM compatible personal computers entitled *The 32 Crystallographic Point Groups* is also available through the Executive Secretary. This program calculates the notation, elements, subgroups, centralizers, normalizers, normal subgroups, and coset and double coset decompositions of the 32 crystallographic point groups.

Ferroelectrics, 1989, Vol. 98, pp. 171–189
Reprints available directly from the publisher
Photocopying permitted by license only

SYMMETRY ANALYSIS OF DOMAIN STRUCTURE IN KSCN CRYSTALS

V. JANOVEC†, W. SCHRANZ‡, H. WARHANEK‡ and Z. ZIKMUND†

†Institute of Physics, Czechoslovak Academy of Sciences, Na Slovance 2, 180 40 Prague 8, Czechoslovakia

‡Institute für Experimentalphysik der Universität Wien, Strudlhofgasse 4, A-1090 Wien, Austria

(Received August 31, 1989)

Basic symmetry properties of domain states, domain pairs, domain twins and walls in KSCN crystals are examined by group theoretical methods. Relations between domain states and domain pairs are expressed in matrix form and by permutation representation. Black and white space groups describing the symmetry of domain pairs are found and layer group symmetries of domain twins and domain walls are determined as their sectional subgroups. Microscopic structures of domain walls are given for coherent ferroelastic walls and for translation (antiphase) walls. Exposition and obtained results provide an illustrative example of symmetry analysis of domain structures.

I. INTRODUCTION

Symmetry analysis of domain structures discloses relations and regularities in these structures that result from a symmetry lowering at the phase transition. Conclusions of this analysis provide a solid basis for deciphering real domain structures.

A KSCN crystal represents a convenient example for studying domain structures. Its crystal structure is simple and well examined, the phase transition can be easily achieved and the experiments with domain structure can be performed at room temperature. The first results of microscopic observations of domain structure and its preliminary analysis are already available.[1] In this paper we complete the analysis within the approximation of zero-thickness domain walls and with simple mathematical tools (without invoking representation theory). A phenomenological theory of domain walls and structures of finite-thickness domain walls in KSCN crystals will be discussed elsewhere.

The aim of the paper is two-fold: besides the symmetry analysis of a particular domain structure in KSCN it should provide an illustrative example of methods and aims of symmetry analysis of domain structures in general. In order to make the paper self-contained we explain basic concepts and recall some relations. Though the treatment is based on simple group-theoretical considerations, we also display graphically the structures of examined objects.

For describing real domain structures the notions of domains and domain walls are used. The symmetry analysis of domain structures treats more idealized objects:

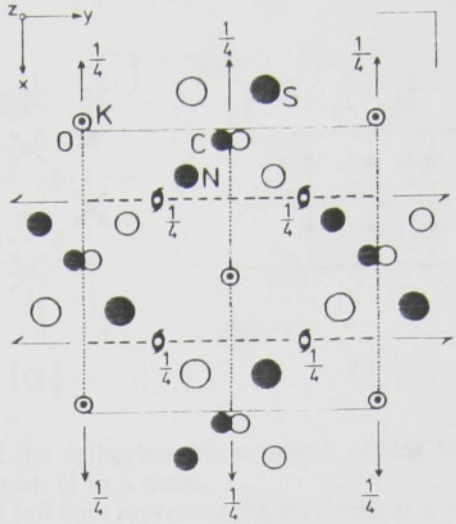

FIGURE 1 Orthorhombic structure of KSCN and its symmetry. Open and full circles represent K^+ ions at $z = \frac{1}{4}c, \frac{3}{4}c$ levels and S, C, N atoms at $z = 0, \frac{1}{2}c$ levels, resp.

domain states, domain pairs and domain twins. These three elementary domain formations are defined and analysed in Parts III, IV, V, resp. First, however, we recall in Part II necessary data about the crystal structure and the phase transition in KSCN.

II. STRUCTURE AND PHASE TRANSITION IN KSCN

1. A crystal of KSCN has at room temperature an orthorhombic structure with four formula units in the primitive unit cell which is depicted in Figure 1. The symmetry is described by the space group $F = Pbcm(D_{2h}^{11})$.[2] Due to strong overlap forces atoms S, C and N form a rather stable formation which we shall treat as a rigid and linear thiocyanate ion $(SCN)^-$. The site symmetries of the ions K^+ and $(SCN)^-$ are given in Table I. From these site symmetries it follows that the K^+ ions can be shifted from $(0,0,\frac{1}{4})$ positions (these spontaneous displacements have been recently determined by X-ray[3]) whereas the $(SCN)^-$ ions can be shifted in $z = 0,\frac{1}{2},\ldots$ planes and can exhibit a spontaneous rotation φ_z about the z direction. A schematic picture of the structure is given in Figure 2.

Above 142° C the structure of KSCN has the tetragonal body-centered structure

TABLE I

Symmetry groups of parent phase and of single domain states, corresponding site symmetries and spontaneous displacements of ions.

Phase	SDS		Symmetry group	K^+		$(SCN)^-$		
				Site sym.	Shift	Site sym.	Shift	Rotat.
parent		G	$I4_z/m_z c_x m_{xy}$	$4_z 2_x 2_{xy}$	(0,0,0)	$m_{xy} m_{x\bar{y}} m_z$	(0,0,0)	0
distorted	1_1	F_1	$Pb_x c_y m_z$	2_x	$(\bar{x},0,0)$	m_z	$(x,y,0)$	φ_z
	1_2	F_1	$Pb_x c_y m_z$	2_x	$(x,0,0)$	m_z	$(\bar{x},\bar{y},0)$	φ_z
	2_1	F_2	$Pc_x a_y m_z$	2_y	$(0,\bar{x},0)$	m_z	$(\bar{y},x,0)$	φ_z
	2_2	F_2	$Pc_x a_y m_z$	2_y	$(0,x,0)$	m_z	$(y,\bar{x},0)$	φ_z

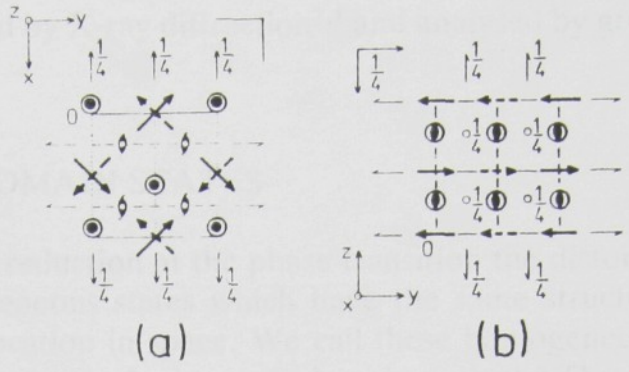

FIGURE 2 Schematic picture of the orthorhombic structure of KSCN. The $(SCN)^-$ ions are represented by oriented bars pointing from N to S atom.
(a) View along z axis. Dashed and full bars represent $(SCN)^-$ ions at $z = 0, \frac{1}{2}c$ levels, resp., open and full circles depict K^+ ions at $z = \frac{1}{4}c, \frac{3}{4}c$, resp. Spontaneous shifts of K^+ ions are exaggerated, shifts of (SCN) are neglected.
(b) View along x direction.

with 2 formula units in the primitive unit cell and with the space group $G = I4/mcm$ (D_{4h}^{18}).[4] The $(SCN)^-$ ions are orientationally disordered. In our schematic picture we represent disordered $(SCN)^-$ ions by non-oriented bars. The site symmetries of ions in this phase are given in Table I from which it follows that both ions have fully determined positions. The schematic representation of this structure is given in the centre of Figure 3.

2. Since the space group $F = Pbcm$ of the room temperature phase is a subgroup of the space group $G = I4/mcm$ of the high-temperature phase, the structural change at 142°C can be interpreted as a phase transition from the parent (high symmetry) phase with symmetry group G to the distorted (low symmetry) phase with symmetry F. This transition, which can be classified as an improper ferroelastic

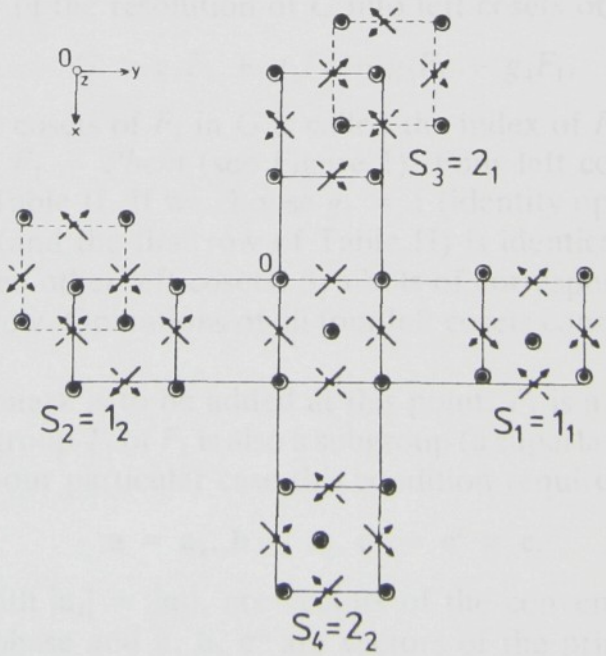

FIGURE 3 Four single domain states of KSCN. Ordered tetragonal structure is depicted in the centre.

one, was examined by X-ray diffraction[3,4] and analysed by group-theoretical methods.[5]

III. SINGLE DOMAIN STATES

Due to symmetry reduction at the phase transition the distorted phase can appear in several homogeneous states which have the same structure but different orientation and/or location in space. We call these homogeneous structures domain states[6,7] (DS's). An equivalent term is domain variant.[8] The equilibrium structure, homogeneous throughout the whole crystal defines a **single domain state (SDS)** which has symmetrically prominent orientation. In this Part we shall discuss SDS's only. Domain states with orientations different from that of SDS's appear in ferroelastic domain twins and will be invoked in Part VI.

The basic symmetry properties of SDS's follow directly from symmetry groups G and F of the parent and distorted phases, resp. Thus, e.g., the number n of SDS's can be calculated from a simple formula[8,9]

$$n = (|G| : |F|)(Z_F:Z_G) = 2.2 = 4, \tag{3.1}$$

where $|G|$, $|F|$ is the order of the point group of G, F, resp. and Z_G, Z_F is the number of the formula units in a primitive unit cell of the group G, F, resp. In our case, $|G| = 16$, $|F| = 8$, $(Z_F:Z_G) = 2$, hence $n = 4$. We can, therefore, designate the SDS's of KSCN as S_1, S_2, S_3, S_4.

Let us denote the symmetry group of S_1 by F_1. All operations that transform S_1 into S_j are comprised in the left coset g_jF_1:

$$S_j = (g_jF_1)S_1, \qquad g_j \in G,\ j = 1,2,3,4. \tag{3.2}$$

This equation defines a one-to-one correspondence between SDS's and left cosets of F_1 which appear in the resolution of G into left cosets of F_1:[10]

$$G = g_1F_1 + g_2F_1 + g_3F_1 + g_4F_1. \tag{3.3}$$

The number of left cosets of F_1 in G is called the index of F_1 in G and is denoted $[G:F]$. In our case $F_1 = Pbcm$ (see Figure 1). Four left cosets of the resolution (3.3) are given in Table II. If we choose $g_1 = 1$ (identity operation) then the first left coset of (3.3) (and the first row of Table II) is identical with F_1. Next three rows represent three other left cosets. Symbols of corresponding SDS's are given at the end of each row. Operations of all four left cosets constitute the whole group $G = I4/mcm$.

An important remark is to be added at this point: F_1 is a subgroup of G only if the translation subgroup T_1 of F_1 is also a subgroup (a superlattice) of the translation subgroup of G. In our particular case this condition requires

$$\mathbf{a} = \mathbf{a}_1,\ \mathbf{b} = \mathbf{a}_2,\ \mathbf{c}^o = \mathbf{c}^t = \mathbf{c}. \tag{3.4}$$

where $\mathbf{a}_1$, $\mathbf{a}_2$, $\mathbf{c}^t$, with $|\mathbf{a}_1| = |\mathbf{a}_2|$, are vectors of the conventional unit cell of the tetragonal parent phase and $\mathbf{a}$, $\mathbf{b}$, $\mathbf{c}^o$ are vectors of the primitive unit cell of the orthorhombic distorted phase. This condition (Equation 3.4), called the **higher symmetry approximation**[7] or **parent clamping approximation (PCA) of the distorted**

TABLE II

Decomposition of $G = I4/mcm$ into left cosets of $F_1 = Pb_xc_ym_z$ and of $K = P2_{1z}/m_z$

Left cosets of F_1								
Left cosets of K				Left cosets of K				SDS's
$\mathbf{T}[(1\|000)$	$+(2_z\|\frac{1}{2}\frac{1}{2}\frac{1}{2})$	$+(\bar{1}\|\frac{1}{2}\frac{1}{2}\frac{1}{2})$	$+(m_z\|000)$	$+(2_x\|00\frac{1}{2})$	$+(2_y\|\frac{1}{2}\frac{1}{2}0)$	$+(m_x\|\frac{1}{2}\frac{1}{2}0)$	$+(m_y\|00\frac{1}{2})]$	S_1 1_1
$\mathbf{T}[(1\|\frac{1}{2}\frac{1}{2}\frac{1}{2})$	$+(2_z\|000)$	$+(\bar{1}\|000)$	$+(m_z\|\frac{1}{2}\frac{1}{2}\frac{1}{2})$	$+(2_y\|\frac{1}{2}\frac{1}{2}0)$	$+(2_y\|00\frac{1}{2})$	$+(m_y\|00\frac{1}{2})$	$+(m_y\|\frac{1}{2}\frac{1}{2}0)]$	S_2 1_2
$\mathbf{T}[(4_z^+\|000)$	$+(4_z^3\|\frac{1}{2}\frac{1}{2}\frac{1}{2})$	$+(\bar{4}_z^+\|\frac{1}{2}\frac{1}{2}\frac{1}{2})$	$+(\bar{4}_z^3\|000)$	$+(2_{xy}\|00\frac{1}{2})$	$+(2_{x\bar{y}}\|\frac{1}{2}\frac{1}{2}0)$	$+(m_{xy}\|\frac{1}{2}\frac{1}{2}0)$	$+(m_{x\bar{y}}\|00\frac{1}{2})]$	S_3 2_1
$\mathbf{T}[(4_z^+\|\frac{1}{2}\frac{1}{2}\frac{1}{2})$	$+(4_z^3\|000)$	$+(\bar{4}_z^+\|000)$	$+(\bar{4}_z^3\|\frac{1}{2}\frac{1}{2}\frac{1}{2})$	$+(2_{xy}\|\frac{1}{2}\frac{1}{2}0)$	$+(2_{x\bar{y}}\|00\frac{1}{2})$	$+(m_{xy}\|00\frac{1}{2})$	$+(m_{x\bar{y}}\|\frac{1}{2}\frac{1}{2}0)]$	S_4 2_2

Symmetry operations related to a conventional coordinate system of $I4/mcm$ (origin at $4/m$). $\mathbf{T} = n_1\mathbf{a}_1 + n_2\mathbf{a}_2 + n_3\mathbf{c}$, where n_1, n_2, n_3 are integers and $\mathbf{a}_1$, $\mathbf{a}_2$, $\mathbf{c}$ are elementary translations of the conventional unit cell of $I4/mcm$. Subscripts x,y,z denote non-zero unit components of a vector along a symmetry axis or non-zero Miller indices of a symmetry plane in the coordinate system of $I4/mcm$. Each row contains symmetry operations constituting one left coset of F_1 and two left cosets of K. Left coset(s) between two horizontal lines constitute(s) one double coset.

phase, is essential in most of our considerations. Thus, e.g., the first left coset in Table II equals F_1 only if Equation (3.4) holds. Unless stated otherwise explicitely, we shall assume that Equation (3.4) is fulfilled. We shall lift this condition only in the last part of Part VI.

The knowledge of left cosets of F_1 enables one to construct all SDS's from the first one, S_1. From Table II we see that in each left coset there always exists a rotation around the axis parallel to z and passing through origin 0 with zero partial translation, i.e. any SDS can be obtained from S_1 by certain pure rotation around this axis. Solid squares in Figure 3 represent parts of the structure that have been obtained in this way from the unit cell (represented by a solid square) of the SDS S_1. When operations with partial translations $(\frac{1}{2},\frac{1}{2},0)$ or $(\frac{1}{2},\frac{1}{2},\frac{1}{2})$—also available in left cosets—are applied, the solid unit cell of S_1 is transformed into structures displayed in Figure 3 within dashed squares, which represent just another regions of the same structures as those within the solid squares.

All SDS's form a class of symmetrically equivalent objects in G. In the language of algebra[10,12] one says that the set $S = \{S_1,S_2,S_3,S_4\}$ forms an orbit of S_1 in G or, shortly, **G-orbit** of S_1. The group comprising all $g \in G$ which leave S_1 invariant, is called the **stabilizer** (isotropy group) of S_1 in G and is denoted $G(S_1)$. In our particular case, the stabilizer of S_1 is identical with the symmetry group of S_1, $G(S_1) = F_1$. As we shall see in Part VI, a *DS* with an orientation deviating from the prominent one of S_1, has the stabilizer different from the symmetry group F_1 of S_1. This difference is significant, since it is the stabilizer, and not the symmetry group of an object, which determines symmetry equivalent objects in G.

3. The set S of all SDS's can be divided into subsets (subclasses) comprising SDS's with the same attribute (property) X. We shall consider three particular attributes:

(i) SDS's with the same macroscopic properties, i.e. with the same orientation of basic translation vectors. Since this attribute corresponds to Aizu's **orientation states**[13] (orientation variants in Reference 8), we shall use this name for the subclasses too. The stabilizer G_0 of an orientation state is the equitranslational sub-

group of $G = I4/mcm$ with the same point group mmm as $F_1 = Pbcm$. In the International Tables[14] we find $G_0 = Ibam$ (D_{2h}^{26}). Since $Pbcm < Ibam < I4/mcm$, the stabilizer G_0 can be resolved into left cosets of F_1. From Table II it follows that

$$G_0 = F_1 + g_2F_1. \tag{3.5}$$

There are, $d_0 = [G_0:F_1] = 2$ SDS's in each orientation state and the first orientation state O_1^{10} includes S_1, S_2. Further, we can conclude from Table II that

$$G = G_0 + g_3G_0, \tag{3.6}$$

i.e. there are $n_0 = [G:G_0] = 2$ orientation states and the second one O_2 can contain S_1 and/or S_2.

The division of SDS's into orientation subclasses provides a useful labelling of SDS's: $S_1 = 1_1$, $S_2 = 1_2$, $S_3 = 2_1$, $S_4 = 2_2$, where the first number denotes the orientation state and the subscript (translation index) specifies the SDS's within the orientation state[11] (cf. Figure 3).

(ii) Subclass of SDS's with the same symmetry group. If we denote by F_i the stabilizer of $S_i = g_iS_1$, $i = 1,2,3,4$, then[10]

$$F_{(i)} = g_iF_{(1)}(g_i)^{-1}. \tag{3.7}$$

The stabilizer $G(F_1)$ of all SDS's with the same symmetry group $F_{(1)}$ consists of all $g \in G$ fulfilling the condition

$$F_{(1)} = gF_{(1)}g^{-1}. \tag{3.8}$$

Equation (3.8) identifies $G(F_1)$ with the normalizer of $F_{(1)}$ in G, $N_G(F_{(1)})$, which can be determined from Euclidean normalizers given in the International Tables,[14] Chapter XV. In our case $N_G(Pbmc) = Ibam = G_0$. We can, therefore, use the results obtained in the preceding part (i). Thus we find that S_1 and S_2 have the common symmetry group

$$F_{(1)} = F_{(2)} = Pbmc = F_1, \tag{3.9}$$

and S_3 and S_4 another common symmetry group

$$F_{(3)} = F_{(4)} = g_3F_1(g_3)^{-1} = Pcam = F_2. \tag{3.10}$$

Though the convention used in International Tables[14] allows in our case to distinguish conjugate groups F_1 and F_2, we can attach indices specifying the orientation of group generators in the coordinate system of the parent phase. In this explicit notation $F_1 = Pb_xc_ym_z$ and $F_2 = Pc_xa_ym_z$.

Any two SDS's from S are related in the following way:

$$S_j = (g_{ji}F_{(i)})S_i, \quad g_{ji} \in G, \quad i,j = 1,2,3,4. \tag{3.11}$$

This relation (where we do not sum over i) expresses the transitivity of SDS's: for any two SDS's, say S_i and S_j, there always exists a left coset of $F_{(i)}$ which transforms S_i into S_j. The explicit form of the matrix of $g_{ji}F_{(i)}$ is given in Table III.

(iii) Subclass of SDS's with the same spontaneous deformation u. It turns out that the corresponding stabilizer G_u is identical with G_0, so that this division coincides with that discussed under (i) and (ii) and orientation states O_1,O_2 are identical with two ferroelastic domain states u_1, u_2.

TABLE III
Transformation matrix of single domain states

S_j	S_i	S_1 1_1	S_2 1_2	S_3 2_1	S_4 2_2
S_1	1_1	$(1\|000)F_1$	$(1\|\frac{111}{222})F_1$	$(4_z\|\frac{111}{222})F_2$	$(4_z\|000)F_2$
S_2	1_2	$(1\|\frac{111}{222})F_1$	$(1\|000)F_1$	$(4_z\|000)F_2$	$(4_z\|\frac{111}{222})F_2$
S_3	2_1	$(4_z\|000)F_1$	$(4_z\|\frac{111}{222})F_1$	$(1\|000)F_2$	$(1\|\frac{111}{222})F_2$
S_4	2_2	$(4_z\|\frac{111}{222})F_1$	$(4_z\|000)F_1$	$(1\|\frac{111}{222})F_2$	$(1\|000)F_2$

IV. DOMAIN PAIRS

1. Domain pairs (DP's) represent an intermediate step between domain states and domain twins. They can be introduced as subsets of order 2 of the set S of SDS's, $\{S_i,S_j\}$, $i,j, = 1,2,3,4$. These are **unordered domain pairs**,[7,10] since, as for any set,

$$\{S_i,S_j\} = \{S_j,S_i\}, \qquad i \neq j. \tag{4.1}$$

A DP $\{S_i,S_j\}$ can be visualized as two overlapping structures S_i and S_j coexisting independently on each other. Thus, e.g., the DP $\{1_1,1_2\}$ can be constructed by extending the structures 1_1 and 1_2 into the whole space. A schematic picture of this DP is presented in Figure 4a, where the squares on left and right sides display

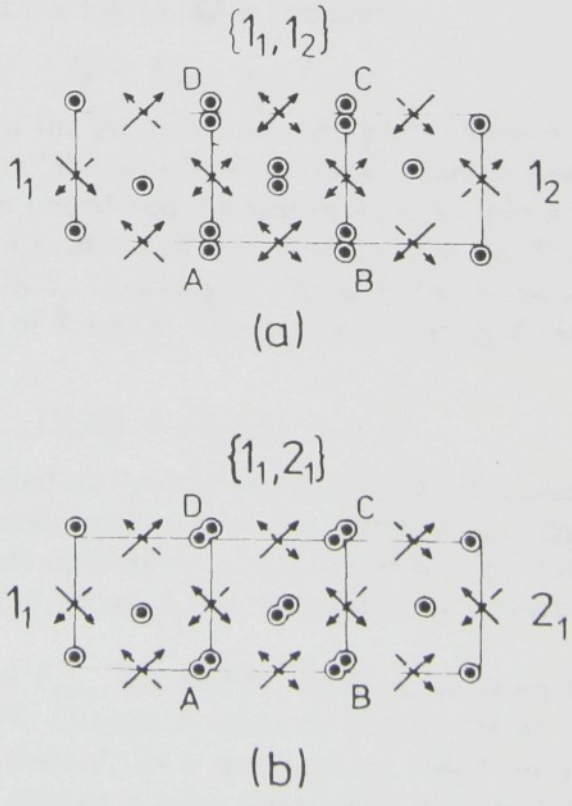

FIGURE 4 Domain pairs of KSCN.
(a) translational domain pair.
(b) ferroelastic domain pair.

structures of 1_1 and 1_2, resp., and the intermediate square, denoted $\{1_1,1_2\}$, represents the overlapping structures of the DP $\{1_1,1_2\}$. In Figure 4b, the DP $\{1_1,2_1\}$ is displayed in a similar manner. As seen from these Figures, a graphical representation of a DP $\{S_i,S_j\}$ allows one to visualize displacements experienced by ions when S_i is switched into S_j. These displacements follow also from a comparison of shifts of ions, given in Table I, for two particular SDS's S_i and S_j.

2. Any DP can be transformed by an operation $g\in G$ into another DP:

$$g\{S_i,S_j\} = \{gS_i,gS_j\} = \{S_k,S_l\},\ g\in G. \tag{4.2}$$

The symmetry group J_{ij} of a DP $\{S_i,S_j\}$ consists of all operations g for which

$$g\{S_i,S_j\} = \{S_i,S_j\}, \qquad g\in G. \tag{4.3}$$

These operations can be divided into two parts:[6,7]

(i) Operations $f\in G$, that leave both S_i and S_j invariant. These operations constitute a group $F_{(i)(j)}$ consisting of operations common to $F_{(i)}$ and $F_{(j)}$:

$$F_{(i)(j)} = F_{(i)} \cap F_{(j)}. \tag{4.4}$$

If S_i,S_j belong to different ferroelastic DS's, the application of the parent clamping approximation is essential since it guarantees the 3-dimensional periodicity of $F_{(i)(j)}$.

(ii) Operations that exchange S_i,S_j (according to Equation (4.1) these are also symmetry operations of $\{S_i,S_j\}$). These operations form a left coset $j'F_{(i)(j)}$ which can be determined from the relation following from Equations (4.4) and (3.10):

$$j'F_{(i)(j)} = g_{ij}F_{(i)} \cap g_{ji}F_{(j)}. \tag{4.5}$$

The symmetry group J_{ij} of the DP $\{S_i,S_j\}$ is the union

$$J_{ij} = F_{(i)(j)} + j'F_{(i)(j)}. \tag{4.6}$$

Division of operations of the group J_{ij} into two parts allows a convenient treatment of DP's: One "colours" the structure S_i "black" and the structure S_j "white". This colouring changes the unordered domain pair $\{S_i,S_j\}$ into an **ordered domain pair** (ODP), denoted (S_i,S_j), in which one distinguishes the first (black) SDS S_i and the second (white) SDS S_j. Contrary to Equation (4.1), the transposition, i.e. a change of order (colour) of S_i and S_j, changes the ODP (S_i,S_j) into another ODP (S_j,S_i):

$$(S_i,S_j) \neq (S_j,S_i), \quad i \neq j. \tag{4.7}$$

Operations (i) can be treated as "colour-preserving" (unprimed) operations and the group $F_{(i)(j)}$ as the symmetry group of the ODP (S_i,S_j). Operations (ii) are "colour-changing" (primed) operations which transform the ODP (S_i,S_j) into a transposed ODP (S_j,S_i). The group J_{ij} can be treated as a black and white space group.[15]

Symmetry groups J_{ij} and $F_{(i)(j)}$ for KSCN, determined from Equations (4.4)–(4.6), are given in Table IV. Groups J_{ij} allow to classify DP's:[6] Thus, $\{S_1,S_2\}$ is a translational domain pair since J_{12} is a space group based on a black-and-white lattice and then j' can be chosen a pure translation. DP $\{S_1,S_3\}$ is a ferroelastic domain pair since $F_{(1)(3)}$ and J_{13} belong to different crystal families, therefore, DS's S_1 and S_3 have different spontaneous deformations.

TABLE IV

Symmetry of domain pairs

Domain pair			Symmetry group of unordered DP			Symmetry group of ordered DP		
			ordinary	black & white	primitive translations			primitive translations
$\{S_1,S_2\}$ $\{S_3,S_4\}$	$\{1_1,1_2\}$ $\{2_1,2_2\}$	J_{12} J_{34}	$Ib_xa_ym_z$	$P_Ib_xc_ym_z$	$\mathbf{a}, \mathbf{b}, \frac{1}{2}(\mathbf{a}+\mathbf{b}+\mathbf{c})$	F_1 F_2	$Pb_xc_ym_z$ $Pc_xa_ym_z$	$\mathbf{a}, \mathbf{b}, \mathbf{c}$
$\{S_1,S_3\}$ $\{S_2,S_4\}$ $\{S_1,S_4\}$ $\{S_2,S_3\}$	$\{1_1,2_1\}$ $\{1_2,2_2\}$ $\{1_1,2_2\}$ $\{1_2,2_1\}$	J_{13} J_{24} J_{14} J_{23}	$Cm_{xy}c_{x\bar{y}}m_z$ $Cc_{xy}m_{x\bar{y}}m_z$	$Cm'_{xy}c'_{x\bar{y}}m_z$ $Cc'_{xy}m'_{x\bar{y}}m_z$	$\mathbf{a}_1,\mathbf{a}_2,\mathbf{c}$	F_{12}	$P2_{1z}/m_z$	$\mathbf{a}_1,\mathbf{a}_2,\mathbf{c}$

Symmetrically equivalent domain pairs are placed between two horizontal lines (cf. TABLE $\overline{V}$).

3. Two **domain pairs**, for which Equation (4.2) holds, are **symmetrically equivalent in G**. The set P of all DP's can be divided into classes of symmetrically equivalent DP's (G-orbits). As proved in Reference 10 (Theorem V), there is a one-to-one correspondence between these classes and the resolution of G into double cosets F_1gF_1 of F_1. From Table II, where the double cosets of $F_1 = Pbcm$ can be found, it follows that there are two classes of symmetrically equivalent DP's, i.e. the set P splits into two G-orbits. From Theorem V it further follows that the representative DP's of these two classes are $\{S_1,S_2\}$ and $\{S_1,S_3\}$.

If we numerate the DP's of P, e.g., $P = \{P_1,P_2,P_3,P_4,P_5,P_6\} = \{\{1_1,1_2\}, \{2_1,2_2\}, \{1_1,2_1\}, \{1_2,2_2\}, \{1_1,2_2\}, \{1_2,2_1\}\}$, we can write the relation between the DP's in the matrix form:

$$P_p = Q_{pq}P_q, \qquad p,q = 1,2, \ldots,6. \tag{4.8}$$

The matrix Q_{pq} is given in Table V. Two diagonal blocks correspond to two classes of symmetrically equivalent DP's (cf. TABLE IV).

4. A generalization of a domain pair is the set of all SDS's. The **unordered set** $\{S_1,S_2,S_3,S_4\}$ is obviously invariant under G. From the transitivity of SDS's it follows that the action of $g \in G$ on the **ordered set** (S_1,S_2,S_3,S_4),

$$g(S_1,S_2,S_3,S_4) = (gS_1,gS_2,gS_3,gS_4) = (S_k,S_l,S_m,S_n), \tag{4.9}$$

results in a permutation of the set. From Equations (3.9), (3.10) we find the stabilizer K of (S_1,S_2,S_3,S_4),

$$K = F_1 \cap F_2 = P2_{1z}/m_z. \tag{4.10}$$

Each left coset of the resolution

$$G = K + g_2K + \ldots + g_8K \tag{4.11}$$

is associated with one permutation of the ordered set. The explicit form of the resolution (4.11) can be found in Table II. The resolution (4.11) defines a homomorphic mapping of G onto the group of permutations of (S_1,S_2,S_3,S_4). This permutation representation of G is isomorphic with the representation according to which the order parameter of the phase transition transforms.[20]

TABLE V

Transformation matrix of domain pairs

$\{S_k,S_l\}$	$\{S_i,S_j\}$	$\{S_1,S_2\}$ $\{1_1,1_2\}$	$\{S_3,S_4\}$ $\{2_1,2_2\}$	$\{S_1,S_3\}$ $\{1_1,2_1\}$	$\{S_2,S_4\}$ $\{1_2,2_2\}$	$\{S_1,S_4\}$ $\{1_1,2_2\}$	$\{S_2,S_3\}$ $\{1_2,2_1\}$
$\{S_1,S_2\}$	$\{1_1,1_2\}$	$(1\|000)J_{12}$	$(4_z\|000)J_{12}$	$\emptyset$	$\emptyset$	$\emptyset$	$\emptyset$
$\{S_3,S_4\}$	$\{2_1,2_2\}$	$(4_z\|000)J_{12}$	$(1\|000)J_{12}$	$\emptyset$	$\emptyset$	$\emptyset$	$\emptyset$
$\{S_1,S_3\}$	$\{1_1,2_1\}$	$\emptyset$	$\emptyset$	$(1\|000)J_{11}$	$(1\|\frac{111}{222})J_{11}$	$(4_z\|000)J_{11}$	$(4_z\|\frac{111}{222})J_{11}$
$\{S_2,S_4\}$	$\{1_2,2_2\}$	$\emptyset$	$\emptyset$	$(1\|\frac{111}{222})J_{11}$	$(1\|000)J_{11}$	$(4_z\|\frac{111}{222})J_{11}$	$(4_z\|000)J_{11}$
$\{S_1,S_4\}$	$\{1_1,2_2\}$	$\emptyset$	$\emptyset$	$(4_z\|\frac{111}{222})J_{11}$	$(4_z\|000)J_{11}$	$(1\|000)J_{11}$	$(1\|\frac{111}{222})J_{11}$
$\{S_2,S_3\}$	$\{1_2,2_1\}$	$\emptyset$	$\emptyset$	$(4_z\|000)J_{11}$	$(4_z\|\frac{111}{222})J_{11}$	$(1\|\frac{111}{222})J_{11}$	$(1\|000)J_{11}$

V. DOMAIN TWINS

1. A **domain twin (DT)** consists of two domains which meet along a planar transition region called **domain wall (DW)**. A normal **n** to the central plane of the DW defines its orientation and the sidedness. The position of the central plane is described by a vector **p**, defined below. Unless stated otherwise, we shall assume that the DW has zero thickness. A DT is defined by specifying domain states on $-$ and $+$ sides of the wall normal **n**. The **symbol of** this **DT** is $(S_i/\mathbf{n},\mathbf{p}/S_j)$, where the DS on the left (right) side corresponds to the DS adhearing to the $-$ ($+$) side of **n**. From this convention follows the identity

$$(S_i/\mathbf{n},\mathbf{p}/S_j) = (S_j/-\mathbf{n},\mathbf{p}/S_i), \tag{5.2}$$

i.e., if we exchange the sides (reverse the normal **n**) of DW and, simultaneously, exchange DS's in both domains we obtain an identical DT.

2. Applying an operation $g\in G$ on a DT we get another DT which is symmetrically equivalent in G with the original one,

$$g(S_i/\mathbf{n},\mathbf{p}/S_j) = (gS_i/g\mathbf{n},g\mathbf{p}/gS_j). \tag{5.3}$$

All $g\in G$ that leave $(S_i/\mathbf{n},\mathbf{p}/S_j)$ invariant constitute the **symmetry group** $T(S_i/\mathbf{n},\mathbf{p}/S_j)$ **of DT**. This group is a layer group.[17] If **n** and **p** are specified in the context, or if they are not significant, we use the symbol T_{ij} only. Generally, group T_{ij} consists of two parts:[6,7]

$$T_{ij} = \hat{F}_{ij} + \underline{t}'_{ij}\hat{F}_{ij}, \tag{5.4}$$

where $\hat{F}_{ij}$ is a group of all operations that leave $S_i,S_j,\mathbf{n},\mathbf{p}$ invariant. This group equals the one-sided sectional layer group[16] of F_{ij} for the central plane of DW, $\underline{t}'_{ij}$ is an operation exchanging S_i and S_j (primed operation) and, simultaneously, transforming **n** into $-\mathbf{n}$ (underlined operation). If such an operation exists, i.e., if $\hat{F}_{ij} < T_{ij}$, then the DT is called a **symmetric DT**. In opposite case, $\hat{F}_{ij} = T_{ij}$, and the DT is denoted a **non-symmetric DT**. There is a close relation between the group T_{ij} and the sectional layer group $\bar{J}_{ij}$ of the DP $\{S_i,S_j\}$ along the central plane of the DT:

$$\bar{J}_{ij} = \hat{F}_{ij} + \underline{t}'_{ij}\hat{F}_{ij} + \underline{r}_{ij}\hat{F}_{ij} + \underline{s}'_{ij}\hat{F}_{ij} = T_{ij} + R_{ij}, \tag{5.5}$$

where $\underline{r}_{ij}$ transforms **n** into $-\mathbf{n}$, $\underline{s}_{ij}$ exchanges S_i and S_j and the complex R_{ij} assembles the operations transforming $(S_i/\mathbf{n},\mathbf{p}/S_j)$ into a **reversed DT** $(S_j/\mathbf{n},\mathbf{p}/S_i)$. If the complex R_{ij} is not empty, i.e. if $T_{ij} < \bar{J}_{ij}$, we call the DT a **reversible DT**. In opposite case, the DT is an **irreversible DT**.

3. The application of these general results on KSCN is summarized in Table VI. For a given DP $\{S_i,S_j\}$ and the normal **n**, expressed by coordinates n_x, n_y, n_z, we find in Table VI the primitive basis (translations) **A** and **B** of the diperiodic lattice of the DT. The vector **C** expresses the minimum shift (periodicity) of DW to a new position with the same structure of the DW. Symmetries T_{ij} and $\bar{J}_{ij}$ repeat with the periodicity $\frac{1}{2}$ **C**. The position **p** of the DW is specified by a fraction p of **C**. The groups T_{ij}, $\bar{J}_{ij}$ and $\hat{F}_{ij}$, specifying symmetry properties of a DT $(S_i/\mathbf{n},p\mathbf{C}/S_j)$, are given in the column Associated layer groups. Two positions of the DW given in the Table VI correspond to symmetrically prominent positions in which additional

TABLE VI

Symmetries of domain twins, associated layer groups, site symmetries and displacements of ions in domain walls

Twin symbol	Periodicity A	B	C	Position p	Associated layer groups		K^+ Site sym.	K^+ Shift	$(SCN)^-$ Site sym.	$(SCN)^-$ Shift	$(SCN)^-$ Rot.
$(1_1/100;p/1_2)$	**b**	**c**	**a**	0	T_{12}	$p\underline{c}'_x c_y m_z$	$2_x 2_y 2_z$	0	$2_z/m_z$	0	φ_z
					$\bar{J}_{12}$	$p\underline{c}'_x c_y m_z$	$2_x 2_y 2_z$	0	$2_z/m_z$	0	φ_z
					F_{12}	$p\underline{2}_x c_y m_z$	2_x	x	m_z	x,y	φ_z
				$\frac{1}{4}$	T_{12}	$p2_x c_y m_z$	off-centre		off-centre		
					$\bar{J}_{12}$	$p\underline{b}_x c_y m_z$					
					F_{12}	$p\underline{2}_x c_y m_z$	2_x	x	m_z	x,y	φ_z
$(1_1/010;p/1_2)$	**a**	**c**	**b**	0	T_{12}	$p\underline{2}'_z/m_z$	2_z	z	$2_z/m_z$	0	φ_z
					$\bar{J}_{12}$	$pc'_x\underline{c}_y m_z$	$2_x 2_y 2_z$	0	$2_z/m_z$	0	φ_z
					F_{12}	pm_z	1	x,y,z	m_z	x,y	φ_z
				$\frac{1}{4}$	T_{12}	$p\underline{2}'_{1x}\underline{a}'_y m_z$	off-centre		off-centre		
					$\bar{J}_{12}$	$pc'_x\underline{a}'_y m_z$					
					F_{12}	pm_z	1	x,y,z	m_z	x,y	φ_z
$(1_1/110;p/2_1)$	**a − b**	**c**	**a**	0	T_{13}	$p\underline{g}'_{xy}\underline{2}'_{1x\bar{y}}\mathrm{m}_z$	1	x,y,z	off-centre		
					$\bar{J}_{13}$	$p\underline{g}'_{xy}c'_{x\bar{y}}m_z$	2_{xy}	$x = y$			
					F_{13}	pm_z	1	x,y,z	m_z	x,y	φ_z
				$\frac{1}{2}$	T_{13}	$p\underline{m}'_{xy}\underline{2}'_{x\bar{y}}m_z$	off-centre		$m_{xy}\underline{2}_{x\bar{y}}m_z$	$x = \bar{y}$	0
					$\bar{J}_{13}$	$p\underline{m}'_{xy}c'_{x\bar{y}}m_z$			$m_{xy}\underline{2}_{x\bar{y}}m_z$	$x = \bar{y}$	0
					F_{13}	pm_z	1	x,y,z	m_z	x,y	φ_z
$(1_1/1\bar{1}0;p/2_1)$	**a + b**	**c**	**a**	0	T_{13}	$p\underline{2}'_{xy}c'_{x\bar{y}}m_z$	2_{xy}	$x = y$	off-centre		
					$\bar{J}_{13}$	$pm'_{xy}\underline{c}'_{x\bar{y}}m_z$	2_{xy}	$x = y$			
					F_{13}	pm_z	1	x,y,z	m_z	x,y	φ_z
				$\frac{1}{2}$	T_{13}	$p\underline{2}'_{1xy}\underline{n}'_{x\bar{y}}m_z$	off-centre		m_z	x,y	φ_z
					$\bar{J}_{13}$	$pm'_{xy}\underline{n}'_{x\bar{y}}m_z$			$m_{xy}\underline{2}_{x\bar{y}}m_z$	$x = \bar{y}$	0
					F_{13}	pm_z	1	x,y,z	m_z	x,y	φ_z

symmetry elements appear in comparison with those available in a general position. A DT with the DW at a general position has the symmetry group $T_{ij} = \hat{F}_{ij}$. Next columns of the Table VI give the site symmetries and corresponding spontaneous displacements (shifts) of ions, and for SCN^- ions also the spontaneous rotation φ_z. Data given in rows T_{ij} and $\bar{J}_{ij}$ concern the structure of the central plane of the DW, whereas the data in the row $\hat{F}_{ij}$ hold not only for the central plane but, in DT's with finite-thickness DW's, also for any out-of-the-central-plane layers. For this reason, symmetry $\hat{F}_{ij}$, corresponding site symmetries and shifts are given even if the particular ions are missing in the central plane. We shall briefly comment particular cases given in the Table VI:

A. TRANSLATION DOMAIN TWINS

1a) DT ($1_1/100;0/1_2$), see Figure 5, upper part.

This DT provides an example of a symmetric, irreversible DT, since $\hat{F}_{12} < T_{12} = J_{12}$. Though the structure of the central layer in DT ($1_1/100;0/1_2$) and in the reversed DT ($1_2/100;0/1_1$) is the same (it corresponds to the structure of the parent phase: K^+ ions at $(00\frac{1}{4})$ positions and SCN^- ions disordered) the arrangement in neighbouring planes on both sides of the central plane is different: for the original DT the K^+ ions are shifted towards the central plane and the ordered SCN^- ions have a head-to-head arrangement. In the reversed DT, K^+ ions are shifted outwords the central plane and the SCN^- ions have a tail-to-tail arrangement.

1b) DT ($1_1/100;\frac{1}{4}/1_2$), see Figure 5, lower part.

This is a non-symmetric, reversible DT since $\hat{F}_{12} = T_{12} < J_{12}$. Though the central plane does not contain any ions, this position is symmetrically prominent one since at a general position $J_{12} = T_{12} = \hat{F}_{12}$, hence the DT is non-symmetric and irreversible. The symmetry T_{12} for position $p = \frac{1}{4}$ is polar. The DW can, therefore, carry a non-zero spontaneous polarization.

Comparison of cases 1a) and 1b) illustrates that the symmetry of a DT may considerably change with changing the position of the central plane of the DW.

2a) DT ($1_1/010;0/1_2$), see Figure 6, upper part.

The central structure of this symmetric, reversible DT is formed by disordered SCN^- ions and K^+ ions shifted alternatively in $-z$ and $+z$ directions. These shifts lower the symmetry of the central layer to the monoclinic symmetry of the entire DT.

2b) DT ($1_1/010;\frac{1}{4}/1_2$), see Figure 6, lower part.

Though the central plane does not contain any ions, this DT is symmetric and reversible. Symmetry T_{12} is polar.

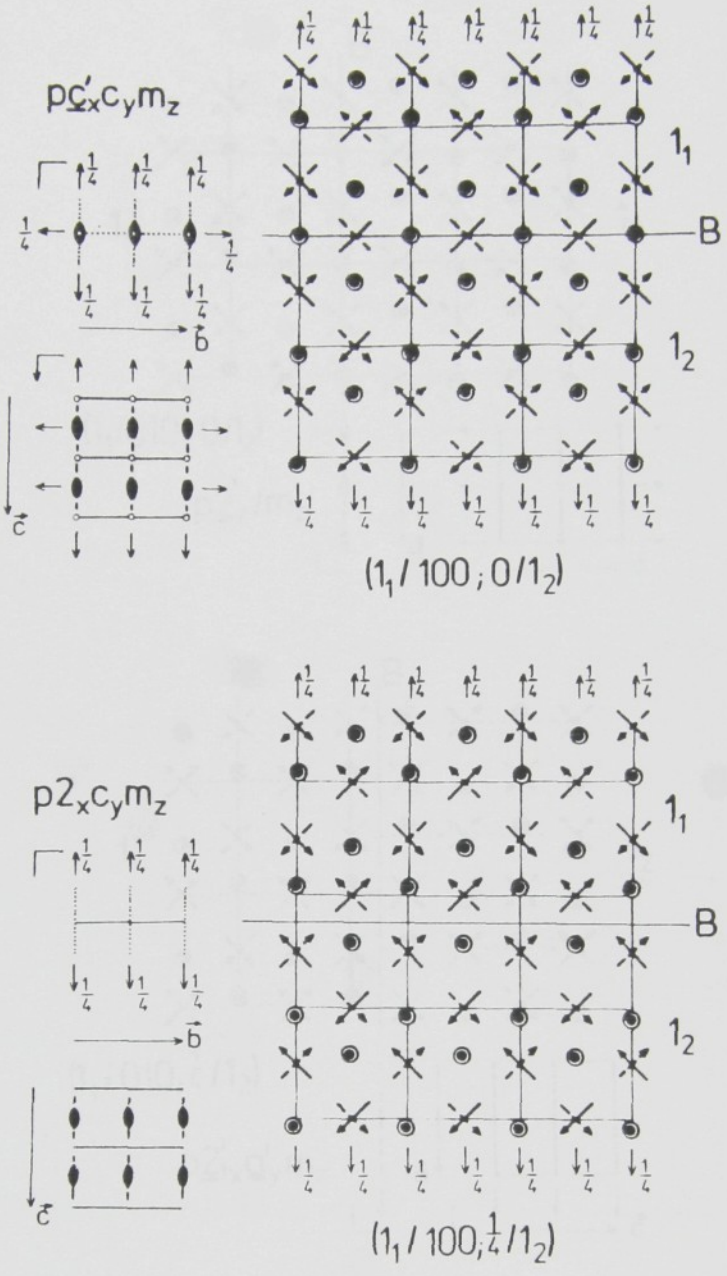

FIGURE 5 Translation domain twins with antiphase boundary of (100) orientation at two symmetrically prominent positions.

A comparison of four DT's considered above illustrates the diversity of symmetries and structures of translation DT's formed from one translational DP $\{1_1,1_2\}$.

B. FERROELASTIC DOMAIN TWINS

For the ferroelastic DP $\{1_1,2_1\}$ there exist just two planes with normals [110] and [1$\bar{1}$0] along which ferroelastic domains can meet coherently. These planes correspond to the mirror planes lost at the phase transition.[9] Because of the different spontaneous deformation in SDS's 1_1 and 2_1, the analysis has to be performed in parent clamping approximation see Equation (3.4).

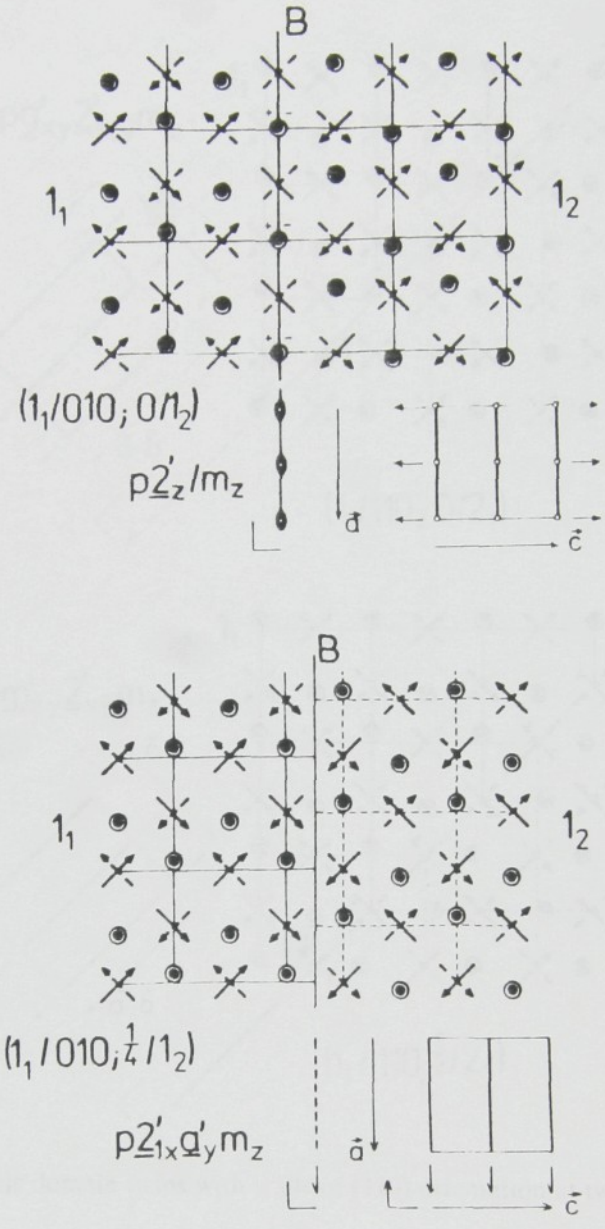

FIGURE 6 Translation domain twins with antiphase boundary of (010) orientation at two symmetrically prominent positions.

From Table VI we see that all ferroelastic DT's with symmetrically prominent positions are symmetric and reversible and possess orthorhombic polar point group symmetry *m2m* (up to the orientation), though with different layer groups T_{13} and J_{13}. We shall comment briefly only the central structure of the ferroelastic DW's.

3a) DT ($1_1/110;0/2_1$), see Figure 7, upper part.

The central structure is formed by K^+ ions. Additional shifts from the SDS's positions have general directions. All these shifts are, however, correlated by the glide planes g_{xy} and mirror planes m_z.

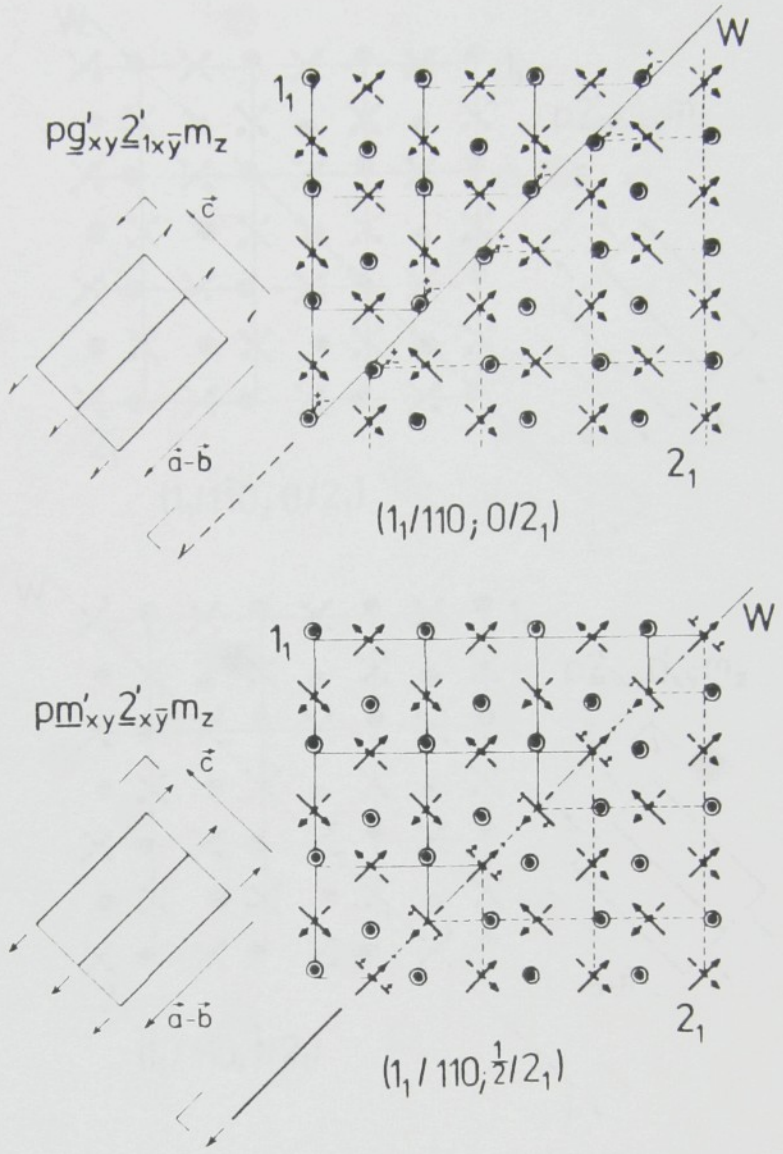

FIGURE 7 Ferroelastic domain twins with walls of (110) orientation at two symmetrically prominent positions.

3b) DT ($1_1/110;\frac{1}{2}/2_1$), see Figure 7, lower part.

The central structure is formed by SCN^- ions. Ions which are perpendicular to the central plane are disordered, whereas ions parallel to that plane are ordered. Both types of SCN^- ions experience additional shifts along [1T0] direction.

4a) DT ($1_1/1T0;0/2_1$), see Figure 8, upper part.

The central structure is formed by K^+ ions. The additional shifts from common positions in SDS's 1_1 and 2_1 are performed along [110] direction. The displacements at positions $(00\frac{1}{4})$ and $(\frac{1}{2}\frac{1}{2}\frac{1}{4})$ are different (arrows and double arrows).

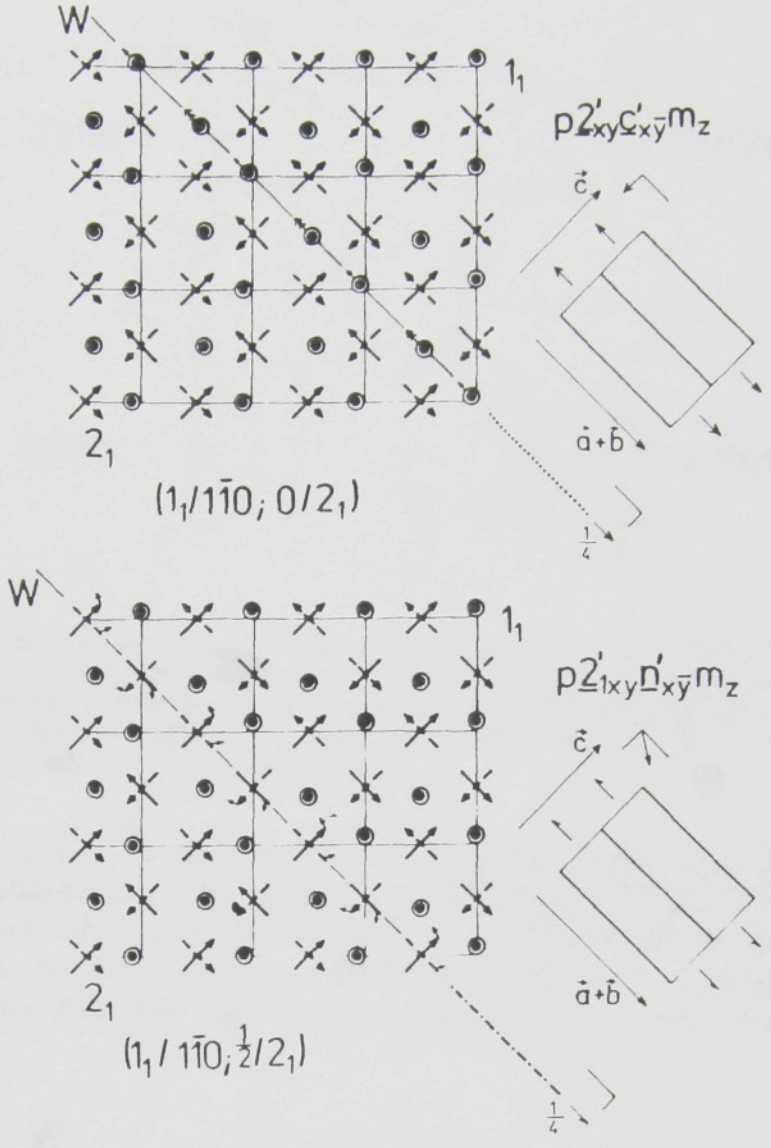

FIGURE 8 Ferroelastic domain twins with walls of (1$\bar{1}$0) orientation at two symmetrically prominent positions.

4b) DT $(1_1/1\bar{1}0;\frac{1}{2}/2_1)$*, see Figure 8, lower part.*

The central plane is formed by SCN^- ions. Contrary to central structure in $(1_1/110;\frac{1}{2}/2_1)$, ions perpendicular to the central plane are alternatively ordered, ions with parallel orientation are disordered. Additional shifts are confined to the mirror planes m_z (see TABLE VI).

VI. LIFTING OF PARENT CLAMPING APPROXIMATION

Introduction of non-zero spontaneous deformations has the following consequences for ferroelastic domain twins:

(i) Orientations of coherent stress-free DW's are confined, in our example, to mirror planes lost at the phase transition.[9]

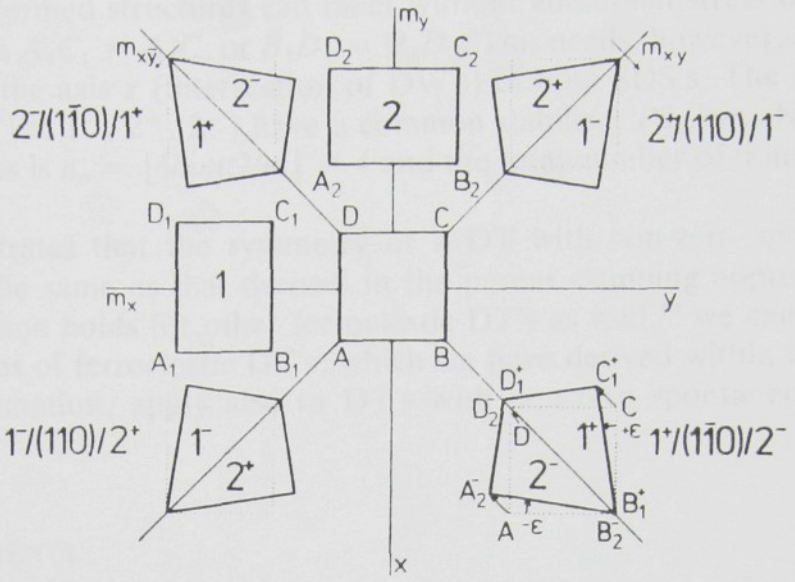

FIGURE 9 Splitting of single domain states in ferroelastic twins. 1, 2 are ferroelastic single domain states, 1^-, 1^+, 2^-, 2^+ are domain states in ferroelastic twins with coherent domain walls with (110) and (1$\bar{1}$0) orientations. Distortion connected with lifting of parent clamping approximation (see text) is depicted in the right-lower part of the Figure. Significant is the rotation $\pm\varepsilon$ which is needed to achieve stress-free contact of adjacent domain states.

(ii) Structures S_i,S_j of domains adhearing to a coherent stress-free DW have orientations different from that of corresponding SDS's.[18,19] This can be seen from Figure 9, where the square ABCD represents the unit cell in parent clamping approximation and $A_iB_iC_iD_i$, $i = 1,2$, the unit cells of SDS's. During the deformation only the diagonals AC and BD experience the same change of length,

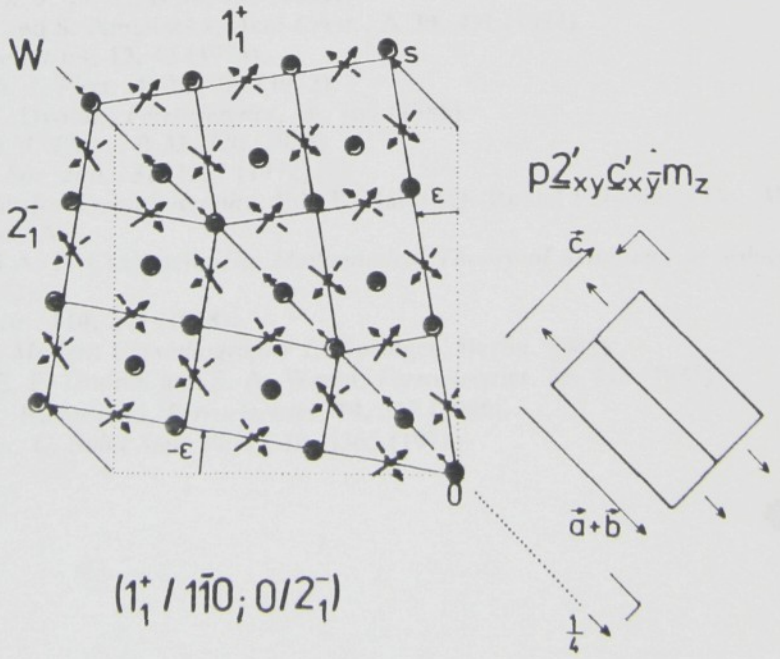

FIGURE 10 Ferroelastic domain twin $(1_1^+/1\bar{1}0;0/2_1^-)$ with exaggerated spontaneous deformation. The symmetry of the twin is not affected by the spontaneous deformation. (cf. Figure 8, upper part and Figure 9).

therefore, the deformed structures can meet without additional stress only along common diagonals $A_1C_1 = A_2C_2$ or $B_1D_1 = B_2D_2$. This needs, however, a rotation $+\varepsilon$ or $-\varepsilon$ along the axis z (intersection of DW's) of both SDS's. The structures in new positions (1^+, 1^-, 2^+, 2^-) have a common stabilizer $P2_{1z}/m_z$. Number of orientational states is $n_o = [4mm{:}2/m] = 4$ and the total number of domain states increases to 8.

Figure 10 illustrates that the symmetry of a DT with non-zero spontaneous deformations is the same as that derived in the parent clamping approximation. Since this conclusion holds for other ferroelastic DT's as well,[19] we can conclude that all symmetries of ferroelastic DT's, which we have derived within the parent clamping approximation, apply also to DT's with non-zero spontaneous deformation.

ACKNOWLEDGEMENTS

This work was supported by the Österreich. Fonds für Förderung der wissenschaftlichen Forschung under the Project number P6758 P. Two of the authors, V. J. and W. S., would like to express thanks to members of the Institut f. Experimentalphysik der Universität Wien and of the Institute of Physics, Czech. Acad. Sci., Prague, resp., for their hospitality during short working stays.

REFERENCES

1. W. Schranz, T. Streuselberger, A. Fuith, H. Warhanek and M. Götzinger, *Ferroelectrics*, **88**, 139 (1988).
2. H. P. Klug, *Z. Krist.*, **85**, 214 (1933).
3. S. Yamamoto, M. Sakuno and Y. Shinnaka, *J. Phys. Soc. Jpn.*, **56**, 4393 (1987).
4. Y. Yamada and T. Watanabe, *Bull. Chem. Soc. Jpn.*, **36**, 1032 (1963).
5. W. Schranz, H. Warhanek and P. Zielinski, *J. Phys.: Condens. Matter*, **1**, 1141 (1989).
6. V. Janovec, *Ferroelectrics*, **35**, 105 (1981).
7. Z. Zikmund, *Czech. J. Phys.*, B **34**, 932 (1984).
8. G. Van Tendeloo and S. Amelinckx, *Acta Cryst.*, A **30**, 431 (1974).
9. V. Janovec, *Ferroelectrics*, **12**, 43 (1976).
10. V. Janovec, *Czech. J. Phys.*, B **22**, 974 (1972).
11. V. Janovec and V. Dvořák, *Ferroelectrics*, **66**, 169 (1986).
12. V. Kopský, *Czech. J. Phys.*, B **33**, 720 (1983).
13. K. Aizu, *J. Phys. Soc. Jpn.*, **32**, 1287 (1972).
14. *International Tables for Crystallography*, Ed. T. Hahn (D. Reidel Publishing Co., Dodrecht, 2nd Edition, 1987), Vol. A.
15. J. C. Bradley and A. P. Cracknell, *The Mathematical Theory of Symmetry in Solids*, (Clarendon Press, Oxford, 1972).
16. W. Holser, *Z. Krist.*, **110**, 249 (1958).
17. B. K. Vainshtein, *Modern Crystallography I*, (Springer, Berlin, 1981).
18. L. A. Shuvalov, E. F. Dudnik and S. A. Wagin, *Ferroelectrics*, **65**, 143 (1985).
19. V. Janovec and L. Richterová, *Ferroelectrics*, **79**, 317 (1988).
20. E. Ascher, *J. Phys. C: Solid State Phys.*, **10**, 1365 (1977).

MODULATED PHASES IN CRYSTALS : SYMMETRIES OF WALLS AND WALL LATTICES . EXAMPLE OF QUARTZ

P. Saint-Gregoire (*) and V. Janovec (**)

(*) GDPC (URA CNRS n°233), USTL,case 026, 34060 MONTPELLIER CEDEX, F
(**) Institute of Physics, CsAV, Na Slovance 2, 18040 PRAGUE 8, CSSR

Abstract. The incommensurate phase of quartz-type is used as

I . INTRODUCTION

The atomic displacements in modulated phases of real crystals obey non-linear equations which do not have in general exact solutions. A possible approach of the problem is to simplify the equations in a drastic way, and, e.g., to treat the system as a linear chain. Another approach is just to keep the maximum number of informations on the concrete system and to try to deduce other properties. In this respect, the tools offered by the theory of symmetry are very important, since they allow to treat the problem without simplifying assumptions.

The aim of this paper is to present such an approach to modulated phases which can be described by a lattice of domain walls, called also discommensurations. The incommensurate phase of quartz-type is used as an illustrative example.

II . STRUCTURE OF INCOMMENSURATE PHASES. EXAMPLE OF QUARTZ

a) General properties of incommensurate phases

Most of incommensurate phases are observed in a temperature region between two periodic crystalline phases labelled N ("normal", at higher temperatures) and C ("commensurate", at lower temperatures). Since the vector **k** associated with the wave of atomic displacements, is temperature dependent, the incommensurate phase cannot be described by a simple order parameter but by a continuous set of order parameters, indexed by **k**. Nevertheless, one gets a simplification by introducing the order parameter η of the N-C phase transition, which is well defined if the symmetry group of phase C is a subgroup of that of N. Then the incommensurate phase can be described as a spatial modulation of phase C. For this reason, the term modulated phase is also used (for further details see e.g. ref /1/ and /2/).

An important class of materials presenting an incommensurate phase, is constituted by those whose order parameter η (of N-C structural change) does not fulfil the so called Lifshitz criterion . It implies the presence, in the free energy expansion, of an antisymmetric term which couples a component of η to the spatial derivative of another one. To be concrete, let us consider the case where η has two components p and q, the expression $(p\,dq/dx - q\,dp/dx)$ (Lifshitz term) being invariant under the symmetry operations of phase N. The free energy density can be written as /2/

$$f(x) = f_o + \frac{\alpha}{2}(p^2+q^2) + ... + \delta\,(p\frac{dq}{dx} - q\frac{dp}{dx}) + \frac{\chi}{2}((\frac{dp}{dx})^2 + (\frac{dq}{dx})^2) + .. \qquad (1)$$

Because of the Lifshitz invariant, the loss of stability when the coefficient α changes sign, does not lead to the C phase but to a state with inhomogeneous displacements. This can be more easily understood after introducing new variables ρ and θ :

$$p = \rho \sin\theta,\ q = \rho\cos\theta \qquad (2)$$

$$f(x) = f_o + \frac{\alpha}{2}\rho^2 + ... - \delta\,\rho^2\frac{d\theta}{dx} + \frac{\chi}{2}((\frac{d\rho}{dx})^2 + \rho^2(\frac{d\theta}{dx})^2) + .. \qquad (3)$$

The third term lowers the energy for inhomogeneous θ but spatial variations of θ are limited by the last positive term. To obtain the wave vector variation and the transition to the C phase, one has to add (at least) another term $\rho^n\cos(n\theta)$ which is called anisotropic because of its θ dependence. With e.g. a positive coefficient in front of it, it is minimal for $n\theta = (2l+1)\pi$. Close to T_i (transition temperature between phases N and I) the amplitude ρ is very small and the anisotropic term is negligible : the solution which minimizes the free energy is sinusoidal. On decreasing the temperature from T_i, there is a competition between the Lifshitz and the anisotropic terms, which results in a change of k and of the form of modulation. These solutions obey the Euler-Lagrange equations derived from the expression of f(x), which are non-linear and which in general do not have exact solutions. However, on approaching the transition temperature T_c (to C phase), in the major part of the period L of the modulation, the order parameter η is associated with values of θ which minimize the anisotropic term and correspond to the different domain states in the C phase. The structure of the incommensurate phase is then rather similar to a domain structure with domain walls regularly disposed in the x direction : far below T_i in the modulated phase, the sinusoidal structure changes into a periodic structure of domain walls of the C phase. One can attribute to them a negative energy in the I phase (because of Lifshitz invariant), and a positive energy in the C phase, where the anisotropic term is preponderant. At the I-C transition,

their density theoretically goes to zero, but this is not the case in real crystals where walls are pinned by defects of crystal lattice.

b) case of quartz type phases

In the preceding paragraph, we presented incommensurate phases formed due to the violation of Lifshitz criterion. Modulated phases can, however, appear between N and C phases even if the order parameter satisfies the Lifshitz criterion /3/. Quartz belongs to this category, since its order parameter has a single component, which can be identified with the angle of rotation of SiO_4 tetrahedra around their twofold axes along x type directions /4/. This mechanism breaks the 6-fold symmetry of β phase (N phase) with the space group $P\,6_2\,2_x\,2_y$. In the α phase (C phase) the twofold symmetry operations 2_y are lost and the hexagonal symmetry is reduced to trigonal $P\,3_2\,2_y$.

In the C phase, there are only two domain states, corresponding to positive and negative value of η. They are referred to as "Dauphiné twins". The loss of stability of β phase does not occur for displacements corresponding to the trigonal α phase, but for a modulated phase /5,6/. This is due to an invariant playing the role of the Lifshitz term, $(U_{xx} - U_{yy})\frac{\partial\eta}{\partial x} - 2\,U_{xy}\frac{\partial\eta}{\partial y}$, and which couples spatial derivatives of the order parameter η to the strain tensor U_{ij}. As a result, there occurs an instability with respect to modulated displacements, with three modulation wave vectors k_i (plus their opposites) lying at T_i along the directions of the lost twofold axes (y axes) /7/.

With such wave vectors at 120° from each other, there are several possibilities : the modulations are, e.g., spatially separated (forming so called stripe phases) or all modulations are superimposed. The latter case corresponds to the observations of the incommensurate phase by means of electron microscopy, where a regular pattern of equilateral triangles reflects the spatial modulation of the order parameter η /8,9/.

Both phases, stripe phase and equilateral triangles phase provide non trivial examples and will be used to illustrate our approach.

III . SYMMETRY OF SINGLE DOMAIN WALLS

Before investigating incommensurate structures, which we shall treat as a regular pattern of domain walls, we recall basic properties of single domain walls. A *domain wall* is a transient region between

$S_i/n/S_j$ is used for a planar coherent wall with domain state S_i on the negative side, and S_j on the positive side of the wall normal n, which determines the orientation of the wall. Within this convention, the identity $S_i/n/S_j = S_j/-n/S_i$ always holds.

Symmetry group T_{ij} of the domain wall $S_i/n/S_j$ contains operations that keep invariant orientation and position of the wall, i.e., T_{ij} is a layer group which consists of two parts /10/ :

$$T_{ij} = F_{ij} + \underline{t}'_{ij} F_{ij} , \qquad (4)$$

where F_{ij} comprises operations leaving invariant both domain states S_i, S_j and the normal n, whereas $\underline{t}'_{ij}$ is an operation that exchanges domain states S_i, S_j and transforms n into -n (the former action is signified by a prime, the latter by underlining). Walls for which $\underline{t}'_{ij}$ exists are called *symmetric walls*.

Two walls are symmetrically equivalent, $S_i/n/S_j \simeq S_k/n'/S_l$, if there exists an operation from the symmetry group of the N phase, that transforms one wall into the other. Symmetrically equivalent walls have the same structure and the same energy. A wall $S_i/n/S_j$ is called *reversible* if it is symmetrically equivalent with the reversed wall $S_j/n/S_i$.

Symmetry group T_{ij} of a domain wall determines the number n_v of symmetrically equivalent domain walls according to a simple formula:

$$n_v = |G| : |T_{ij}|, \qquad (5)$$

where $|G|, |T_{ij}|$ are orders (numbers of operations) of point groups G (symmetry of the N phase) and T_{ij}, resp.

The knowledge of wall symmetry T_{ij} is very useful in locating orientations with extremal wall energy and identifying the specific tensor properties of walls.

As an illustrative example, we shall investigate symmetry properties of domain walls in quartz. For simplicity, we use continuum description and consider walls parallel to z axis (6-fold axis of the β phase). Then, the orientation of a wall is specified by the angle θ between the axis y_2 and the axis ξ attached to the wall (see fig.1c).

First examine the symmetry of a domain wall perpendicular to the coordinate axis x_2, $1/-\frac{\pi}{2}/2$, where $(-\frac{\pi}{2})$ specifies the angle θ and 1 and 2 denote domain states $-\eta_0$ and $+\eta_0$, resp. (fig. 1a). This wall is transformed into itself by any 2-fold rotation axis 2_{x2} perpendicular to the wall, further by any 2-fold axis 2_{y2} and 2_z lying in the plane of the wall and parallel to the coordinate axis y_2 and z, resp. The former operations 2_{x2}, belonging to the symmetry group $3\,2_x$, preserve both domain states 1, 2 and also leave invariant the normal n, whereas the latter rotations $\underline{2}'_{y2}$, $\underline{2}'_z$, which were lost at the phase transition,

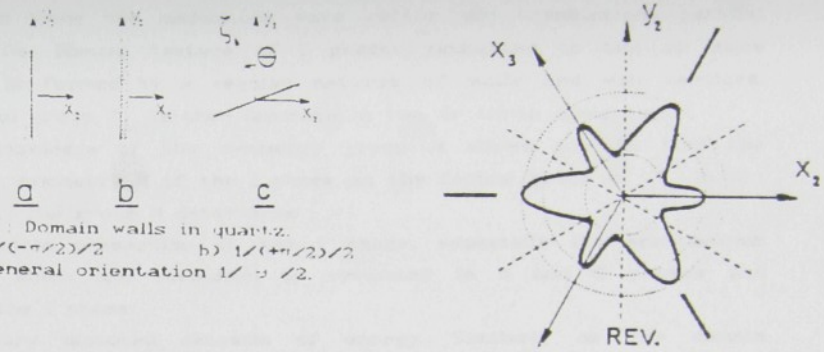

Fig.1 : Domain walls in quartz.
a) $1/(-\pi/2)/2$ b) $1/(+\pi/2)/2$
c) general orientation $1/\theta/2$.

Fig.2 : Angular dependence $E(\theta)$ of the wall energy. Reversible and prominent orientations are indicated.

exchange both domain states 1, 2 and, simultaneously, transform the wall normal n into antiparallel -n. All above mentioned operations transforming the wall into itself form the group $\mathcal{L}\, 2_{x2}\underline{2}'_{y2}\underline{2}'_z$ where $\mathcal{L}$ signifies a layer group.

The reversed domain wall $2/-\frac{\pi}{2}/1 = 1/\frac{\pi}{2}/2$ (see fig. 1b) has the same symmetry $\mathcal{L}\, 2_{x2}\underline{2}'_{y2}\underline{2}'_z$ as the original wall $1/-\frac{\pi}{2}/2$. There is, however, no operation from the symmetry group $6\,2_x2_y$ of the β phase, which would transform the wall $1/-\frac{\pi}{2}/2$ into reversed wall $2/-\frac{\pi}{2}/1$. These two walls are, therefore, not symmetrically equivalent; i.e., they have different structure and different energy.

The wall 1/0/2, which is perpendicular to y_2 (fig.1c with $\theta=0$), has a symmetry expressed by the layer group $\mathcal{L}\,\underline{2}'_z$. The operations $2'_{y2}$, that exchange domain states only, and operations $\underline{2}_{x2}$ reversing the wall normal only, are no more symmetry operations of the wall but they transform the wall 1/0/2 into reversed wall 2/0/1 and vice versa, i.e., these walls are reversible.

It is easy to show that a wall parallel to z, with a general orientation θ (fig. 1c) has the symmetry $\mathcal{L}\,\underline{2}'_z$ as well, but, contrary to walls with special orientation $\theta = 0$, it is not reversible. From eq.(5) we find the number of symmetrically equivalent walls: for walls with $T_{12} = \mathcal{L}\, 2_{x2}\underline{2}'_{y2}\underline{2}'_z$ we obtain $n_v = 12 : 4 = 3$, for $T_{12} = \mathcal{L}\,\underline{2}'_z$ we get $n_v = 6$. Symmetrically equivalent walls can be generated by applying operations of $6\,2_x2_y$ on one wall. Thus, e.g., from $1/-\frac{\pi}{2}/2$ one gets symmetrically equivalent walls $1/\frac{\pi}{6}/2$ and $1/\frac{5}{6}\pi/2$ with the symmetry groups $\mathcal{L}\, 2_{x3}\underline{2}'_{y3}\underline{2}'_z$ and $\mathcal{L}\, 2_{x1}\underline{2}'_{y1}\underline{2}'_z$, resp.

All walls parallel to z are symmetric walls, i.e., the order parameter η is an odd function of the distance ξ from the central plane

of the wall. Symmetry of a wall does not, therefore, depend on the form of the function $\eta(\xi)$, unless the condition $\eta(-\xi) = -\eta(\xi)$ is violated. In particular, symmetry of a wall does not depend on the thickness of the wall.

Symmetry T_{12} of the wall is useful in locating the extrema of wall energy /11/. The angles $\Theta = (2k + 1)\frac{\pi}{6}$, $k = 0, \pm1, \pm2, \ldots$, represent symmetrically prominent orientations with $T_{12} = \{2_{x_i}, 2'_{y_i}, 2'_z\}$, $i = 1, 2, 3$, whereas for any other orientation, $T_{12} = \{2'_z\}$. Symmetrically prominent orientations present a sufficient condition for local extrema of wall energy. Taking into account experimental fact that the equilibrium orientation of Θ changes smoothly with temperature (and cannot therefore correspond to any symmetrically prominent orientations which are fixed), one can draw the quantitative form of the angular dependence of the wall energy $E(\Theta)$ (fig. 2). Orientations corresponding to minimal wall energy are rotated away from $\Theta = 2k\pi/3$ by an angle $\pm\varepsilon$. Orientation parallel to z, which we have been considering, is also a symmetrically prominent one, since any tilt of the wall decreases the wall symmetry to $\{1\}$.

From the monoclinic symmetry $\{2'_z\}$ of an equilibrium wall, it directly follows that the wall carries spontaneous polarization P_z parallel to z; P_z has the same sign for three walls related by operations 3 and 3^2 and opposite sign for walls related by any 2-fold axis. The spontaneous deformation of the wall includes a volume dilatation and a shear. These spontaneous properties can also be deduced from a phenomenological theory /12/.

If n walls meet along a common line we call this line a *n-fold domain vertex*. For topological reasons, only 2-, 4-, and 6-fold vertices exist in quartz /8/. Their symmetry is described by rod groups, but we shall not discuss this point here.

IV . REGULAR LATTICE OF WALLS

1) Symmetry of a regular pattern of walls

As already mentioned in part II, an incommensurate phase close to the I-C transition can be approximated by a regular domain texture formed by domain walls of negative energy /13/. Symmetry of this domain texture is, within the continuum approach, described by a group $\mathcal{M}$ with translation subgroup $\mathcal{T}_m$. Domain texture of I phases modulated in one direction only (so called stripe phase) is formed by an array of parallel domain walls in which a certain basic sequence of walls is regularly repeated. The translation subgroup contains discrete

translations along the modulation wave vector and translations parallel to the walls. Domain texture of I phases modulated in two or more directions is formed by a regular network of walls and wall vertices. Translational group $\mathcal{T}_m$ is then discrete in two or three directions.

The knowledge of the symmetry group $\mathcal{M}$ allows one to find the macroscopic symmetry M of the I phase as the factor group of $\mathcal{T}_m$ in $\mathcal{M}$: $M \simeq \mathcal{M}/\mathcal{T}_m$. The group M determines :

(i) macroscopic properties of the I phase, especially its spontaneous properties which are forbidden by symmetry in N and C phases and allowed in the I phase;

(ii) symmetry dictated extrema of energy. Similarly as for domain walls, symmetrically prominent orientations can be helpful in locating orientations with minimal energy of I phase. We shall see, however, that a texture can have prominent orientations different from that of single walls which form the texture;

(iii) number n_b of symmetrically equivalent variants of I phase, $n_b = |G|:|M|$. These variants, related by operations of G not contained in M, have the same energy and can coexist as textural *blocks*. Interfaces between blocks are called *block boundaries*.

2) Example of the stripe phase in quartz

To construct a stripe phase, in which walls are parallel (and under the assumption that they have the same energy), one needs reversible walls. From the preceding results it follows that this phase should be built up from walls 1/0/2 and 1/$\bar{1}$/2 (=2/0/1) regularly

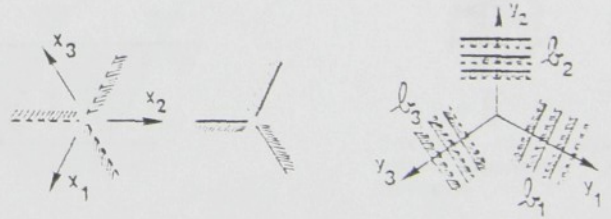

Fig.3 : Reversible domain walls with $-P_z$ and $+P_z$ polarizations, and symmetrically equivalent stripe phases.

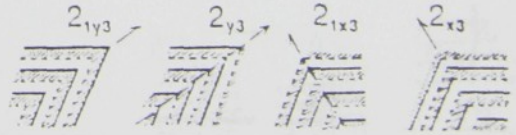

Fig.4 : Block boundaries between stripe phases with polar 2-fold symmetries.

disposed in the y_2 direction (fig. 3). Such a pattern has an orthorhombic symmetry $\mathcal{3} = 2_{x2}2'_{y2}2'_z$ with 2_{x2} axes in between two walls and $2'_z$ axes in the walls. There are $n_s = |G|:|\mathcal{3}| = 3$ symmetrically equivalent stripe phases which we call blocks. These blocks are built up from walls perpendicular to y_i (i= 1, 2, 3) and the corresponding macroscopic symmetries of blocks are $\mathcal{3}_i = 2_{xi}2_{yi}2_z$, resp. Each block can be identified with a ferroelastic domain since by symmetry one can predict that in block b_i $(U_{xi\,xi} - U_{yi\,yi}) \neq 0$, but the symmetry is non-polar, in agreement with the fact that consecutive walls carry opposite polarizations.

This macroscopic symmetry is important in considerations concerning block boundaries, which join two ferroelastic blocks. The orientation corresponding to minimal energy of the boundary is given by the condition of mechanical compatibility, as in usual ferroelastic materials. Let us consider, for instance, the pair of blocks b_1,b_2. Orientations of stress-free block boundaries are in this case perpendicular to x_3 and y_3. The symmetry of a boundary depends on the relative phase of modulations on opposite sides of the boundary. The highest symmetry cases are represented in figure 4 : since 2_{yi} axes exchange the stripe phases b_1 and b_2, whereas 2_{xi} axes do not, the symmetries of block boundaries are expressed by following layer groups $\ell\, 2_{1y3}$ (fig. 4a), $\ell\, 2_{y3}$ (fig. 4b), $\ell\, 2_{1x3}$ (fig. 4c), or $\ell\, 2_{x3}$ (fig.4d). These higher symmetry configurations have extremal energy. It is interesting to note that in fig. 4 the boundaries represented in (a) and (d) do not involve other walls than 1/0/2 and 2/0/1 whereas this is not the case for (b) and (c). In (b), the supplementary walls are perpendicular to x_3 and have maximal energy (fig. 2 & 4b). In (c), walls are perpendicular to y_3 and then (for $\varepsilon = 0$) their energy is minimal (and negative). From this one can expect that the real structure of block boundaries corresponds to cases (a) and (c). Block boundaries are always formed by a regular array of two-fold or four-fold vertices.

Another interesting feature concerns ferroelectricity: whereas the blocks are ferroelastic but not ferroelectric, a spontaneous polarization either parallel to y_3 (fig. 4a) or to x_3 (fig. 4c) is allowed by symmetry.

Parallel block boundaries are reversible: $b_1/\theta/b_2$ and $b_2/\theta/b_1$ are related by the 2_z operation and have, therefore, opposite spontaneous polarizations ($\theta = -\frac{\pi}{3}$ or $\frac{\pi}{6}$).

Evidence of stripe phase has been obtained by neutron diffraction in /14/ but observations in direct space are not available.

3) Analysis of the 3-q phase of quartz

The superposition of the three waves with equal amplitudes can lead to different patterns formed out of triangles or hexagons, depending on the relative phase of the modulations. Here, we shall consider the pattern of equilateral triangles since it corresponds to observations. To construct it, one has two possibilities, either from walls carrying a polarization P_z or from walls carrying $(-P_z)$. Let us now consider the symmetry of such a structure diperiodic in the plane (001). For any $\theta \neq \pm \frac{\pi}{2}$ (and symmetrically related orientations), the group leaving the figure invariant is $p6'_z$, whose symmetry axes are shown in fig.5. It can also be written as $p6'_z = p3 + 2'_z(p3)$, and one can note that this symmetry is polar (all walls carry the same polarization, and the macroscopic P_z is non zero). It is interesting to note that the modulated phase is ferroelectric, though neither x nor 2 phases is polar. For the special orientation $\theta = \pm \frac{\pi}{2}$, the structure has a higher symmetry since now 2_x and $2'_y$ leave the pattern invariant. For this special orientation, the polarization P_z therefore vanishes, and one has an extremum of energy, which is a maximum. However, as the structures with $\theta = +\frac{\pi}{2}$ and $\theta = -\frac{\pi}{2}$ cannot be related by any symmetry operation of $6'_z2_x2'_y$, there is no symmetry requirement that both maxima of energy coincide. From this one can conclude that the angular dependence of energy is similar to that of a single wall (fig. 2). In particular, the positions of minima are not determined by symmetry. It follows, that both blocks with $\pm P_z$, which are related, e.g., by $2'_y$, are rotated in opposite directions (fig. 6).

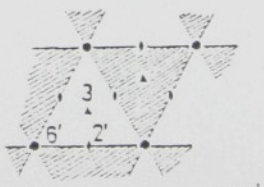

$P6'$

Fig.5 : Symmetry $p6'$ of the 3-q phase.

Fig.6 : 3-q phase: blocks with opposite polarization along z.

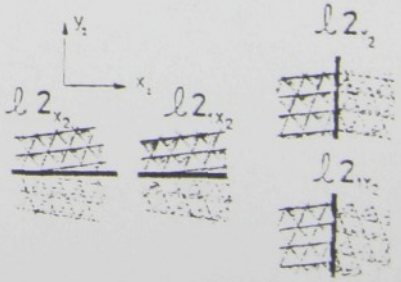

Fig.7 : 3-q phase : block boundaries with prominent orientations.

Since the blocks can be identified with ferroelectric non-ferroelastic domains, there is no strong requirement concerning block boundary orientation. However, special orientations normal to x and to y can have higher symmetries, depending on the difference of phase of modulations on opposite sides of the boundary (fig. 7). In all cases, a polarization normal to [001], lying within the boundary, is allowed. Within the boundary, the polarization rotates in an analogous manner as does magnetization in ferromagnetic Bloch walls.

V . CONCLUSION

On the example of quartz, we have shown that some important conclusions about properties of non-linear objects, like domain walls and incommensurate phases, can be obtained from symmetry analysis without solving non-linear equations. Though this approach has limitations (it cannot yield quantitative values, temperature dependences, etc), conclusions are rigorous, reflect specific features of complicated systems and disclose tiny effects not considered in simplified models. In crystal physics, symmetry analysis represents a useful first step in examining properties of real non-linear systems.

REFERENCES :

/1/ V.Dvořák, in *Modern Trends in the Theory of Condensed Matter*, Ed. A. Pekalski and J. Przystawa (Springer, Berlin),p447 (1980).
/2/ A.P. Levanyuk, in *Incommensurate Phases in Dielectrics*, Ed. R. Blinc and A.P. Levanyuk (North Holland, Amsterdam), Vol. 1, p1 (1986).
/3/ Y. Ishibashi, H. Shiba, J. Phys. Soc. Jpn 45, 409 (1978).
/4/ H. Grimm, B. Dorner, J. Phys. Chem. Solids 36, 407 (1975).
/5/ K. Gouhara, Y. Hao Li, N. Kato, J. Phys. Soc. Jpn 52, 3697 (1983) G. Dolino, J.P. Bachheimer, and C.M.E. Zeyen, Solid State Commun.45, 295 (1983).
/6/ G. Dolino, in *Incommensurate Phases in Dielectrics*, Ed. R. Blinc and A.P. Levanyuk (North Holland, Amsterdam), Vol. 2, p205 (1986).
/7/ T.A. Aslanyan, A.P. Levanyuk, M. Vallade, and J. Lajzerowicz, J. Phys. C 16, 6705 (1983).
/8/ J. Van Landuyt, G. Van Tendeloo, S. Amelinckx, M.B. Walker, Phys. Rev. B 31, 2986 (1985).
/9/ C. Roucau, E. Snoeck, P. Saint-Grégoire, J. Physique 47, 2041 (1986).
/10/ V. Janovec, Ferroelectrics 35, 105 (1981).
/11/ G. Kalonji, J. Physique, Colloque C4, sup.n°4, 46, 249 (1985).
/12/ M.B. Walker and R.J. Gooding, Phys. Rev. B 32, 7408 (1985).
/13/ V. Janovec and V. Dvorak, Ferroelectrics 66, 169 (1986).
/14/ P. Bastie, F. Mogeon, C.M.E. Zeyen, Phys. Rev. B 38, 786 (1988).

Anales de Física. Monografías

1

M. A. del Olmo, M. Santander and J. Mateos Guilarte
(Eds.)

Group Theoretical Methods in Physics

Proceedings of the XIX International Colloquium
Salamanca, Spain, June 29 – July 4, 1992.

Volume II.

Super Physics, Super Mathematics
Geometry, Topology and Quantum Field Theory
Atomic, Molecular and Condensed Matter Physics
Nuclear and Particle Physics
Symmetry and Foundations of Classical and Quantum Mechanics

CIEMAT Real Sociedad Española de Física

Space Group Coset Decompositions: Software and Applications to Phase Transitions

B. L. DAVIES
School of Mathematics, U.C.N.W., Bangor, U.K.

R. DIRL, P. ZEINER
Institut fur Theoretische Physik, T.U., Wien, Austria

V. JANOVEC
Institute of Physics, Czechoslovak Academy of Sciences, Prague, CSFR

Introduction

In order to assist the study of structural phase transitions in crystals, the need arose for a computer program to run on IBM-compatible PCs to compute left coset and double coset decompositions of a space group $\mathcal{G}_0$ of the high symmetry phase with respect to the sub-space group $\mathcal{G}$ of the low symmetry phase. The homogeneous high symmetry phase splits at a phase transition into a heterogeneous aggregate consisting of homogeneous regions of lower symmetry called domains. Crystallographic relations between domains and domain pairs are deduced form these left coset and double coset decompositions respectively.

Coset Decompositions of Space Groups

Let $\mathcal{G}_0$ be a super-space and $\mathcal{G}$ a sub space group of finite index. Every set $\mathcal{G} * \{g\} * \mathcal{G}$ defines a double coset of $\mathcal{G}_0$ with respect to $\mathcal{G}$. The task consists of computing minimal subsets of left coset representatives (LCRs) of $\mathcal{G}_0$ with respect to $\mathcal{G}$ such that for every pair $g_1, g_2 \in \mathcal{PG}_0(\mathcal{G})$ their intersections $\mathcal{G} * \{g_1\} * \mathcal{G} \cap \mathcal{G} * \{g_2\} * \mathcal{G} = \emptyset$ are mutually disjoint and that their total union presents $\mathcal{G}_0$. The double cosets are either self-inverse (ambivalent) or non-self inverse (complementary) according to:

$$\text{Ambivalent Double Cosets:} \quad \mathcal{G} * \{g\} * \mathcal{G} = \mathcal{G} * \{g^{-1}\} * \mathcal{G} \tag{1}$$

$$\text{Complementary Double Cosets:} \quad \mathcal{G} * \{g\} * \mathcal{G} \cap \mathcal{G} * \{g^{-1}\} * \mathcal{G} = \emptyset \tag{2}$$

The first approach is to apply the Frobenius Theorem [1], [2] which has been implemented in the software package or to tailor an alternative approach which exploits the specific structure of space groups [3]. Frobenius Theorem reads:

$$\begin{aligned} \mathcal{G} * \{g\} * \mathcal{G} &= \textstyle\sum_{n_i} \{a_i g\} * \mathcal{G} \\ \mathcal{G} &= \textstyle\sum_{n_i} \{a_i\} * \mathcal{G}(g) \\ \mathcal{G}(g) &= \mathcal{G} \cap \{g\} * \mathcal{G} * \{g^{-1}\} \end{aligned} \tag{3}$$

Space Group Cosets Program: PCDC.PAS

A Pascal program for IBM compatible PCs has been developed to compute coset decompositions of space groups. The input and output are summarized here. The program is used below in an actual application to structural phase transitions. The notation and conventions adopted are given in [1].

Input: (1) Space group $\mathcal{G}_0$, (2) Setting data (new origin/re orientation), (3) Matri $\mathcal{M}(Z)$ which maps the lattice $\mathcal{T}(\mathcal{G}_0)$ of $\mathcal{G}_0$ onto the sublattice $\mathcal{T}(\mathcal{G})$ of $\mathcal{G}$, (4) Isogonal poin group $\mathcal{P}(\mathcal{G})$ of $\mathcal{G}$, (5) Non-primitive translations assigned to all elements of $\mathcal{P}(\mathcal{G})$.

Output: (1) Specification of elements of $\mathcal{G}_0$ and $\mathcal{G}$, (2) Left cosets of $\mathcal{T}(\mathcal{G}_0)$ with respec to $\mathcal{T}(\mathcal{G})$, (3) Left cosets of $\mathcal{P}(\mathcal{G}_0)$ with respect to $\mathcal{P}(\mathcal{G})$, (4) Double cosets of $\mathcal{P}(\mathcal{G}_0)$ wit respect to $\mathcal{P}(\mathcal{G})$, (5) Double cosets of $\mathcal{G}_0$ with respect to $\mathcal{G}$, (6) Self inverse and non-sel inverse classification of double cosets in (5).

Applications to Structural Phase Transitions

In a structural phase transition accompanied by a symmetry reduction the space group $\mathcal{G}$ the ordered (distorted) phase is a proper subgroup of the space group $\mathcal{G}_0$ of the disordere (parent) phase. Due to this symmetry reduction the ordered phase is degenerate: it ca appear in several crystallographically equivalent (with respect to $\mathcal{G}_0$) homogeneous ordere structures that differ only in orientation and/or position (with respect to the coordinat system of the disordered phase). These crystallographically equivalent ordered structur are called single domain states (SDSs) and will be denoted $\mathbf{S}_1, \mathbf{S}_2, \ldots \mathbf{S}_n$. For any two SD $\mathbf{S}_i, \mathbf{S}_j$ there exists an operation $g \in \mathcal{G}_0$, such that

$$\mathbf{S}_j = g \circ \mathbf{S}_i \qquad (4$$

The set of all SDSs forms a $\mathcal{G}_0$-orbit. The stabilizer of $\mathbf{S}_i$ in $\mathcal{G}_0$ is the maximal subgrou of $\mathcal{G}_0$ that leaves $\mathbf{S}_i$ invariant. It equals the space group $\mathcal{G}_i$ of the ordered phase in the SI $\mathbf{S}_i$. There is a one-to-one correspondence between the SDSs of the orbit of $\mathbf{S}_1$ and the le cosets of $\mathcal{G}_0$ with respect to $\mathcal{G}_1$. Consequently the number of SDSs equals the index of $\mathcal{G}$ in $\mathcal{G}_0$ respectively.

Structures of SDSs can co-exist in a domain structure that consists of domains (connect regions with homogeneous structures of SDSs) and domain walls (boundaries between neig bouring domains). To study possible relations between structures of two domains the conce of a domain pair has been introduced [5]. An ordered domain pair (ODP) consists of t first SDS $\mathbf{S}_i$ and a second SDS $\mathbf{S}_j$ both from the same orbit; such an ODP will be denot $(\mathbf{S}_i, \mathbf{S}_j)$. An ODP with reversed order of SDSs is called a transposed ODP. An ODP $(\mathbf{S}_i, \mathbf{S}$ is not equal to the transposed ODP $(\mathbf{S}_j, \mathbf{S}_i)$ unless $i = j$ (trivial ODP). The stabilizer $\mathcal{G}_{($ of an ODP $(\mathbf{S}_i, \mathbf{S}_j)$ is equal to the intersection of the stabilizers of $\mathbf{S}_i$ and $\mathbf{S}_j$. Two OD $(\mathbf{S}_i, \mathbf{S}_j)$ and $(\mathbf{S}_k, \mathbf{S}_l)$ are crystallographically equivalent with respect to $\mathcal{G}_0$ if an operati $g \in \mathcal{G}_0$ exists such that

$$\begin{aligned} (\mathbf{S}_k, \mathbf{S}_l) &= (g \circ \mathbf{S}_i, g \circ \mathbf{S}_j) \\ \mathcal{G}_{(k,l)} &= g * \mathcal{G}_{(i,j)} * g^{-1} \end{aligned}$$

ODPs can be classified in the following manner. An ODP $(\mathbf{S}_i, \mathbf{S}_j)$ is ambivalent if it is $\mathcal{G}_0$ with the transposed ODP $(\mathbf{S}_j, \mathbf{S}_i)$. If this condition cannot be fulfilled then the O is polar, in which case the ODP and the transposed ODP are called complementary p ODPs. The crystallographical equivalence defined by (6) divides the set of all conceiva ODPs that can be formed from $\mathcal{G}_0 \circ \mathbf{S}_1$ into orbits (classes of symmetrically equivalent OD $\mathcal{G}_0 \circ (\mathbf{S}_i, \mathbf{S}_j)$. From (4) it follows that a representative ODP of $\mathcal{G}_0 \circ (\mathbf{S}_i, \mathbf{S}_j)$ can always chosen in such a way that its first SDS is $\mathbf{S}_1$, i.e. the representative has the form $(\mathbf{S}_1, \mathbf{S}$ The attributes "ambivalent" and "complementary polar" are class properties, i.e. O

in an orbit are either all ambivalent or all polar and all transposed ODPs of a polar orbit constitute another disjoint polar orbit, a complementary polar orbit.

The relation between double cosets $\mathcal{G}_1 * \{g_j\} * \mathcal{G}_1$ and all possible orbits of ODPs formed from the orbit $\mathcal{G}_0 \diamond S_1$ is expressed by the following theorem: There is a one-to-one correspondence between ambivalent and complementary polar double cosets of $\mathcal{G}_0$ with respect to $\mathcal{G}_1$ and ambivalent and complementary polar orbits of ODPs. The representative ODPs of these orbits can be found in the form $(S_1, g_j \diamond S_1)$, where $g_j \in \mathcal{G}_0$ are properly chosen double coset representatives of $\mathcal{G}_0$ with respect to $\mathcal{G}_1$.

ODPs from different orbits differ in at least some inherent properties, whereas ODPs from the same orbit have "essentially equal" properties. The double coset decomposition thus reduces the task of examining $n(n-1)$ ODPs to a considerably lower (especially for large n) number q of double coset representatives. Properties significant for the whole orbit of ODPs can be found by examining the representative ODPs of the orbits. The main advantage of the coset analysis described above is that the only input data are just two space groups $\mathcal{G}_0$ and $\mathcal{G}_1$. No further information, e.g. crystal structures of both phases, is needed.

Example

To illustrate the importance of coset decompositions in the symmetry analysis of domain structures, let us consider the triply commensurate charge-density-wave domain states in 2H polytype $TaSe_2$. The disordered phase has $\mathcal{G}_0 = P6_3/mmc$ (#194) symmetry and the ordered commensurate phase exhibits $\mathcal{G}_1 = Cmcm$ (#63) symmetry with tripled periodicity along two hexagonal primitive lattice vectors. There are $d = |6/mmm : mmm| = 24 : 8 = 3$ orientational SDSs and within each of them $d = 9$ SDSs related by lost translations may exist. Thus, in all, there are $n = 3 \times 9 = 27$ SDSs.

The output from the program PCDC provides the left coset and double coset decompositions of $6/mmm$ with respect to mmm which are omitted owing to lack of space. The left coset representatives of the translation group $\mathcal{T}(\mathcal{G}_0)$ with respect to the translation subgroup $\mathcal{T}(\mathcal{G}_1)$ (coordinates relative to the primitive lattice vectors of $\mathcal{G}_0$) and the double coset representatives $\mathcal{G}_0$ with respect to $\mathcal{G}_1$ (including left coset partition) are:

Table I:

NUMBER	LCR
1	(0,0,0)
2	(0,1,0)
3	(0,2,0)
4	(1,0,0)
5	(1,1,0)
6	(1,2,0)
7	(2,0,0)
8	(2,1,0)
9	(2,2,0)

Table II:

NUMBER	DCR	LCRs
1	(1,1)	(1,1)
2	(1,2)	(1,2) (1,3)
3	(1,4)	(1,4) (1,5) (1,7) (1,9)
4	(1,6)	(1,6) (1,8)
5	(2,1)	(2,1) (3,1)
6	(2,2)	(2,2) (2,3) (3,2) (3,3)
7	(2,4)	(2,4) (2,7) (3,5) (3,9)
8	(2,5)	(2,5) (2,9) (3,1) (3,7)
9	(2,6)	(2,6) (2,8) (3,6) (3,8)

N.B. The DCR and LCR symbols in the second table are to be interpreted as in this example: (2,1) means the product of the Seitz space group symbols (2|v(2)) * (E|1), where v(2) denotes the non primitive translation associated with the rotation 2, and 1 denotes

the translation LCR number 1 [= (0,0,0)] in Table I above. The point group symmetry operations are labelled numerically in the notation of Ref.[1].

The last table outputted by the program gives the types of double cosets. This table shows that all the double cosets are self- inverse except for those numbered 6 and 8 in Table II which form a pair of non-self-inverse double cosets. Thus all double cosets except two are ambivalent; double cosets 6 and 8 are complementary polar double cosets. Thus the set of $27 \times 26 = 702$ non-trivial ODP's is partitioned into 8 orbits and the representatives of these orbits are samples of all significantly different relations between two SDSs. The value of the PC software is obvious !

Complementary double cosets are worthy of further attention since they indicate the possible appearance of incommensurate phases in between parent and ordered phases. More detailed analysis has shown that one of these polar double cosets can generate 54 symmetry equivalent coherent domain walls with negative formation energy; from these 9 different symmetry equivalent incommensurate stripe phases can be formed. These stripe phases have equal energy and can, therefore, co exist like domains. Rather complicated incommensurate structures consisting of such stripe phases were really observed by electron microscopy [6].

References

[1] F.G. Frobenius: J. reine u. angewandte Mathematik **101**, 273 (1895)

[2] C.J. Bradley, A.P. Cracknell
The Mathematical Theory of Symmetry in Solids
(Clarendon, Oxford, 1972)

[3] R. Dirl, P. Zeiner, B.L. Davies, V. Janovec
Coset Decompositions of Space Groups – Applications to Structural Phase Transitions
(in preparation)

[4] A.P. Cracknell, B.L. Davies, S.C. Miller, W.F. Love
Kronecker Product Tables, Volume 1
(Plenum, New York, 1979)

[5] V. Janovec: Czech. J. Phys. **B 22**, 974 (1972)
V. Janovec: Ferroelectrics, **12**, 43 (1976)
V. Dvorak, V. Janovec: J.Phys. **C 18**, 269 (1985)
V. Janovec, E. Dvorkov, T.R. Wike, D.B. Litvin: Acta Cryst. **A 45**, 801 (1989)
V. Janovec, L. Richterov, D.B. Litvin: Ferroelectrics, **126**, 287 (1992)

[6] C.H. Chen, J.M. Gibson, R.M. Fleming: Phys.Rev. **B 26**, 184 (1982)

Ferroelectrics, 1993, Vol. 140, pp. 89–94
Reprints available directly from the publisher
Photocopying permitted by license only

MICROSCOPIC STRUCTURE OF DOMAIN WALLS AND ANTIPHASE BOUNDARIES IN CALOMEL CRYSTALS

V. JANOVEC and Z. ZIKMUND

Institute of Physics, Czechoslovak Academy of Sciences,
Na Slovance 2, 180 40 Prague 8, Czechoslovakia

We present examples of microscopic structures of finite thickness ferroelastic domain walls and antiphase boundaries in Hg_2Cl_2 crystals obtained by symmetry analysis. They illustrate positional dependencies of the structure of domain walls, topologically different structures of antiphase boundaries and the role of gradient effects.

INTRODUCTION

Crystals of calomel Hg_2Cl_2 have attracted attention not only for exceptionally high optical and elastic anisotropy with practical implications but also for a structural phase transition from a tetragonal to an orthorhombic phase. Its very simple molecular structure makes calomel an appealing model material for investigating the microscopic mechanism of the transition and the microscopic structures of domain walls and antiphase boundaries.

A ferroelastic domain structure has been observed optically in the orthorhombic phase.[1] Basic symmetry properties of this domain structure have been determined in Ref. 2 and the first results concerning the structure of domain walls have been reported in Ref. 3. Here we present examples of microscopic structures of domain walls and antiphase boundaries deduced from symmetry analysis.[4–6]

SINGLE DOMAIN STATES

Calomel crystals are built up of linear molecules $Cl - Hg - Hg - Cl$ that form at room temperature a body-centered tetragonal lattice with space group symmetry $I4/mmm - D_{4h}^{17}$ and molecules aligned parallel to the **c** axis. At 185K calomel undergoes an improper ferroelastic phase transition to an orthorhombic phase with the space group symmetry $Bbmm(Cmcm) - D_{2h}^{17}$ and doubling of the primitive unit

cell volume.[7] A direct consequence of this symmetry reduction is a degeneracy of the orthorhombic phase which can be formed in four single domain states. These are the same orthorhombic structures that differ only in orientation and/or position and are related by symmetry operations lost at the transition. We label these single domain states 1_1, 1_2, 2_1, 2_2. The first number in the symbol signifies one of two possible orientations corresponding to two ferroelastic single domain states with spontaneous deformation $+e_{xy}$ and $-e_{xy}$, resp., whereas the lower index distinguishes two single domain states that have the same orientation but different location.

The structure of Hg_2Cl_2 projected onto the $z = 0$ plane is depicted in Figure 1. The full and open circles correspond to the centres of gravity of Hg_2Cl_2 molecules at levels $z = 0$, $\frac{1}{2}\mathbf{c}$, resp. The conventional unit cell of the tetragonal phase (basic vectors **a, b, c**) is represented by a solid square in the centre of the Figure. Unit cells of the orthorhombic phase (basic vectors $\mathbf{a} - \mathbf{b}, \mathbf{a} + \mathbf{b}, \mathbf{c}$, see upper left corner of the Fig. 1) are depicted as dotted squares (spontaneous deformation is neglected). The arrows represent spontaneous shifts of the centres of gravity of the molecules. These shifts are frozen-in displacements of a transverse acoustic soft mode with the **k** vector at the X point of the Brillouin zone boundary.[8] In the domain state 1_1 all molecules in the (110) plane passing through the origin O

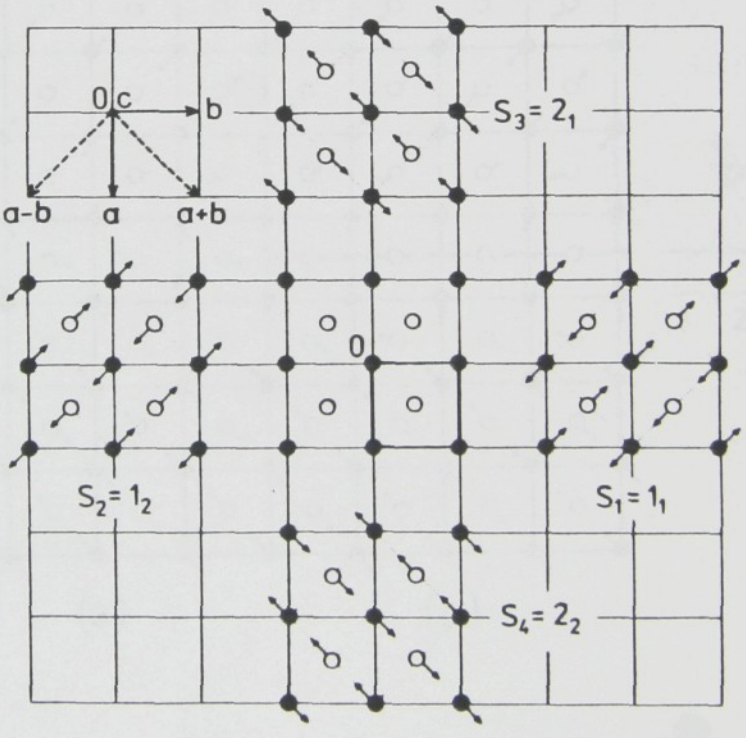

FIGURE 1 Parent tetragonal phase and single domain states 1_1, 1_2, 2_1, 2_2 of the orthorhombic improper ferroelastic phase.

are shifted along the $[1\bar{1}0]$ direction and in the neighbouring parallel planes along antiparallel direction $[\bar{1}10]$ (indices specifying the orientation of planes and directions are related to the tetragonal coordinate system). The shifts in the domain state 2_1 can be obtained by applying on 1_1 the mirror plane (010) passing through the origin O or performing the rotation 4_z about **c**. The structure of 1_2 (or 2_2) is identical with that of 1_1 (or 2_1) shifted by the lost translation **a** or **b**.

Within Landau theory the phase transition can be described by an order parameter (OP) with two components p and q.[7] The domain states are represented in the OP space by points $1_1(a_o, a_o)$, $1_2(-a_o, -a_o)$, $2_1(-a_o, a_o)$, $2_2(a_o, -a_o)$.

FERROELASTIC DOMAIN WALLS

A ferrelastic domain wall joining domain states 1_1 and 2_1 is coherent only for orientations (100) and (010). This wall is represented in the order parameter space by an oriented path connecting the point 1_1 with the point 2_1.

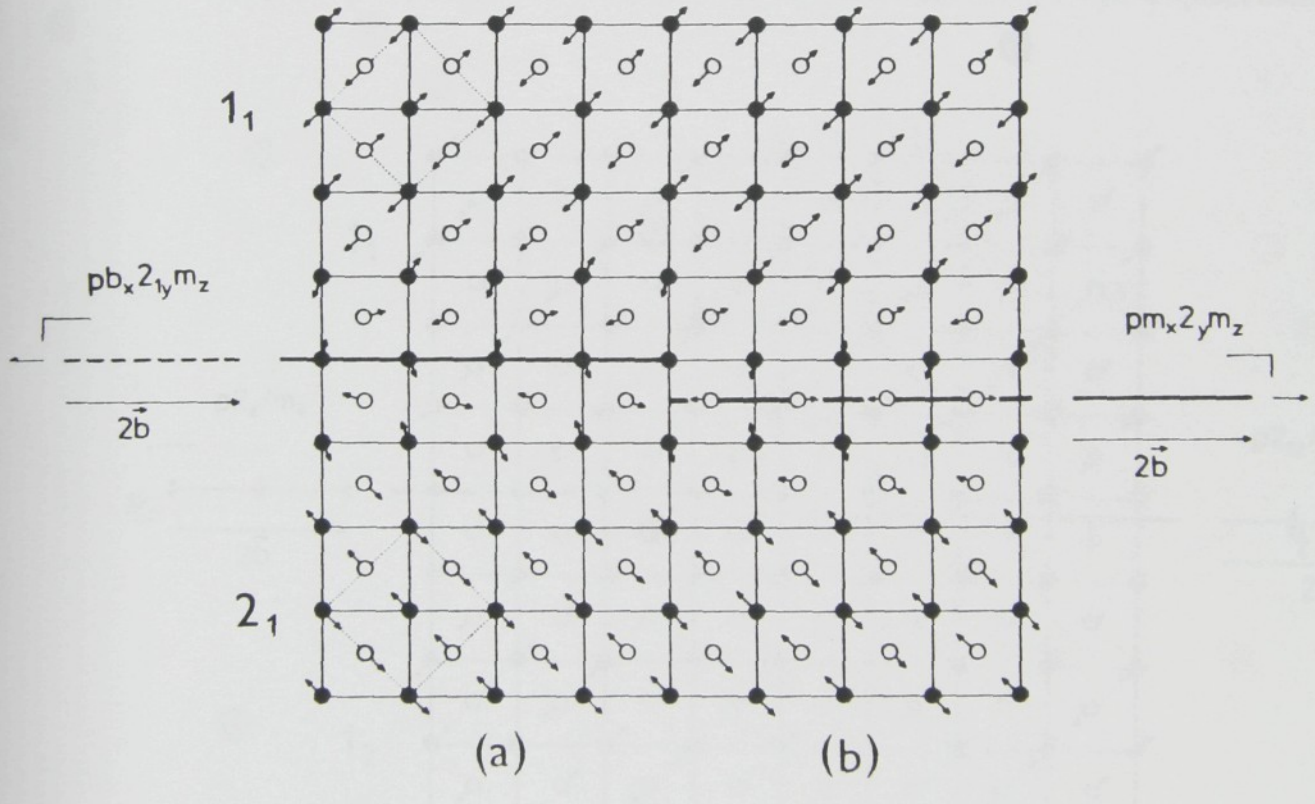

FIGURE 2 Microscopic structure of a coherent ferroelastic domain wall in two symmetrically prominent positions.

The microscopic structure of a coherent ferroelastic domain wall in two symmetrically prominent positions is depicted in Fig. 2. The shifts of the molecules inside the wall have been deduced from the site symmetries of diperiodic layer groups describing the symmetry of the the wall.[4–6] The diagrams of these layer groups, determined in Ref. 2, are given on the left and right sides of the Figure (the letter p signifies a two-dimensional net with basic vectors $2\mathbf{b}$, $\mathbf{c}$).

It follows from the Figure that when one passes through the wall in the $[1\bar{1}0]$ direction the molecular shifts are experiencing rotations through $\frac{\pi}{2}$ about the $\mathbf{c}$ direction in opposite senses for "black" and "white" molecules. The molecules in the central layer of the wall on Fig. 2(a) exhibit nearly antiparallel displacements perpendicular to the wall. Strictly perpendicular shifts would represent "averaged" displacements of domain states 1_1 and 2_1 and would correspond to the central point $(0, a)$ on the wall path which has the symmetry (isotropy group) $P4_2/mnm$. The deviations (tilts) from this structure exemplify an additional degree of freedom allowed by the wall symmetry and represent gradient effects in the wall.

A wall with a central plane shifted in the [100] direction about $\frac{1}{2}\mathbf{a}$ is depicted in Fig. 2(b). In this wall the molecules at the central plane shift alternatively in [010] and $[0\bar{1}0]$ directions. The symmetry (mirror plane m) keeps displacements in

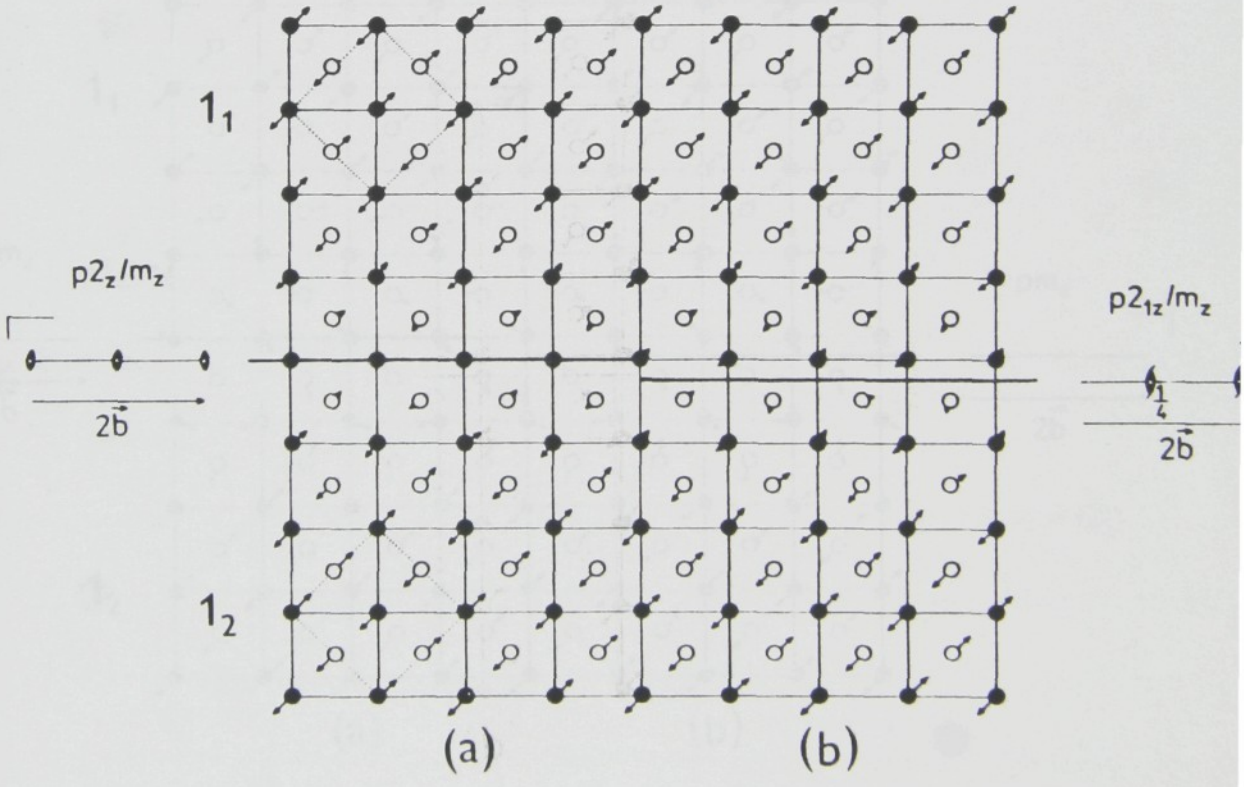

FIGURE 3 Microscopic structure of a linear antiphase boundary in two symmetrically prominent positions.

the central plane strictly antiparallel. In an "averaged" central structure have these displacements equal lenght. The gradient effects manifest themselves as shifts of unequal length in neighbouring molecules.

In both positions the wall symmetries are polar and allow the appearance of a non-zero spontaneous polarization parallel or antiparallel to **b**. Structures (a) and (b) have extreme energy but symmetry considerations cannot decide which of them has minimum energy.

ANTIPHASE BOUNDARIES

The transition region between domain states 1_1 and 1_2 (or between 2_1 and 2_2) is called an *antiphase boundary (APB)* or a *translational domain wall.* The parallel shifts in the (110) planes have to change sign when passing through the *APB* (see Fig. 3 and 4). This can be accomplished in two topologically different ways:

(i) In a *linear APB* the molecular shifts diminish to zero at the central plane without essentially changing directions (Fig. 3). The corresponding path in the

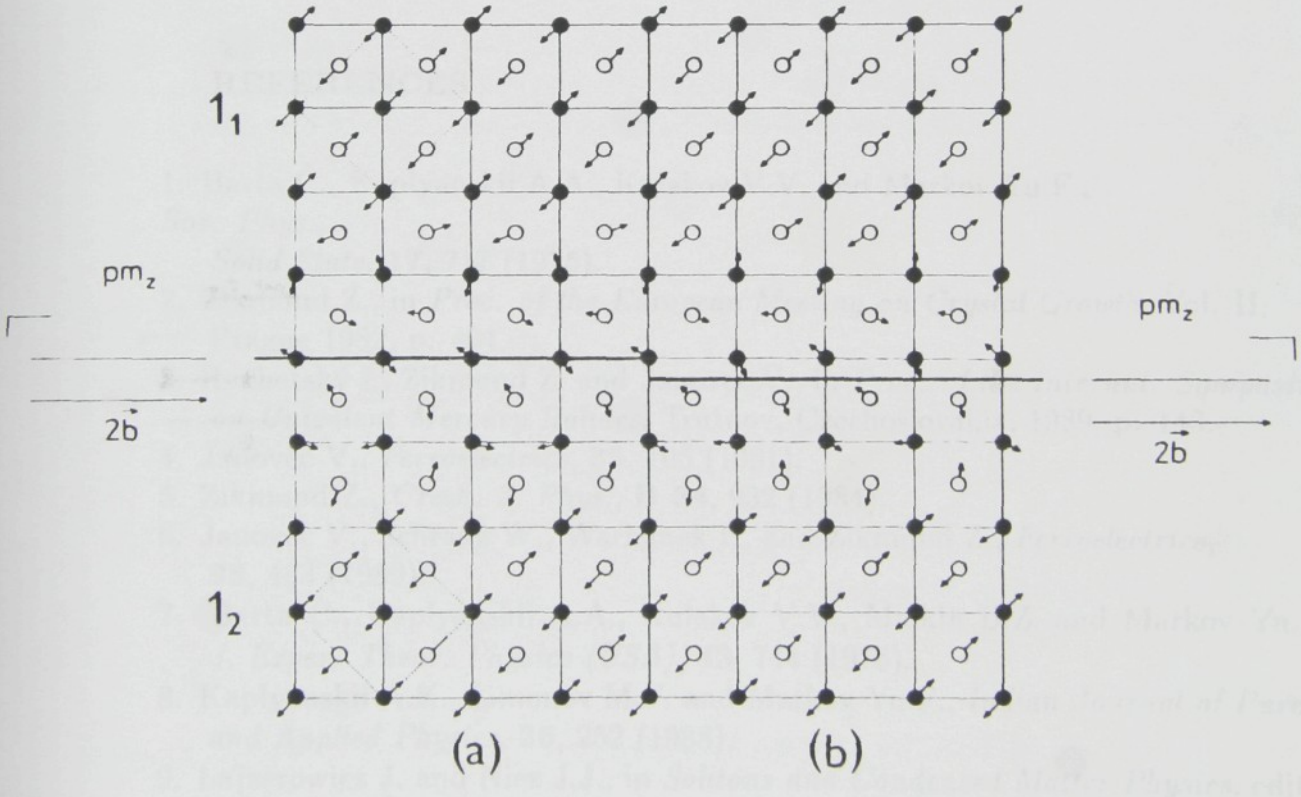

FIGURE 4 Microscopic structure of a rotational antiphase boundary with no symmetrically prominent position.

OP space is a line $p(x) = q(x)$ (where x is the distance from the central plane) passing through the origin $p(x = 0) = q(x = 0) = 0$ with tetragonal symmetry of the parent phase. The structure of the central layer in Fig. 3(a) and a double layer in Fig. 3(b) is identical with that of a tetragonal parent phase (up to small additional tilts in the latter case connected with gradient effects).

(ii) In a *rotational APB* the direction of shifts rotates through π about the **c** direction (Fig. 4). The APB path in the OP space is an arc with a centre at the point $(-a, a)$ or $(a, -a)$. Molecules at the central layer are displaced alternatively along the [110] and $[\bar{1}\bar{1}0]$ directions and the structure of the central layer corresponds to that of the domain state 2_1 or 2_2, resp. These two topologically distinct variants of an APB differ in the sense of rotation of both black and white molecules. The APB in Fig. 4 has the central structure corresponding to the domain state 2_1 (cf., Fig. 2 and Fig. 4).

The symmetry of the rotational APB does not change with its position contrary to that of the linear APB which is positionally dependent.

We notice that the rotational APB structure in Fig. 4 has lower symmetry than that of the linear APB structure in Fig. 3. The change from the linear to the rotational structure is accomplished by the appearance and growth of a plate-like nucleus of domain 2_1 in the center of the APB. This change can be performed as a Landau type of a phase transition in the APB.[4,9–12]

REFERENCES

1. Barta Č., Kaplyanskii A.A., Kulakov V.V. and Markov Yu.F., *Sov. Phys., Solid State*, **17**, 717 (1975).
2. Zikmund Z., in *Proc. of the European Meeting on Crystal Growth*, Vol. II, Prague 1982, p. 404.
3. Rychetský I., Zikmund Z. and Janovec V., in *Proc. of the Internat. Symposium on Univalent Mercury Halides*, Trutnov, Czechoslovakia, 1989, p. 143.
4. Janovec V., *Ferroelectrics*, **35**, 105 (1981).
5. Zikmund Z., *Czech. J. Phys.*, **B 34**, 932 (1984).
6. Janovec V., Schranz W., Warhanek H. and Zikmund Z., *Ferroelectrics*, **98**, 483 (1989).
7. Barta Č., Kaplyanskii A.A., Kulakov V.V., Malkin B.Z. and Markov Yu.F., *J. Exper. Theor. Physics (USA)*, **43**, 744 (1976).
8. Kaplyanskii A.K., Limonov M.F. and Markov Yu.F., *Indian Journal of Pure and Applied Physics*, **26**, 252 (1988).
9. Lajzerowicz J. and Niez J.J., in *Solitons and Condensed Matter Physics*, edited by Bishop A.R. and Schneider T. (Springer, Berlin, 1978), p. 195.
10. Bulbich A.A. and Gufan Yu.M., *Ferroelectrics*, **98**, 277 (1989).
11. Sonin E.B. and Tagancev A.K., *Ferroelectrics*, **98**, 291 (1989).
12. Rychetský I., *J. Phys.: Condens. Matter*, **3**, 7117 (1991).

Ferroelectrics, 1993, Vol. 140, pp. 95–100
Reprints available directly from the publisher
Photocopying permitted by license only

NON-FERROELASTIC TWIN LAWS AND DISTINCTION OF DOMAINS IN NON-FERROELASTIC PHASES

V. JANOVEC(1), L. RICHTEROVÁ(2) and D. B. LITVIN(3)

(1)Institute of Physics, Czechoslovak Academy of Sciences, Na Slovance 2, 180 40 Prague 8, CSFR

(2) Comenius University, Faculty of Mathematics and Physics, Mlynská dolina F1, 842 15 Bratislava, CSFR

(3) Department of Physics, The Pennsylvania State University, The Berks Campus, P.O.Box 7009, Reading, PA 19610-6009, U.S.A.

We show that within continuum description there exist 48 possible relations (twin laws) between structures of two non-ferroelastic domains. All these twin laws can be expressed by dichromatic point groups. For each twin law we give the number of components of important material property tensors that have opposite sign in the two domains under consideration.

INTRODUCTION

Domains in non-ferroelastic phases cannot be simply observed in a polarizing microscope. There exist, however, other properties (expressible by appropriate material property tensors) that allow to distinguish such domains. Distinction of ferroelectric non-ferroelastic domains has been discussed recently in Ref. 1. Here we shall present an extension of this work to all non-ferroelastic domain structures that can appear in non-ferroelastic phases. Since we shall be interested in tensor distinction of domains we shall use continuum description and point groups only.

DOMAIN STATES IN NON-FERROELASTIC PHASES

We consider a ferroic transition from a prototype (parent) phase with symmetry G to a ferroic (distorted) phase with symmetry F, where $F < G$. The ferroic phase is degenerate: it can appear in n_o homogeneous single domain orientational states

$S_1, S_2, ..., S_n$ which have the same structure and differ only in spatial orientation.[2] We call these states *single domain states (SDS's)*. The number n_o of SDS's equals

$$n_o = |G| : |F|, \tag{1}$$

where $|G|$ and $|F|$ denotes the number of symmetry operations in G and F, resp. Symmetry groups of SDS's $S_1, S_2, ..., S_n$ are $F_1, F_2, ..., F_n$, resp. Further, we introduce a more general concept of *domain states (DS's)* which denote bulk structures (or their orientations) of domains in polydomain samples. Several disconnected domains can possess the same DS. DS's of a polydomain sample thus represent structures that appear in the sample, irrespectively in which domain.

According to Aizu[2] a ferroic phase is *non-ferroelastic* if all of the SDS's have the same (zero) spontaneous deformation. A simple criterion can be formulated in terms of crystal families[§] : A ferroic phase is non-ferroelastic if and only if

$$F < G, \quad \mathrm{Fam}(F) = \mathrm{Fam}(G); \tag{2}$$

if $\mathrm{Fam}(F) < \mathrm{Fam}(G)$ the ferroic phase is full or partial ferroelastic one.[2]

Domain states of non-ferroelastic phases have the following specific properties:

(i) DS's have a common lattice and their orientation is not affected by the coexistence, number and shape of domains in a domain structure. (DS's in ferroelastic phases depend on these factors). DS's coincide with SDS's (in contrast to polydomain ferroelastic phases where SD's differ from SDS's due to disorientations[4]) and the number of possible DS's equals the number of SDS's n_o given by Eq. (1).

(ii) All DS's have the same symmetry group, $F_1 = F_2 = ... = F_n = F$. (This groups may be different for ferroelastic SDS's and DS's.)

NON-FERROELASTIC DOMAIN PAIRS AND THEIR TWIN LAWS

Macroscopic properties that are different in two chosen domains are determined by the relation between their DS's. Two DS's S_i and S_k form a *domain pair* (DP)[5] $\{S_i, S_k\} = \{S_k, S_i\}$. An DP $\{S_i, S_k\}$ is *ambivalent* if there exists $g'_{ik} \in G$ such that

$$g'_{ik} S_i = S_k \quad \text{and} \quad g'_{ik} S_k = S_i. \tag{3}$$

Symmetry group J_{ik} of an ambivalent DP $\{S_i, S_k\}$ can be expressed as[6]

$$J_{ik} = F_{(ik)} + g'_{ik} F_{(ik)} , \tag{4}$$

where $F_{ik} = F_i \cap F_k$ and g'_{ik} fulfils (3). Group J_{ik} has the structure of a dichromatic group in which unprimed operations $F_{(ik)}$ represent trivial symmetry operations and primed operations $g'_{ik} F_{(ik)}$ non-trivial operations of the DP $\{S_i, S_k\}$. The group J_{ik} specifies in a convenient way the relation between S_i and S_k. We shall call it the *twin law of the ambivalent domain pair* $\{S_i, S_k\}$.

[§] *Crystal family* of a point group P = crystal system of P, with exception of trigonal groups which belong to the hexagonal family.[3] We shall represent crystal family of P by the holohedral point group of P, $\mathrm{Fam}(P)$ = holohedral group of P, where we put Fam(trigonal group) = $6/mmm$

A *domain pair* $\{S_i, S_k\}$ is *non-ferroelastic* if S_i and S_k possess the same (zero) spontaneous deformation. A necessary and sufficient condition for an ambivalent DP to be non-ferroelastic is

$$\mathrm{Fam}(F_{(ik)}) = \mathrm{Fam}(J_{ik}). \tag{5}$$

It can be shown that *all* $\frac{1}{2}n_o(n_o - 1)$ *DP's that can be formed from* n_o *DS's of a non-ferroelastic phase are ambivalent, non-ferroelastic and their twin law has the form*

$$J_{ik} = F + g'_{ik}F, \tag{6}$$

where F is the common symmetry group of the DS's S_i and S_k.

TABLE I Symmetry reductions $G \rightarrow F$ generating twin law J_{ik}

G	F	J_{ik}
$\bar{1}$, $2/m$ (mmm, $4/m$, $4/mmm$, $\bar{3}$, $\bar{3}1m$, $\bar{3}m1$ $6/m$, $6/mmm$, $m\bar{3}$, $m\bar{3}m$)	1	$\bar{1}'$
$2/m$ (mmm, $4/m$, $4/mmm$, $\bar{3}1m$, $\bar{3}m1$, $6/m$, $6/mmm$, $m\bar{3}$, $m\bar{3}m$)	2	$2/m'$
$2/m$ (mmm, $4/m$, $4/mmm$, $\bar{3}1m$, $\bar{3}m1$, $6/m$, $6/mmm$, $m\bar{3}$, $m\bar{3}m$)	m	$2'/m$
mmm ($4/mmm$, $6/mmm$, $m\bar{3}$, $m\bar{3}m$)	222	$m'm'm'$
mmm ($4/mmm$, $6/mmm$, $m\bar{3}$, $m\bar{3}m$)	$mm2$	mmm'
$4/m$, $4/mmm$ ($m\bar{3}m$)	4	$4/m'$
$4/m$, $4/mmm$ ($m\bar{3}m$)	$\bar{4}$	$4'/m'$
422 $4/mmm$, 432 ($m\bar{3}m$)	4	$42'2'$
$4mm$ $4/mmm$ ($m\bar{3}m$)	4	$4m'm'$
$\bar{4}2m$, $4/mmm$, $\bar{4}3m$ ($m\bar{3}m$)	$\bar{4}$	$\bar{4}2'm'$
$\bar{4}m2$, $4/mmm$, $\bar{4}3m$ ($m\bar{3}m$)	$\bar{4}$	$\bar{4}m'2'$
$4/mmm$ ($m\bar{3}m$)	$4/m$	$4/mm'm'$
$4/mmm$ ($m\bar{3}m$)	422	$4/m'm'm'$
$4/mmm$ ($m\bar{3}m$)	$4mm$	$4/m'mm$
$4/mmm$ ($m\bar{3}m$)	$\bar{4}2m$	$4'/m'm'm$
$\bar{3}$, $\bar{3}m1$, $\bar{3}1m$, $6/m$, $6/mmm$ ($m\bar{3}$, $m\bar{3}m$)	3	$\bar{3}'$
321, $\bar{3}m1$, 622, $\bar{6}2m$, $6/mmm$ (432, $m\bar{3}m$)	3	32'1
312, $\bar{3}1m$, 622, $\bar{6}m2$, $6/mmm$ (432, $m\bar{3}m$)	3	312'
$3m1$, $\bar{3}m1$, $6mm$, $\bar{6}m2$, $6/mmm$ ($\bar{4}3m$ $m\bar{3}m$)	3	$3m'1$
$31m$, $\bar{3}1m$, $6mm$, $\bar{6}2m$, $6/mmm$ ($\bar{4}3m$ $m\bar{3}m$)	3	$31m'$
$\bar{3}m1$, $6/mmm$ ($m\bar{3}m$)	$\bar{3}$	$\bar{3}m'1$
$\bar{3}1m$, $6/mmm$ ($m\bar{3}m$)	$\bar{3}$	$\bar{3}1m'$
$\bar{3}m$, $6/mmm$ ($m\bar{3}m$)	32	$\bar{3}'m'$
$\bar{3}m$, $6/mmm$ ($m\bar{3}m$)	$3m$	$\bar{3}'m$
6, $6/m$, 622 $6mm$, $6/mmm$	3	6'
$\bar{6}$, $6/m$ $\bar{6}2m$ $\bar{6}m2$, $6/mmm$	3	$\bar{6}'$

TABLE I, *cont.*

G	F	J_{ik}
$6/m$, $6/mmm$	$\bar{3}$	$6'/m'$
$6/m$, $6/mmm$	6	$6/m'$
$6/m$, $6/mmm$	$\bar{6}$	$6'/m$
622, $6/mmm$	32	6'22'
622, $6/mmm$	6	62'2'
$6mm$, $6/mmm$	$3m$	$6'mm'$
$6mm$, $6/mmm$	6	$6m'm'$
$\bar{6}2m$, $6/mmm$	32	$\bar{6}'2m'$
$\bar{6}2m$, $6/mmm$	$\bar{6}$	$\bar{6}2'm'$
$\bar{6}m2$, $6/mmm$	$3m$	$\bar{6}'m2'$
$\bar{6}m2$, $6/mmm$	$\bar{6}$	$\bar{6}m'2'$
$6/mmm$	$\bar{3}m$	$6'/m'mm'$
$6/mmm$	$6/m$	$6/mm'm'$
$6/mmm$	622	$6/m'm'm'$
$6/mmm$	$6mm$	$6/m'mm$
$6/mmm$	$\bar{6}2m$	$6'/mm'm$
$m\bar{3}$, $m\bar{3}m$	23	$m'\bar{3}$
432, $m\bar{3}m$	23	$4'32'$
$\bar{4}3m$, $m\bar{3}m$	23	$\bar{4}'3m'$
$m\bar{3}m$	$m\bar{3}$	$m\bar{3}m'$
$m\bar{3}m$	432	$m'\bar{3}m'$
$m\bar{3}m$	$\bar{4}3m$	$m'\bar{3}m$

There are 48 crystallographically different dichromatic point groups that fulfil condition (5). These groups represent all possible twin laws of non-ferroelastic DP's and are displayed in the third column of Table I, together with symmetry groups F (second column). This list is identical with 48 dichromatic point groups used by Curien and Le Corre to designate twins by merohedry and reticular merohedry (except cubic reticular merohedry).[7]

Groups G that fulfil for given F and J_{ik} the relation

$$F < J_{ik} \leq G \qquad (7)$$

represent symmetries of possible prototype phases for which the phase transition $G \rightarrow F$ leads to the appearance of the twin law J_{ik} in the non-ferroelastic phase (for G's in the first column without brackets) or in the partial ferroelastic phase (G's within the brackets).

TENSOR DISTINCTION OF NON-FERROELASTIC DOMAINS

Let us consider a material property tensor $\mathbf{T}$ and a specific twin law (6) of a DP $\{S_i, S_k\}$. If $m_J^{\mathbf{T}}$ denotes the number of components of $\mathbf{T}$ in J_{ik} and $m_F^{\mathbf{T}}$ that in F then the difference $m^{\mathbf{T}} = m_F^{\mathbf{T}} - m_J^{\mathbf{T}}$ gives the number of components that are different in DS's S_i and S_k. Numbers $m_F^{\mathbf{T}}$ and $m_J^{\mathbf{T}}$ can be found e.g. in Ref. 8. Numbers $m^{\mathbf{T}}$ for all non-ferroelastic twin laws J_{ik} and important material property tensors $\mathbf{T}$ are given in Table II.

There is an alternative and more elegant method for determining $m^{\mathbf{T}}$: Distinct components of $\mathbf{T}$ transform as basis functions of an alternating representation $D_a^{\mathbf{T}}$ of J_{ik} which subduces the identity representation in F (the representation $D_a^{\mathbf{T}}$ is given in the fourth column of Table II). The components of the tensor $\mathbf{T}$ transform as a set of basis functions of a representation $D^{\mathbf{T}}$. The number $m^{\mathbf{T}}$ equals the multiplicity of $D_a^{\mathbf{T}}$ in $D^{\mathbf{T}}$.

The results can be applied also to twins by merohedry[7] (twin-lattice symmetry[9]).

TABLE II Non-ferroelastic twin laws and numbers of distinct tensor components. F...symmetry of both domain (twin) components S_i and S_k, J_{ik}...dichromatic point group expressing the twin law, fe: n = non-ferroelectric domain pair, e = ferroelectric domain pair (see Ref. 1), $D_a^{\mathbf{T}}$ ... alternating irreducible representation of J_{ik} that subduces the identity representation in F, ϵ...enantiomorphism, V...spontaneous polarization, $\epsilon[V^2]$...optical activity, $V[V^2]$...piezoelectricity, electrooptics, $\epsilon V[V^2]$...electrogyration, $[[V^2]^2]$...linear elasticity, $[V^2]^2$...piezooptics, electrostriction.

F	J_{ik}	fe	$D_a^{\mathbf{T}}$	ϵ	V	$\epsilon[V^2]$	$V[V^2]$	$\epsilon V[V^2]$	$[[V^2]^2]$	$[V^2]^2$
1	$\bar{1}'$	e	A_u	1	3	6	18	0	0	0
2	$2/m'$	e	A_u	1	1	4	8	0	0	0
m	$2'/m$	e	B_u	0	2	2	10	0	0	0
222	$m'm'm'$	n	A_u	1	0	3	3	0	0	0
$mm2$	mmm'	e	B_{1u}	0	1	1	5	0	0	0
4	$4/m'$	e	A_u	1	1	2	4	0	0	0
$\bar{4}$	$4'/m'$	n	B_u	0	0	2	4	0	0	0
4	$42'2'$	e	A_2	0	1	0	3	3	1	3
4	$4m'm'$	n	A_2	1	0	2	1	3	1	3
$\bar{4}$	$\bar{4}2'm'$	n	A_2	0	0	1	2	3	1	3
$\bar{4}$	$\bar{4}m'2'$	n	A_2	0	0	1	2	3	1	3
$4/m$	$4/mm'm'$	n	A_{2g}	0	0	0	0	3	1	3
422	$4/m'm'm'$	n	A_{1u}	1	0	2	1	0	0	0
$4mm$	$4/m'mm$	e	A_{2u}	0	1	0	3	0	0	0
$\bar{4}2m$	$4'/m'm'm$	n	B_{1u}	0	0	1	2	0	0	0
3	$\bar{3}'$	e	A_u	1	1	2	6	0	0	0
3	32'1	e	A_2	0	1	0	4	4	1	4
3	312'	e	A_2	0	1	0	4	4	1	4
3	$3m'1$	n	A_2	1	0	2	2	4	1	4
3	$31m'$	n	A_2	1	0	2	2	4	1	4
$\bar{3}$	$\bar{3}m'1$	n	A_{2g}	0	0	0	0	4	1	4
$\bar{3}$	$\bar{3}1m'$	n	A_{2g}	0	0	0	0	4	1	4
32	$\bar{3}'m'$	n	A_{1u}	1	0	2	2	0	0	0
$3m$	$\bar{3}'m$	e	A_{2u}	0	1	0	4	0	0	0
3	6'	n	B	0	0	0	2	2	2	4
3	$\bar{6}'$	e	A''	1	1	2	4	2	2	4
$\bar{3}$	$6'/m'$	n	B_g	0	0	0	0	2	2	4
6	$6/m'$	e	A_u	1	1	2	4	0	0	0
$\bar{6}$	$6'/m$	n	B_u	0	0	0	2	0	0	0
32	6'22'	n	B_1	0	0	0	1	1	1	2
6	62'2'	e	A_2	0	1	0	3	3	0	2

TABLE II, *cont.*

F	J_{ik}	fe	$D_a^{\mathbf{T}}$	ϵ	V	$\epsilon[V^2]$	$V[V^2]$	$\epsilon V[V^2]$	$[[V^2]^2]$	$[V^2]^2$
$3m$	$6'mm'$	n	B_2	0	0	0	1	1	1	2
6	$6m'm'$	n	A_2	1	0	2	1	3	0	2
32	$\bar{6}'2m'$	n	A_1''	1	0	2	1	1	1	2
$\bar{6}$	$\bar{6}2'm'$	n	A_2'	0	0	0	1	3	0	2
$3m$	$\bar{6}'m2'$	e	A_2''	0	1	0	3	1	1	2
$\bar{6}$	$\bar{6}m'2'$	n	A_2'	0	0	0	1	3	0	2
$\bar{3}m$	$6'/m'mm'$	n	B_{1g}	0	0	0	0	1	1	2
$6/m$	$6/mm'm'$	n	A_{2g}	0	0	0	0	3	0	2
622	$6/m'm'm'$	n	A_{1u}	1	0	2	1	0	0	0
$6mm$	$6/m'mm$	e	A_{2u}	0	1	0	3	0	0	0
$\bar{6}2m$	$6'/mm'm$	n	B_{2u}	0	0	0	1	0	0	0
23	$m'\bar{3}$	n	A_u	1	0	1	1	0	0	0
23	$4'32'$	n	A_2	0	0	0	1	1	0	1
23	$\bar{4}'3m'$	n	A_2	1	0	1	0	1	0	1
$m\bar{3}$	$m\bar{3}m'$	n	A_{2g}	0	0	0	0	1	0	1
432	$m'\bar{3}m'$	n	A_{1u}	1	0	1	0	0	0	0
$\bar{4}3m$	$m'3m$	n	A_{2u}	0	0	0	1	0	0	0

This work has been partially supported by the grant No 11074 of the CSAS Grant Agency.

REFERENCES

1. V. Janovec, L Richterová and D.B. Litvin, *Ferroelectrics*, **126**, 287 (1992).
2. K. Aizu, *J. Phys. Soc. Japan*, **34**, 121 (1973).
3. *International Tables for Crystallography*, Vol.A, edited by T. Hahn (D. Reidel Publishing Company, Dordrecht, Holland, 1983), pp.12, 747.
4. V. K. Wadhawan, *Phase Transitions*, **34**, 3 (1991).
5. V. Janovec, *Czech. J. Phys.*, **B 22**, 974 (1972).
6. V. Janovec, *Ferroelectrics*, **35**, 105 (1981).
7. H. Curien and Y. Le Corre, *Bull. Soc. franç. Minér. Crist.*, **81**, 126 (1958).
8. Y. I. Sirotin and M. P. Shaskol'skaya, *Osnovy Kristallofiziki* (Nauka, Moskva, 1975). English translation: *Fundamentals of Crystal Physics* (Mir, Moscow, 1982).
9. G. Donnay and J. D. H. Donnay, *Candian Mineralogist*, **12**, 422 (1974).

Presented at the Eighth International Meeting on Ferroelectricity
Gaithersburg, Maryland, U.S.A., 8-13 August, 1993
To appear in Ferroelectrics

TENSOR DISTINCTION OF FERROELASTIC DOMAIN STATES IN COMPLETELY TRANSPOSABLE DOMAIN PAIRS

V. JANOVEC*, D. B. LITVIN† and L. RICHTEROVÁ§

**Institute of Physics, Academy of Sciences of the Czech Republic, Na Slovance 2, 180 40 Prague 8, Czech Republic*
† Department of Physics, The Pennsylvania State University, The Berks Campus, P.O.Box 7009, Reading, PA 19610-6009, U.S.A.
§ Comenius University, Faculty of Mathematics and Physics, Mlynská dolina F1, 842 15 Bratislava, Slovakia

We present tensor distinction of ferroelastic domains for a large class of ferroelastic domain states that form so called completely transposable domain pairs. We give the 15 possible relations (twin laws) between these ferroelastic domain states. For each twin law we list the numbers of components of important material property tensors that are different and that are equal in the two single domain states of the domain pair. We demonstrate how these twin laws and tensor distinction can be influenced by disorientations, i.e. rotations of single domain states needed to achieve coherent junction of two ferroelastic domain states along a planar domain wall.

1. INTRODUCTION

Domain structures consist of domains. Bulk structures $S_i, S_k, \ldots$ of domains, called *domain states*, have the same low symmetry structure and in the continuum description differ only in spatial orientation. When observed from one laboratory coordinate system they may exhibit different tensor properties. This tensor distinction is important, e.g., for finding and applying appropriate methods for observing domains, for determining average tensor properties of polydomain samples and for discussing the behavior of domain structures in external fields.

Recently, we have examined tensor distinction in non-ferroelastic phases.[1] In this contribution we demonstrate specific features of relations between bulk structures of ferroelastic domains and present tensor distinction for a class of ferroelastic domain states that form so called completely transposable pairs.

2. FERROELASTIC DOMAIN PAIRS AND DISORENTATIONS

When examining tensor distinction of two domains D_i and D_k we are comparing tensor properties of their domain states S_i and S_k. Instead of describing S_i and S_k by their orientations we shall characterize the relation between S_i and S_k by a suitable point group which will allow us to determine tensor distinction by group-theoretical procedures.

Two domain states S_i, S_k considered irrespectively of their coexistence form a *domain pair* $\{S_i, S_k\}$. Domain pair can be treated algebraically as an unordered set $\{S_i, S_k\} = \{S_k, S_i\}$ or, geometrically, as a superposition of domain states S_i and S_k. Symmetrically, the domain pair is specified by the symmetry group F_i of S_i which consists of the operations of the symmetry group G of the high-symmetry (parent) phase that leave S_i invariant,

$$F_i = \{g \in G \mid gS_i = S_i\}\,, \tag{1}$$

and by an operation $j'_{ik} \in G$ that transforms S_i into S_k, $j'_{ik}S_i = S_k$. If, further, j'_{ik} transforms also S_k into S_i , i.e. if $j'_{ik}S_i = S_k$, and $j'_{ik}S_k = S_i$, then the domain pair is referred to as a *transposable (ambivalent*[1]*) domain pair.* The operation j'_{ik} exchanging the domain states can be considered a symmetry operation of $\{S_i, S_k\}$. If, moreover, the domain states S_i and S_k have the same symmetry group, $F_i = F_k$, then the pair is called a *completely transposable domain pair.* The symmetry group of such a pair can be expressed in the form of a dichromatic group

$$J_{ik} = F_i + j'_{ik}F_i\,, \tag{2}$$

where the unprimed operations of F_i leave invariant both S_i and S_k whereas primed operations of the left coset $j'_{ik}F_i$ exchange S_i and S_k. The group J_{ik} fully specifies the domain pair $\{S_i, S_k\}$ and we say that J_{ik} in Eq. (3) expresses the *twin law* of a completely transposable domain pair $\{S_i, S_k\}$.

Depending on the spontaneous deformations $e^{(i)}$ and $e^{(k)}$ of S_i and S_k, resp., we can distinguish between *non-ferroelastic domain pairs* for which $e^{(i)} = e^{(k)}$ and *ferroelastic domain pairs* for which $e^{(i)} \neq e^{(k)}$. For completely transposable domain pairs a simple criterion holds: $\{S_i, S_k\}$ is ferroelastic if and only if $\mathrm{Fam}F_i \subset \mathrm{Fam}J_{ik}$, where the symbol Fam denotes the crystal family of a group.[1]

There are 15 dichromatic groups of the form (2) that satisfy conditions $\mathrm{Fam}F_i \subset \mathrm{Fam}J_{ik}$ and $F_i = F_k$. These twin laws are listed in the first three columns of Table I. Before discussing the tensor distinction in these domain pairs we recall some specific features of ferroelastic domain structures.

In non-ferroelastic phases the number and orientations of possible domain states are not influenced by coexistence of domain states and do not depend on the form of the domain structure. Domain states in the polydomain sample are identical with *single domain states*, i.e. with bulk structures of single domains. All possible domain pairs in non-ferroelastic phases are completely transposable.[1]

The basic difference, and the main source of complications for ferroelastic phases lies in the fact that the number and orientation of ferroelastic domain states in polydomain samples differ from that of single domain states and depend on the specific form of the domain structure. In each case, however, domain states can be related in a unique way to single domain states which thus form a reliable reference system of domain states.

To illustrate this let us consider possible coexistence of two ferroelastic domain states that appear in the ferroelastic phase of the phase transition with $G = 4/mmm$ and $F = m_x m_y m_z$. In Figure 1 the tetragonal parent phase is represented by dotted square P

TABLE I Twin laws, axes, permissible walls and tensor distinction of ferroelastic domain states in completely transposable domain pairs

$F_i = F_k$...symmetry of domain states S_i and S_k, j'_{ik}...operation exchanging domain states S_i and S_k, J_{ik}...dichromatic point group expressing the twin law, D_a...alternating representation of J_{ik} subducing the identity representation in F_i
tensor designation: ϵ...enantiomorphism, V...polarization, $[V^2]$...deformation, permittivity, $\epsilon[V^2]$...optical activity, $V[V^2]$...piezoelectricity, electrooptics, $\epsilon V[V^2]$...electrogyration, $[[V^2]^2]$...elasticity, $[V^2]^2$...piezooptics, electrostriction

completely transposable ferroelastic domain pair							opposite (equal) tensor components							
$F_i = F_k$	j'_{ik}	J_{ik}	D_a	axis	permis. walls		ϵ	V	$[V^2]$	$\epsilon[V^2]$	$V[V^2]$	$\epsilon V[V^2]$	$[[V^2]^2]$	$[V^2]^2$
1	$2'$	$2'$	B	$[k\bar{h}0]$	(001)	$(hk0)_e$	0(1)	2(1)	2(4)	2(4)	10(8)	10(8)	8(13)	16(20)
1	m'	m'	A''	$[k\bar{h}0]$	$(001)_e$	$(hk0)$	1(0)	1(2)	2(4)	4(2)	8(10)	10(8)	8(13)	16(20)
$\bar{1}$	m'	$2'/m'$	B_g	$[k\bar{h}0]$	(001)	$(hk0)$	0(0)	0(0)	2(4)	0(0)	0(0)	10(8)	8(13)	16(20)
2_z	$2'_x$	$2'2'2$	B_1	[001]	(100)	(010)	0(1)	1(0)	1(3)	1(3)	5(3)	5(3)	4(9)	8(12)
2_z	m'_x	$m'm'2$	A_2	[001]	(100)	(010)	1(0)	0(1)	1(3)	3(1)	3(5)	5(3)	4(9)	8(12)
m_z	m'_x	$m'2'm$	B_2	[010]	$(100)_e$	(010)	0(0)	1(1)	1(3)	1(1)	5(5)	5(3)	4(9)	8(12)
$2_z/m$	m'_x	$m'm'm$	B_{1g}	[001]	(100)	(010)	0(0)	0(0)	1(3)	0(0)	0(0)	5(3)	4(9)	8(12)
2	$4'$	$4'$	B	[001]	$(hk0)$	$(k\bar{h}0)$	0(1)	0(1)	2(2)	2(2)	4(4)	4(4)	6(7)	10(10)
2	$\bar{4}'$	$\bar{4}'$	B	[001]	$(hk0)$	$(k\bar{h}0)$	1(0)	1(0)	2(2)	2(2)	4(4)	4(4)	6(7)	10(10)
$2_z/m$	$4'$	$4'/m$	B_g	[001]	$(hk0)$	$(k\bar{h}0)$	0(0)	0(0)	2(2)	0(0)	0(0)	4(4)	6(7)	10(10)
2_x22	$2'_{xy}$	$4'22'$	B_1	[001]	(110)	$(1\bar{1}0)$	0(1)	0(0)	1(2)	1(2)	2(1)	2(1)	3(6)	5(7)
m_xm2	m'_{xy}	$4'mm'$	B_1	[001]	(110)	$(1\bar{1}0)$	0(0)	0(1)	1(2)	1(0)	2(3)	2(1)	3(6)	5(7)
m_xm2	$2'_{xy}$	$\bar{4}'m2'$	B_2	[001]	(100)	(010)	0(0)	1(0)	1(2)	0(1)	3(2)	2(1)	3(6)	5(7)
2_x22	m'_{xy}	$\bar{4}'2m'$	B_1	[001]	(110)	$(1\bar{1}0)$	1(0)	0(0)	1(2)	2(1)	1(2)	2(1)	3(6)	5(7)
m_xmm	m'_{xy}	$4'/mmm'$	B_{2g}	[001]	(110)	$(1\bar{1}0)$	0(0)	0(0)	1(2)	0(0)	0(0)	2(1)	3(6)	5(7)

and the two orthorhombic single domain states $S_i = 1$ and $S_k = 2$ by dashed rectangles 1 and 2 with symmetry $F_1 = F_2 = m_x m_y m_z$. A geometrical representation of the *single domain pair* {1,2} is given on the left side of Figure 2. An operation $j'_{12} = m'_{\bar{x}y}$ exchanges 1 and 2, hence the domain pair {1,2} is completely transposable. The symmetry group of this pair is $J_{12} = m_x m_y m_z + m'_{\bar{x}y}\{m_x m_y m_z\} = 4'/m_z m_x m'_{xy}$.

It has been shown[2,3,4] that for a ferroelastic domain pair there exist two mutually perpendicular planes, called *permissible walls*, along which two domain states can meet in a compatible way, i.e. without dislocations or other singular defects. To achieve such a connection the single domain states must be rotated by a *disorientation angle* φ and $-\varphi$ about the intersecton of permissible domain walls called an *axis of the domain pair*. The rotated structures will be called *disoriented domain states* and domain pairs in which two disoriented domain states have a common plane (permissible wall) will be called *compatible domain pairs*.

In our example permissible domain walls are denoted W^I and W^{II} and the axes of the domain pair passes through the origin O. From Figures 1 and 2 it follows that disoriented domain states 1^+ and 2^- form a compatible domain pair $\{1^+, 2^-\}$ with a common plane W^{II} whereas 1^- and 2^+ in the compatible pair $\{1^-, 2^+\}$ share the plane W^I. Domain states in both compatible domain pairs have a common symmetry group in G which is, according to Eq. (1), $F_{1-} = F_{1+} = F_{2-} = F_{2+} = 2_z/m_z$. Domain states in both compatible domain pairs are exchanged by the operation $j'_{1+2-} = m'_{\bar{x}y}$, both compatible domain pairs are, therefore, completely transposable and have the same symmetry group $J_{1+2-} = J_{1-2+} = \{2_z/m_z\} + m'_{\bar{x}y}\{2_z/m_z\} = m'_{xy} m'_{\bar{x}y} m_z$. Thus disorientation reduces symmetry of domain states and of domain pairs as well.

In Table I we list for each of the 15 twin laws the orientation of the axis of the domain pair and of two perpendicular permissible walls. It can be easily shown that for the first 7 twin laws (given in the upper box) neither the symmetry of the domain states nor that of domain pairs are influenced by disorientations. For the remaining 8 twin laws the symmetry (twin law) $\hat{J}_{ik}$ of the compatible domain pairs is lower than the symmetry (twin law) J_{ik} of the corresponding single domain pair (see Table II). In the first three cases of Table II (middle box of Table I) the symmetry of domain states is not influenced by disorientations, therefore $\hat{J}_{ik} = F_i$ and the compatible pairs are no more transposable. In remaining five cases of Table II (lower box of Table I) not only J_{ik} but also the symmetry of domain states $F_i = F_k$ is lowered by disorientations and the compatible domain pairs with reduced symmetry $\hat{J}_{ik}$ remain completely transposable (see our example).

TABLE II Symmetry reduction of tetragonal twin laws by disorientation

J_{ik}	$4'_z$	$\bar{4}'_z$	$4'_z/m_z$	$4'_z 2_x 2'_{xy}$	$4'_z m_x m'_{xy}$	$\bar{4}'_z m_x 2'_{xy}$	$\bar{4}'_z 2_x m'_{xy}$	$4'_z/m_z m_x m'_{xy}$
$\hat{J}_{ik}$	2_z	2_z	$2_z/m_z$	$2'_{xy} 2'_{\bar{x}y} 2_z$	$m'_{xy} m'_{\bar{x}y} 2_z$	$2'_{xy} 2'_{\bar{x}y} 2_z$	$m'_{xy} m'_{\bar{x}y} 2_z$	$m'_{xy} m'_{\bar{x}y} m_z$

3. TENSOR DISTINCTION OF FERROELASTIC DOMAIN STATES

Discussion of tensor distinction in completely transposable ferroelastic domain pairs is similar to that in non-ferroelastic domain pairs.[1] Let us consider a material property tensor **T** and a specific twin law J_{ik}. Components of **T** transform as a set of basis functins of a (generally reducible) representation $D^{\mathbf{T}}$ of J_{ik}. Distinct components of **T** transform as basis functions of an alternating representation D_a of J_{ik} which subduces the identity representation in F (this representation D_a is given in the fourth column of Table); equal non-zero components of **T** transform as basis function of the identity representation D_1

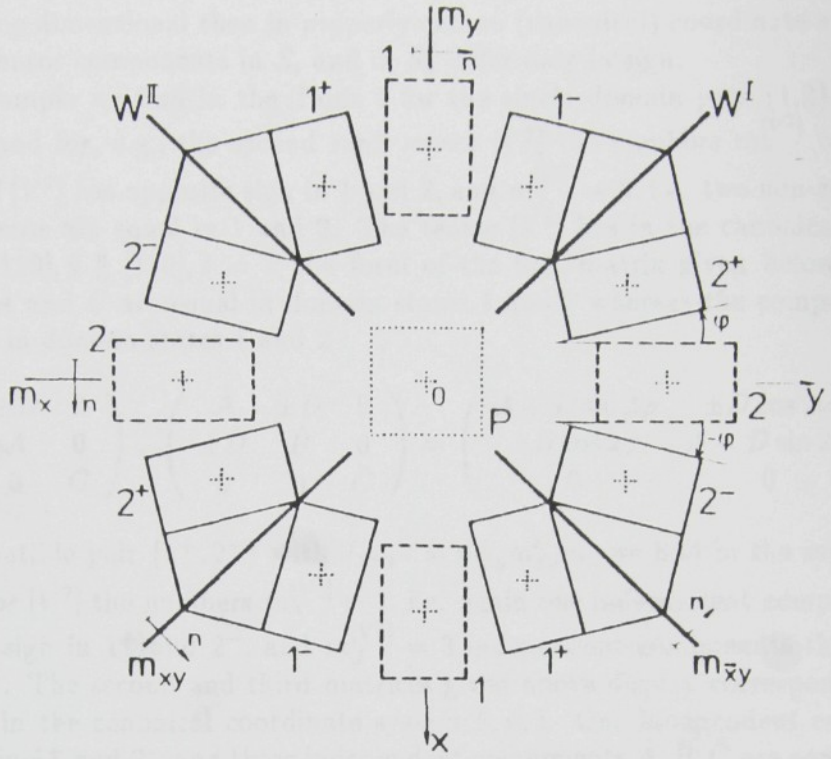

FIGURE 1 Exploded view of the single domain states 1, 2 and disoriented domain states $1^+, 1^-, 2^+, 2^-$. W^I and W^{II} are permissible walls, the axis of the ferroelastic domain pair {1,2} is perpendicular to the plane of the Figure and passes through the origin O. Rectangles representing domain states should be shifted so that their centers (dotted crosses) are at the axis.

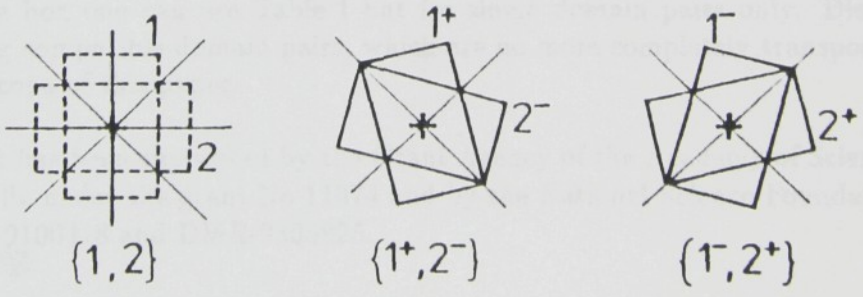

FIGURE 2 Single domain pair {1,2} and compatible domain pairs $\{1^+, 2^-\}$, $\{1^-, 2^+\}$. Diagonal solid lines passing through the center represent mirror planes and two-fold axes which exchange domain states. Vertical and horizontal lines represent mirror planes and two-fold axes which leave domain states 1 and 2 invariant.

of J_{ik}. Number $m_a^{\mathbf{T}}$ of distinct components and number $m_J^{\mathbf{T}}$ of equal componets of $\mathbf{T}$ in domain states of a domain pair are equal to the multiplicity of D_a and D_1 in $D^{\mathbf{T}}$, resp. In Table I numbers $m_a^{\mathbf{T}}$ and $m_J^{\mathbf{T}}$ (given in the parenthesis) are presented for all 15 ferroelastic completely transposable twin laws J_{ik} and for 8 important material property tensors $\mathbf{T}$. Since D_a is one dimensional then in properly chosen (canonical) coordinate system $\hat{x}, \hat{y}, \hat{z}$ the distinct tensor components in S_i and in S_k differ only in sign.

In our example we find in the Table I for the single domain pair $\{1,2\}$ with $J_{12} = 4'/mm_x m'_{xy}$ and for, e.g., the second rank tensor $[V^2]$ the numbers $m_a^{[V^2]} = 1$, i.e. one component of $[V^2]$ has opposite sign in 1 and 2, and $m_J^{[V^2]} = 2$, i.e. two non-zero independent components are equal in 1 and 2. The tensor $[V^2]$ has in the canonical coordinate system $\hat{x} \parallel [110], \hat{y} \parallel [\bar{1}10], \hat{z} = z$ the form of the first matrix given below, where the components A and C are equal in domain states 1 and 2 whereas the component D has opposite sign in domain states 1 and 2 :

$$\begin{pmatrix} A & \pm D & 0 \\ \pm D & A & 0 \\ 0 & 0 & C \end{pmatrix}, \begin{pmatrix} \hat{A} & \pm\hat{D} & 0 \\ \pm\hat{D} & \hat{B} & 0 \\ 0 & 0 & \hat{C} \end{pmatrix} = \begin{pmatrix} A + D\sin 2\varphi & \pm D\cos 2\varphi & 0 \\ \pm D\cos 2\varphi & A - D\sin 2\varphi & 0 \\ 0 & 0 & C \end{pmatrix}$$

For the compatible pair $\{1^+, 2^-\}$ with $J_{1^+2^-} = m'_{xy} m'_{\bar{x}y} m_z$ we find in the seventh line of the Table I for $[V^2]$ the numbers $m_a^{[V^2]} = 1$, i.e. again one independent component which has opposite sign in 1^+ and 2^-, and $m_J^{[V^2]} = 3$ independent components that are equal in 1^+ and 2^-. The second and third matrices given above display corresponding matrix form of $[V^2]$ in the canonical coordinate system $\hat{x}, \hat{y}, \hat{z}$. One independent component $\hat{D}$ changes sign in 1^+ and 2^- and three independent components $\hat{A}, \hat{B}, \hat{C}$ are equal in 1^+ and 2^-. As the last matrix shows all these four components are functions of A, C, D from the first matrix and the angle of disorientation φ.

In general, for 7 twin laws in the upper box of Table I the numbers $m_a^{\mathbf{T}}$ and $m_J^{\mathbf{T}}$ of opposite and equal tensor components are not influenced by disorientatins, i.e. the numbers given in the upper box of Table I hold both for single domain pairs and for compatible domain pairs. For 5 twin laws in the lower box of Table I the numbers $m_a^{\mathbf{T}}$ and $m_J^{\mathbf{T}}$ are smaller for single domain pairs than for compatible domain pairs and both can be determined from Tables I and II, similarly as in our example. For 3 remaining cases in the middle box one can use Table I but for single domain pairs only. Discussion of corresponding compatible domain pairs, which are no more completely transposable, falls outside the scope of this paper.

This work has been supported by the Grant Agency of the Academy of Sciences of the Czech Republic under the grant No 11074 and by the National Science Foundation under grants DMR-9100418 and DMR-9305825.

REFERENCES

1. V. Janovec, L Richterová and D.B. Litvin, *Ferroelectrics*, **126**, 287 (1992).
2. J. Fousek and V. Janovec, *J. Appl. Phys.*, **40**, 135 (1969).
3. J. Sapriel, *Phys. Rev. B*, **12**, 5128 (1975).
4. E. F. Dudnik and L. A. Shuvalov, *Ferroelectrics*, **98**, 207 (1989).

U 635 P